

**NEW CALIBRATION APPROACHES IN SOLID PHASE
MICROEXTRACTION FOR ON-SITE ANALYSIS**

by

Yong Chen

A thesis
presented to the University of Waterloo
in fulfillment of the
thesis requirement for the degree of
Doctor of Philosophy
in
Chemistry

Waterloo, Ontario, Canada, 2004

©Yong Chen, 2004

Declaration

I hereby declare that I am the sole author of this thesis. This is a true copy of the thesis, including any required final revisions, as accepted by my examiners.

I understand that my thesis may be made electronically available to the public.

Abstract

Calibration methods for quantitative on-site sampling using solid phase microextraction (SPME) were developed based on diffusion mass transfer theory. This was investigated using adsorptive polydimethylsiloxane/divinylbenzene (PDMS/DVB) and Carboxen/polydimethylsiloxane (CAR/PDMS) SPME fiber coatings with volatile aromatic hydrocarbons (BTEX: benzene, toluene, ethylbenzene, and o-xylene) as test analytes. Parameters that affected the extraction process (sampling time, analyte concentration, water velocity, and temperature) were investigated. Very short sampling times (10-300 s) and sorbents with a strong affinity and large capacity were used to ensure a 'zero sink' effect calibrate process. It was found that mass uptake of analyte changed linearly with concentration. Increase of water velocity increased mass uptake, though the increase is not linear. Temperature did not affect mass uptake significantly under typical field sampling conditions (5-30°C). To further describe rapid SPME analysis of aqueous samples, a new model translated from heat transfer to a circular cylinder in cross flow was used. An empirical correlation to this model was used to predict the mass transfer coefficient. Findings indicated that the predicted mass uptake compared well with experimental mass uptake. The new model also predicted rapid air sampling accurately.

To further integrate the sampling and analysis processes, especially for on-site or *in-vivo* investigations where the composition of the sample matrix is very complicated and/or agitation of the sample matrix is variable or unknown, a new approach for calibration was developed. This involved the loading internal standards onto the extraction fiber prior to the extraction step. During sampling, the standard partially desorbs into the sample matrix and the rate at which this process occurs, was for calibration. The kinetics of the absorption/desorption was investigated, and the isotropy of the two processes was demonstrated, thus validating this approach for calibration.

A modified SPME device was used as a passive sampler to determine the time-weighted average (TWA) concentration of volatile organic compounds (VOCs) in air. The sampler collects the VOCs by the mechanism of molecular diffusion and sorption on to a coated fiber as collection medium. This process was shown to be described by Fick's first

law of diffusion, whereby the amount of analyte accumulated over time enable measurement of the TWA concentration to which the sampler was exposed. TWA passive sampling with a SPME device was shown to be almost independent of face velocity, and to be more tolerant of high and low analyte concentrations and long and short sampling times, because of the ease with which the diffusional path length could be changed. Environmental conditions (temperature, pressure, relative humidity, and ozone) had little or no effect on sampling rate. When the SPME device was tested in the field and the results compared with those from National Institute of Occupational Health and Safety (NIOSH) method 1501 good agreement was obtained.

To facilitate the use of SPME for field sampling, a new field sampler was designed and tested. The sampler was versatile and user-friendly. The SPME fiber can be positioned precisely inside the needle for TWA sampling, or exposed completely outside the needle for rapid sampling. The needle is protected within a shield at all times hereby eliminating the risk of operator injury and fiber damage. A replaceable Teflon cap is used to seal the needle to preserve sample integrity. Factors that affect the preservation of sample integrity (sorbent efficiency, temperature, and sealing materials) were studied. The use of a highly efficient sorbent is recommended as the first choice for the preservation of sample integrity. Teflon was a good material for sealing the fiber needle, had little memory effect, and could be used repeatedly. To address adsorption of high boiling point compounds on fiber needles, several kinds of deactivated needles were evaluated. RSC-2 blue fiber needles were the more effective. A preliminary field sampling investigation demonstrated the validity of the new SPME device for field applications.

Acknowledgements

I'd like to thank Dr. Janusz Pawliszyn for providing me the opportunity to work on this interesting and challenging project, and for guiding me to excel in this work.

I next thank and acknowledge the efforts of all my committee members, Dr. Dixon, Dr. Lipkowski, Dr. Mills, Dr. Power, and Dr. Sloan.

Finally, I thank all the group members for their help and friendship, especially Dr. Tiemin Huang, Dr. Guohua Xiong, Maria, Helen, Limei, Xinyu, Yan, Fang, Winston, Michael, Dr. Zhen Liu, Heather, Shokouh, Marcel.

Dedication

In memory of my father.

I dedicate this thesis to Diane. I have a special dedication for my mother.

Table of Contents

Declaration	ii
Abstract	iii
Acknowledgements	v
Dedication	vi
Table of Contents	vii
List of Figures	xi
List of Tables	xvii
Chapter 1 Introduction	1
1.1 Field Analysis	1
1.2 Solid Phase Microextraction	3
1.3 Calibration in Solid Phase Microextraction	7
1.3.1 <i>Equilibrium Extraction</i>	8
1.3.2 <i>Exhaustive Extraction</i>	11
1.3.3 <i>Pre-equilibrium Extraction</i>	11
1.3.4 <i>Calibration Based on First-Order Reaction Rate Constant</i>	12
1.3.5 <i>Calibration Based on Diffusion</i>	16
1.3.5.1 Diffusion	16
1.3.5.2 Diffusion-Based Rapid SPME	22
1.3.5.3 Time-Weighted Average Passive Sampling	26
1.4 Thesis Objective.....	31
1.5 References.....	31
Chapter 2 Rapid Solid Phase Microextraction	34
2.1 Introduction.....	34
2.2 Theory	36

2.3	Experimental Section	39
2.3.1	<i>Chemicals and Supplies</i>	39
2.3.2	<i>Flow-Through System</i>	40
2.3.3	<i>Monitoring Toluene Concentration in Deionized Water.</i>	42
2.3.4	<i>Rapid Air Sampling</i>	42
2.3.4.1	Standard Gas Generator	42
2.3.4.2	Sampling Chamber.....	43
2.3.5	<i>Indoor Air Sampling</i>	43
2.3.6	<i>Gas Chromatography</i>	44
2.4	Results and Discussion	46
2.4.1	<i>Extraction Time Profiles for Aqueous Solutions</i>	46
2.4.2	<i>Effects of Sample Velocity</i>	48
2.4.3	<i>Mass Uptake Rate Vs. Analyte Concentration</i>	50
2.4.4	<i>Validation of the Theoretical Model</i>	52
2.4.5	<i>Effect of Water Temperature</i>	55
2.4.6	<i>Monitoring Toluene Concentration in Deionized Water</i>	57
2.4.7	<i>Rapid Air Sampling</i>	59
2.4.8	<i>Indoor Air Sampling</i>	60
2.5	Conclusion	63
2.6	References.....	64
Chapter 3	Standards on A Fiber	66
3.1	Introduction.....	66
3.2	Theory	68
3.3	Experimental Section	73
3.3.1	<i>Chemicals, Supplies, and Standard Gases</i>	73
3.3.2	<i>Flow-Through System</i>	74
3.3.3	<i>Gas Chromatography</i>	75
3.4	Results and Discussion	76
3.4.1	<i>Desorption</i>	76
3.4.2	<i>Absorption Vs. Desorption</i>	77
3.4.3	<i>Calibration of Rate of Absorption using Rate of Desorption</i>	82

3.4.4	<i>Effect of Extraction Temperature</i>	92
3.4.4.1	The Temperature Dependence of Distribution Coefficient K	92
3.4.4.2	The Temperature Dependence of Time Constant a	94
3.5	Conclusion	98
3.6	References.....	99
Chapter 4	Time-Weighted Average Passive Sampling	101
4.1	Introduction.....	101
4.2	Theory	104
4.3	Experimental Section	104
4.3.1	<i>Chemicals</i>	104
4.3.2	<i>Materials</i>	104
4.3.3	<i>Standard Gas Generator</i>	105
4.3.4	<i>Sampling Chamber</i>	105
4.3.5	<i>Instrumentation and Methods for SPME and Liquid Injections</i>	106
4.3.6	<i>Field TWA Sampling with SPME using A CAR/PDMS-75 Fiber</i>	107
4.4	Results and Discussion	107
4.4.1	<i>Three Prerequisites</i>	107
4.4.1.1	Zero Sink.....	107
4.4.1.2	Response Time.....	111
4.4.1.3	Effect of Face Velocity	112
4.4.2	<i>TWA Passive Sampling with The CAR/PDMS-75 Fiber</i>	113
4.4.3	<i>Sensitivity to Ambient Conditions</i>	117
4.4.3.1	Effects of Temperature and Pressure	118
4.4.3.2	Effect of Humidity	120
4.4.3.3	Effect of Ozone.....	121
4.4.4	<i>Storage Stability</i>	122
4.4.5	<i>Field TWA Sampling</i>	122
4.5	Conclusion	123
4.6	References.....	125
Chapter 5	A New SPME Field Sampler	127

5.1	Introduction.....	127
5.2	Experimental Section.....	129
5.2.1	<i>Standard Gas Generator</i>	129
5.2.2	<i>Sampling Chamber</i>	129
5.2.3	<i>Gas Chromatography</i>	129
5.3	Results and Discussion.....	130
5.3.1	<i>The SPME Field Sampler</i>	130
5.3.2	<i>Preservation of Sample Integrity</i>	134
5.3.3	<i>Cross Contamination</i>	138
5.3.4	<i>Deactivated Needles</i>	142
5.4	Field Sampling.....	144
5.5	Conclusion.....	145
5.6	References.....	145
Chapter 6	Summary.....	147
6.1	Calibration for Different Extraction Modes of SPME.....	147
6.2	Contributions of This Thesis.....	150
6.3	Perspective.....	151
	Glossary.....	153

List of Figures

Figure 1-1 Field analysis.....	2
Figure 1-2 The custom-made SPME device based on the Hamilton 7000 series syringe.	4
Figure 1-3 Thermal desorption of the analytes from a SPME fiber in a GC injector.....	5
Figure 1-4 Microextraction with SPME. V_f , volume of fiber coating; K_{fs} , fiber/sample distribution coefficient; V_s , volume of sample; C_0 , initial concentration of analyte in the sample.	7
Figure 1-5 Various calibration methods in SPME.	8
Figure 1-6 SPME derivatization techniques	13
Figure 1-7 In-coating derivatization technique with fiber doping method.	14
Figure 1-8 The derivation of Fick's Second Law of Diffusion.....	18
Figure 1-9 (A) Schematic of conduction of electricity through two resistances r_1 and r_2 , and B) schematic of mass diffusion through two tubes.	20
Figure 1-10 Extraction using absorptive (a) and adsorptive (b) extraction phases immediately after exposure of the phase to the sample ($t=0$) and after completion of the extraction ($t=t_e$).	23
Figure 1-11 Schematic diagram of the diffusion-based calibration model for cylindrical geometry. The terms are defined in the text.	24
Figure 1-12 Use of SPME for in-needle time-weighted average sampling. a) adaptation of commercial SPME manual extraction holder, b) Schematic.....	27
Figure 2-1 Schematic of rapid extraction with a SPME fiber in cross flow.	37
Figure 2-2 Flow-through system for rapid direct sampling of standard aqueous BTEX solution using SPME.....	41
Figure 2-3 Schematic of experimental setup for indoor air sampling.....	44
Figure 2-4 Extraction time profiles of BTEX at concentration of 20.8 ng/mL and water velocity of 0.2 cm/s using a 75 μm CAR/PDMS fiber: Benzene, \diamond ; toluene, \square ; ethylbenzene, Δ ; o-xylene, \times	46

Figure 2-5 Extraction time profiles of BTEX at concentration of 20.8 <i>ng/mL</i> and water velocity of 0.2 <i>cm/s</i> using a 65 μm PDMS/DVB fiber. Benzene, \diamond ; toluene, \square ; ethylbenzene, Δ ; o-xylene, \times	47
Figure 2-6 Effects of water velocity on the adsorption of BTEX onto the 75 μm CAR/PDMS fiber for various sampling times and concentrations. Only error bars signifying +1 standard deviation from the mean of the sampling rate of benzene for various sampling times and concentrations are displayed for better view. Relative experimental errors of other compounds are comparable to those of benzene.	49
Figure 2-7 Validation of rapid SPME extraction of standard aqueous BTEX solution at concentration of 20.8 <i>ng/mL</i> and water velocity of 0.2 <i>cm/s</i> using model 1: benzene, \diamond ; toluene, \square ; ethylbenzene, Δ ; o-xylene, \times ; and model 2: benzene, \circ , $y = 1.31x - 0.07$, $R^2 = 0.993$; toluene, $+$, $y = 1.33x - 0.07$, $R^2 = 0.989$; ethylbenzene, $*$, $y = 1.24x - 0.06$, $R^2 = 0.987$; o-xylene, $-$, $y = 1.06x - 0.05$, $R^2 = 0.991$	53
Figure 2-8 Validation of rapid SPME extraction of standard aqueous BTEX solution at various sampling times, concentrations, and water velocities using model 2 (equation 2.3, benzene as the example). Only parts of data are presented because of limit of the space. 2.8 <i>ng/ml</i> , 0.7 <i>cm/s</i> , —; 2.8 <i>ng/ml</i> , 2.7 <i>cm/s</i> , \blacklozenge ; 4.9 <i>ng/ml</i> , 0.2 <i>cm/s</i> , \circ ; 4.9 <i>ng/ml</i> , 0.7 <i>cm/s</i> , $*$; 4.9 <i>ng/ml</i> , 1.5 <i>cm/s</i> , \blacktriangle ; 4.9 <i>ng/ml</i> , 2.7 <i>cm/s</i> , \times ; 4.9 <i>ng/ml</i> , 5.4 <i>cm/s</i> , \blacksquare ; 11.0 <i>ng/ml</i> , 0.2 <i>cm/s</i> , \diamond ; 11.0 <i>ng/ml</i> , 0.7 <i>cm/s</i> , \square ; 11.0 <i>ng/ml</i> , 2.7 <i>cm/s</i> , Δ ; 20.8 <i>ng/ml</i> , 0.2 <i>cm/s</i> , $+$; 20.8 <i>ng/ml</i> , 0.7 <i>cm/s</i> , $-$	54
Figure 2-9 Effect of temperature on the adsorption of BTEX onto the 75 μm CAR/PDMS fiber.....	56
Figure 2-10 Chromatograms obtained from monitoring toluene concentration in deionized water by a) headspace SPME and b) rapid SPME.	57
Figure 2-11 Concentration profiles of toluene in the deionized water determined by rapid SPME (\circ) and headspace SPME (\times).	58
Figure 2-12 Comparison of experimental and predicted mass uptakes of BTEX for rapid air sampling using a CAR/PMS fiber. Air velocity is 2.8 <i>cm/s</i>	59

Figure 2-13 Concentration profile of toluene determined from rapid SPME sampling in a chemistry laboratory. o : Rapid SPME sampling; — : TWA concentration calculated from rapid SPME sampling using equation 2.7; - - - : TWA concentration determined by SPME passive sampling; — — — : TWA concentration determined by the NIOSH method 1501.....	62
Figure 3-1 Schematic of the calibration of the extraction of hydrocarbons by the desorption of a standard from a SPME fiber coated with a liquid polymeric coating to an aqueous solution. A steady state of diffusion is assumed when the aqueous solution is agitated constantly. A linear concentration gradient is assumed in both the polymer and the boundary layers.....	69
Figure 3-2 Desorption time profiles of benzene (◇), toluene (□), ethylbenzene (Δ), and o-xylene (x). Desorption of BTEX from a 100 μm PDMS fiber into water at a rate of 0.25 cm/s (at 25 °C).....	77
Figure 3-3 The isotropy of absorption and desorption in SPME. Simultaneous absorption of toluene (x) and desorption of deuterated toluene (<i>d</i> -8) (o) onto and from a 100 μm PDMS fiber from and into water at a rate of 0.25 cm/s (at 25 °C). (▲) represents of the sum of $\frac{Q}{q_0}$ and $\frac{n}{n_0}$	79
Figure 3-4 Desorption of o-xylene from a 100 μm PDMS fiber into clean air at various flow velocities (at 25 °C).....	83
Figure 3-5 Desorption time profile of constant <i>a</i> : desorption of benzene (◇), toluene (□), ethylbenzene (Δ), and o-xylene (x) from a 100 μm PDMS fiber into water at a rate of 0.25 cm/s (at 25 °C).....	87
Figure 3-6 The dependence of mass transfer coefficient on the linear velocity of water. Error bars signify ±1 standard deviation from the mean of the mass transfer coefficient of benzene and o-xylene. Relative experimental errors of toluene and ethylbenzene are comparable to those of o-xylene.....	89
Figure 3-7 Validation of the calibration of uptake of PAHs (fluorene as the example) onto a 100 μm PDMS fiber by the use of desorption of a standard from the same fiber into a standard PAHs aqueous solution of 0.27cm/s at 25 °C. Experimental	

mass uptake vs. predicted mass uptake with benzene (\diamond), toluene (\square), ethylbenzene (Δ), and o-xylene (x) as the standard.	90
Figure 3-8 Calibration of the uptake of PAHs (fluorene as the example) onto a 100 μm PDMS fiber by the desorption of o-xylene from the same fiber into a standard PAHs aqueous solution at a rate of 1.2 cm/s (at 25 $^{\circ}\text{C}$), when the axis of the fiber is in different orientations to the flow direction of the standard solution.	91
Figure 3-9 The temperature dependence of constant a . Desorption of benzene (\diamond), toluene (\square), ethylbenzene (Δ), and o-xylene (x) from a 100 μm PDMS fiber into water at a rate of 0.25 cm/s at various temperatures. Relative experimental errors of ethylbenzene and o-xylene are comparable to those of toluene.	95
Figure 3-10 The temperature dependence of the mass transfer coefficient. Desorption of benzene (\diamond), toluene (\square), ethylbenzene (Δ), and o-xylene (x) from a 100 μm PDMS fiber into water at a rate of 0.25 cm/s at various temperatures. Error bars signify ± 1 standard deviation from the mean of the mass transfer coefficient of o-xylene. Relative experimental errors of other compounds are comparable to those of o-xylene.	96
Figure 3-11 Calibration of uptake of PAHs (fluorene as the example) onto a 100 μm PDMS fiber by the desorption of o-xylene from the same fiber into a standard PAHs aqueous solution at a rate of 0.25cm/s (at 15 (o) and 25 (x) $^{\circ}\text{C}$). (A) Desorption time profile of o-xylene. (B) Mass uptake profile of fluorene. —: prediction for 15 $^{\circ}\text{C}$; ---: prediction for 25 $^{\circ}\text{C}$	97
Figure 4-1 Continuous (15 min) and intermittent (15 min total) retracted-fiber exposure to the standard gas with a total of 15 min exposure to clean air.	108
Figure 4-2 Amounts (%) of analytes on PDMS-100, PDMS/DVB-65, and CAR/PDMS-75 fibers after intermittent exposure, relative to the amounts after continuous exposure.	109
Figure 4-3 Sampling rate determined by TWA passive sampling of <i>n</i> -hexane with PDMS-100, PDMS/DVB-65, and CAR/PDMS-75 fibers ($Z=0.48$ cm).	110
Figure 4-4 Relationship between face velocity and sampling rate ($Z=0.45$ cm).	113
Figure 4-5 TWA passive sampling of <i>n</i> -alkanes with a CAR/PDMS-75 fiber ($Z=1.47$ cm).	114

Figure 4-6 Plot of the dependence of experimental and theoretical R/D on the carbon number of each analyte for the CAR/PDMS-75 fiber (Z=1.47 cm).	115
Figure 4-7 Comparison of the sampling rates determined by use of a PDMS/DVB-65 fiber with a deactivated needle and a Carboxen-75 fiber with a stainless steel needle (Z=1.50 cm).	115
Figure 4-8 Relationship between sampling rate and diffusion path length.....	117
Figure 4-9 Effect of temperature on mass loading rate.....	119
Figure 4-10 Effect of relative humidity on TWA passive sampling of <i>n</i> -alkanes with a CAR/PDMS-75 fiber (Z=1.44 cm).	120
Figure 4-11 Effect of ozone on TWA sampling of <i>n</i> -alkanes with a CAR/PDMS-75 fiber (Z=1.42 cm).	121
Figure 4-12 Field testing. Comparison of results from use of a charcoal tube (NIOSH method1501) and SPME with a CAR/PDMS-75 fiber.	123
Figure 5-1 Schematic of the new SPME field sampler. Parts (a) and (b) are the fiber holder. Part (c) is a commercialized fiber assembly. Part (d-1) is the cross view of the adjustable cylinder, and Part (d-2) is the side view of the adjustable cylinder. Part (e) is the protecting shield. Part (e) is a replaceable Teflon cap.....	131
Figure 5-2 Operation of the new SPME field sampler. (a) is the status of standby, storage, or transportation. (b) is the status when the protecting shield is pulled outward and locked at the sampling position. (c-1) is the model for TWA sampling, and (c-2) is the model for grab sampling.	133
Figure 5-3 Introduction of the fiber into a GC injector. (a): the fiber is protected. (b): the protecting shield is removed. (c): exposure of the fiber.	134
Figure 5-4 Effect of storage temperature. A PDMS fiber was used. The storage time was 24 hours.	136
Figure 5-5 The reusability of a Teflon cap with the use of a PDMS fiber. The storage time was 24 hours at ~ 25 °C.	137
Figure 5-6 Test of adsorption of <i>n</i> -undecane onto deactivated needles. The sampling rates of Silicosteel were translated from reference 6.	143
Figure 6-1 Extraction modes of SPME and the corresponding calibration methods.....	148

Figure 6-2 Extraction modes of SPME when the fiber is extended outside its needle:

(a) direct extraction, (b) headspace extraction, (c) membrane-protected extraction.149

List of Tables

Table 1.1 Physical processes that obey the gradient-flux law.....	19
Table 2.1 Constant of equation 2.1 for the fiber in cross flow.....	38
Table 3.1 Distribution coefficients of BTEX between the PDMS coating* and water at various temperatures.	94

Chapter 1 Introduction

1.1 Field Analysis

The analyte concentrations in the field are usually too low to be detected directly by modern instruments. Modern instruments are also not compatible with the complex composition of the sample matrices in the field. An extraction step, including “clean up” procedures for very complex “dirty” samples, is often required to bring the analytes to a suitable concentration level for detection. The current state of the art in sample preparation techniques employs multi-step procedures involving large amounts of organic solvents, thus creating environmental and occupational hazards. For example, toxic chemical management and disposal are required when analyzing for the presence of organic pollutants in different matrices using conventional approaches such as Soxhlet extraction for solid samples, liquid-liquid extraction (LLE) for aqueous matrices, or the charcoal tube method with carbon disulfide desorption for gas analysis. To reduce the use of solvents, supercritical fluid extraction (SFE), solid-phase extraction (SPE), and sorbent traps were developed as less-solvent-consuming alternatives to Soxhlet extraction, LLE, charcoal tube, respectively. The evolution of extraction techniques followed, with single drop extraction, hot water extraction, and solid-phase microextraction (SPME). While the extraction techniques evolve towards less solvent consumption or solvent free, the applications of the extraction techniques are moving rapidly to on-site where the investigated systems are located.^{1,2}

Basically, there are four approaches for field analysis (Figure 1-1).¹⁻³ The most widely used is field sampling, followed by sample transportation, storage, preparation, and analysis in a laboratory. This approach, however, is costly and does not provide large data

sets of spatial distributions or temporal evolutions of the parameters of interest. In addition, delicate analyses, such as the determination of dissolved gases or trace compounds, are often prone to significant artifacts. Another disadvantage of this approach is that some samples, such as living plants, cannot be transported to the laboratory. The second approach is field sampling and sample preparation followed by sample/sampler transportation, storage, and analysis in laboratory. The amount of samples to be transported to laboratory is significantly reduced.

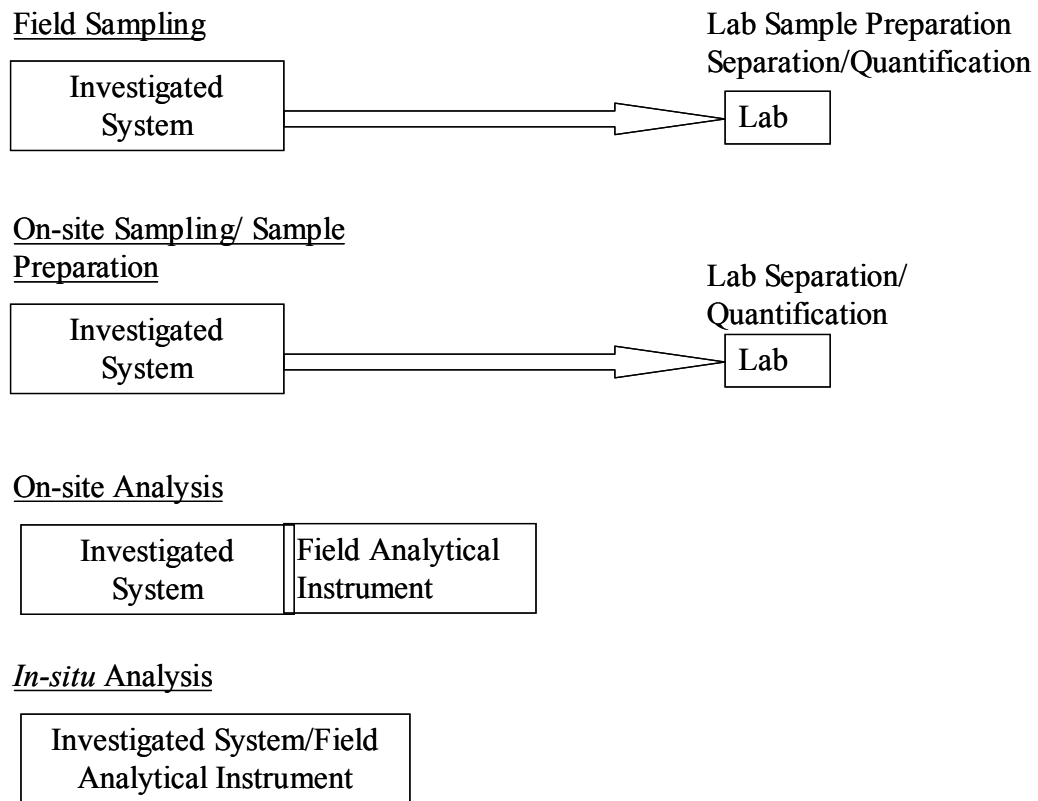


Figure 1-1 Field analysis.

Sometimes only samplers are transported to laboratory. However, loss of analytes and artifacts associated with sample transportation and storage are the main issues with this

approach. The third approach consists of performing the analysis directly at the field sites after manual or automatic sampling and sample preparation. This approach is called on-site analysis. It often uses laboratory procedures and instruments, adapted to site-specific conditions. On-site analyses approach the ideal of real-time measurement and minimize loss of analytes and appearance of artifacts associated with sample transportation and storage. In the fourth approach, measurements are made at the location of interest (e.g. at a certain depth in water, or within a sediment or soil). This approach is called *in-situ* analysis. It minimizes most of the artifacts, including those due to transportation and storage and those due to sampling and sample preparation, such as changes in pressure (e.g. gas evolution). It also allows for automatic real-time measurement, sometimes in locations difficult to access, such as great depths, or in environmental systems that should not be perturbed. Instruments and analytical procedures, however, should be specially developed for this purpose.

This thesis focuses on the development of calibration methods for quantitative on-site sampling and sample preparation using SPME, which is very important for the last three field analysis approaches described above.

1.2 Solid Phase Microextraction

SPME was developed to address the need for rapid sampling/sample preparation, both in the laboratory and on-site (in the field where the investigated system is located).⁴ It presents many advantages over conventional analytical methods by combining sampling, sample preparation, and direct transfer of the analytes into a standard gas chromatograph (GC), thus minimizing analyte losses due to multi-step processes. Since its introduction in

the early 1990s,⁵ SPME has been successfully applied to the sampling and analysis of environmental samples.⁶

Figure 1-2 shows the schematic of the first SPME device, which was implemented by incorporating coated fibers into a microsyringe.⁵ The metal rod, which serves as the piston in a microsyringe, is replaced with stainless steel microtubing with an inside diameter (i.d.) slightly larger than the outside diameter (o.d.) of the fused silica rod. Typically, the first 5 mm of the coating is removed from a 1.5 cm long fiber, which is then inserted into the microtubing. High temperature epoxy glue is used to permanently mount the fiber. The

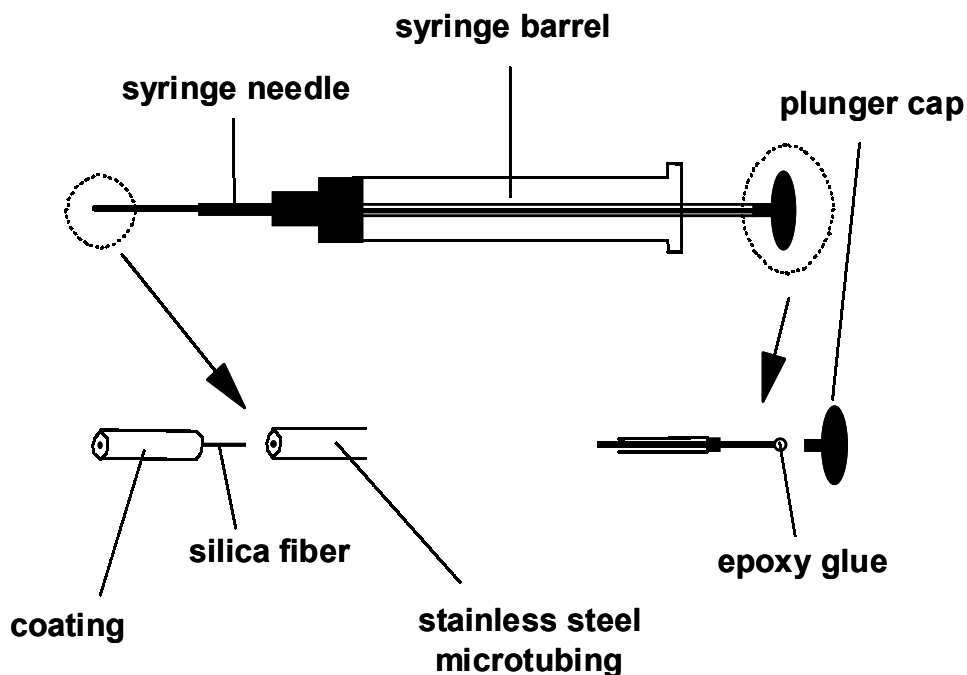


Figure 1-2 The custom-made SPME device based on the Hamilton 7000 series syringe.

coated fiber can be moved into and out of a stainless steel needle that serves the purposes of protecting the fiber when not in use and guiding the fiber into the injector. As demonstrated

herein, the needle can also serve a further purpose, specific to time-weighted average (TWA) passive sampling with SPME, which is, in fact, no more difficult than placing the coating inside the needle during sampling. This contrasts with conventional SPME, in which the coating is extended outside the needle and exposed directly to target analytes from a number of matrices, and the analytes then reach equilibrium with the coating.

Several different coatings are commercially available, including polydimethylsiloxane (PDMS), polyacrylate (PA), PDMS/divinylbenzene (PDMS/DVB), and Carboxen. The PDMS and PA coatings are a non-porous, amorphous polymeric phase whereas the PDMS/DVB and Carboxen are predominantly porous polymeric phases. Analyte uptake on PDMS and PA is by absorption whereas it is adsorptive for PDMS/DVB and Carboxen.

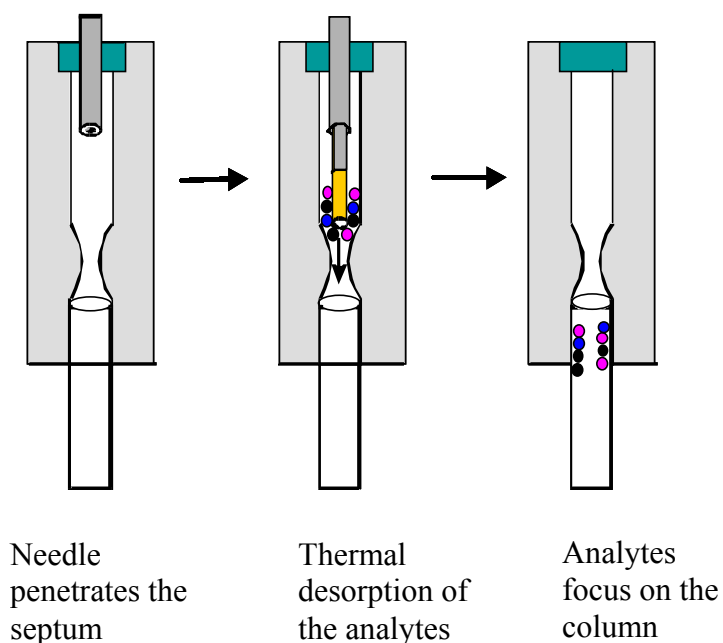


Figure 1-3 Thermal desorption of the analytes from a SPME fiber in a GC injector.

The use of SPME devices is very simple. When the plunger is depressed, the fiber is extended outside the needle and exposed to the sample matrix. After a certain amount of extraction time, the fiber is withdrawn into the needle. The needle is then introduced into the hot injector of a GC, where the analytes are thermally desorbed from the coating (Figure 1-3). The analytes then pass into the GC column for separation and quantification.

At this point it should be emphasized that one of the major advantages of SPME is that all of the sorbed analytes are analyzed. This is a significant advantage of SPME over traditional sampling methods, which only deliver small fractions of the total mass of the analytes collected. In addition, no solvent vehicle is used with SPME; background noise from the solvent is, therefore, absent. Narrower peak widths are also obtained, thus increasing the overall analytical efficiency. Other quite important advantages are that the SPME sampling system is fully re-usable and that when an SPME coating is analyzed it is immediately available for a subsequent sampling session (the coating is clean). SPME is also readily amenable to field portability and automation.⁷

Simplicity and convenience of operation make SPME a superior alternative to more established techniques for a number of applications. In some cases, the technique facilitates unique investigations. The most visible advantages of SPME exist at the extremes of sample volumes. Because the setup is small and convenient, coated fibers can be used to extract analytes from very small samples. For example, SPME devices are used to probe for substances emitted by a single flower bulb during its life span.⁶ Since SPME does not often extract target analytes exhaustively, its presence in a living system should not result in significant disturbance.⁸ In addition, the technique facilitates speciation in natural systems, since the presence of a minute fiber, which removes small amounts of analyte, is not likely to

disturb the chemical equilibrium in a system. It should be noted, however, that the fraction of analyte extracted increases as the ratio of coating to sample volume increases. Complete extraction can be achieved for small sample volumes when distribution constants are reasonably high. This observation can be important if exhaustive extraction is required. It is very difficult to work with small sample volumes using conventional sample preparation techniques. Also, SPME allows rapid extraction and transfer to an analytical instrument. These features result in an additional advantage when investigating intermediates in a system. An other advantage is that this technique can be used for studies of the distribution of analytes in a complex multiphase system,⁹ and allows for the speciation of different forms of analytes in a sample.¹⁰

1.3 Calibration in Solid Phase Microextraction

In SPME, a small amount of the extracting phase associated with a solid support is placed in contact with the sample matrix for a pre-determined time (Figure 1-4).

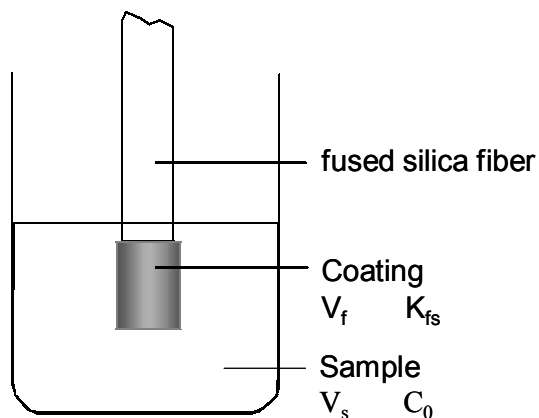


Figure 1-4 Microextraction with SPME. V_f , volume of fiber coating; K_{fs} , fiber/sample distribution coefficient; V_s , volume of sample; C_0 , initial concentration of analyte in the sample.

To date, there are several calibration approaches developed for SPME, as shown in Figure 1-5. Equilibrium extraction is the most frequently used method. When a sample volume is very small, exhaustive extraction might occur in SPME and can be used for calibration. To shorten long equilibrium extraction times, and/or address the displacement effects that occur when porous coatings are used, extraction can be interrupted before equilibrium, and calibration is still feasible if the agitation and the extraction time are kept constant. While performing derivatization/SPME, when the reaction is the rate-limiting step, the first-order reaction rate constant can be used for calibration. The last approach, the diffusion-based calibration method, is very important for field sampling. This method eliminates the use of conventional calibration curves. Fast on-site analysis and long-term monitoring are thus possible.

$$\text{Calibration in SPME} \left\{ \begin{array}{l}
 \text{Equilibrium extraction : } n = \frac{K_{fs} V_f V_s}{K_{fs} V_f + V_s} C_0 \\
 \text{Exhaustive extraction : } n = V_s C_0 \\
 \text{Pre - equilibrium extraction : } n = [1 - \exp(-at)] \frac{K_{fs} V_f V_s}{K_{fs} V_f + V_s} C_0 \\
 \text{First - order reaction rate constant : } v = K^* C_0 \\
 \text{Diffusion : } \left\{ \begin{array}{l}
 \text{Grab sampling : various empirical mass transfer correlations} \\
 \text{Time - weighed average sampling : Fick's First Law of Diffusion}
 \end{array} \right.
 \end{array} \right.$$

Figure 1-5 Various calibration methods in SPME.

1.3.1 Equilibrium Extraction

If the extraction time is long enough, a concentration equilibrium is established between the sample matrix and the extraction phase. When equilibrium conditions are

reached, exposing the fiber for a longer time does not result in the accumulation of more analytes. Typically, SPME extraction is considered to be complete when the analyte concentration has reached distribution equilibrium between the sample matrix and the fiber coating. The equilibrium conditions can be described by equation 1.1, according to the law of mass conservation, if only two phases, for example, the sample matrix and the fiber coating, are considered:¹¹

$$C_0V_s = C_s^\infty V_s + C_f^\infty V_f \quad \text{Equation 1.1}$$

where C_0 is the initial concentration of a given analyte in the sample, V_s is the sample volume, V_f is the fiber coating volume, C_s^∞ is the equilibrium concentration of analyte in the sample, C_f^∞ is the equilibrium concentration of analyte in the fiber. The fiber coating/sample matrix distribution coefficient K_{fs} is defined as:

$$K_{fs} = \frac{C_f^\infty}{C_s^\infty} \quad \text{Equation 1.2}$$

Combining equations 1.1 and 1.2, rearrangement results in:

$$n = \frac{K_{fs} V_f V_s}{K_{fs} V_f + V_s} C_0 \quad \text{Equation 1.3}$$

where n is the number of moles extracted by the coating. Equation 1.3 indicates that the amount of analyte extracted onto the coating (n) is linearly proportional to the analyte concentration in the sample (C_0), which is the analytical basis for quantification using SPME.

Strictly speaking, the above discussion is practically limited to partitioning equilibrium involving liquid polymeric phases such as PDMS. The method of analysis for solid sorbent coatings is analogous for low analyte concentrations, since the total surface area available for adsorption is proportional to the coating volume, if constant porosity of the

sorbent is assumed. For high analyte concentrations, saturation of the surface can occur, resulting in nonlinear isotherms. Similarly, high concentrations of a competitive interference compound can displace the target analyte from the surface of the sorbent.

Equation 1.3, which assumes that the sample matrix can be represented as a single homogeneous phase and that no headspace is present in the system, can be modified to account for the existence of other components in the matrix, by considering the volumes of the individual phases and the appropriate distribution constants.

In addition, when the sample volume is very large, i.e. $V_s \gg K_{fs}V_f$, equation 1.3 can be simplified to:

$$n = K_{fs}V_fC_0 \quad \text{Equation 1.4}$$

which points to the usefulness of the technique for field applications. In this equation, the amount of extracted analyte is independent of the volume of the sample. In practice, there is no need to collect a defined sample prior to analysis, as the fiber can be exposed directly to the ambient air, water, production stream, etc. The amount of extracted analyte will correspond directly to its concentration in the matrix, without being dependent on the sample volume. When the sampling step is eliminated, the whole analytical process can be accelerated, and errors associated with analyte losses through decomposition or adsorption on the sampling container walls will be prevented.

Equation 1.4 also implies another important quantification method for field sampling using SPME. That is, by knowing the distribution coefficient, the concentration of analyte can be determined by the amount of the analyte on the fiber under extraction equilibrium. In other words, quantification is possible without external calibrations. This is a very desirable feature for field analysis, because external calibrations slow down the analytical process, and

introduce additional errors. One of the applications of this approach is the determination of parameters like total petroleum hydrocarbons (TPH) in air.¹²

1.3.2 Exhaustive Extraction

As mentioned above, when the sample volume is very small, and the distribution coefficient is very large, such as sampling of semi-volatile organic compounds (semi-VOCs) in small volumes of a sample matrix, or sampling of VOCs in small volumes of a sample matrix using a cold fiber,¹³ V_s is far smaller than the product of $K_{fs}V_f$, and equation 1.3 can be simplified to:

$$n = V_s C_0 \quad \text{Equation 1.5}$$

This implies that all analytes in the sample matrix are extracted onto the fiber coating.

Calibration for exhaustive extraction is very simple, as suggested by equation 1.5. However, it is not often used in SPME because of the small volume of the extraction phase. Only when the volume of sample matrix is small is it possible to extract all analytes onto the fiber coating.

1.3.3 Pre-equilibrium Extraction

When a SPME fiber is exposed to the sample matrix, transportation of the analyte from the sample matrix to the fiber coating occurs. The time to reach the extraction equilibrium, ranging from minutes to hours, is dependent on the agitation conditions, the physicochemical properties of analytes and the fiber coating, and the physical dimensions of the sample matrix and the fiber coating. The amount of analyte extracted onto the fiber

coating is at a maximum when the equilibrium is reached, thus achieving highest sensitivity. If sensitivity is not a major concern of analysis, shortening the extraction time is desirable. In addition, the equilibrium extraction approach is not practical for solid porous coatings due to the displacement effect at high concentrations. For these circumstances, the extraction is stopped and the fiber is analyzed before the equilibrium is reached.

The kinetics of absorption of analytes onto a liquid fiber coating is described as:¹⁴

$$n = [1 - \exp(-at)] \frac{K_{fs} V_f V_s}{K_{fs} V_f + V_s} C_0 \quad \text{Equation 1.6}$$

where t is the extraction time, and a is a time constant, representing how fast an equilibrium can be reached.

When the extraction time is long, equation 1.6 becomes equation 1.3, characterizing equilibrium extraction. If the extraction equilibrium is not reached, equation 1.6 indicates that there is still a linear relationship between the amount (n) of analyte extracted onto the fiber and the analyte concentration (C_0) in the sample matrix, if the agitation, the extraction time, and the extraction temperature remain constant.

1.3.4 Calibration Based on First-Order Reaction Rate Constant

The main challenge in organic analysis is polar compounds. They are difficult to extract from environmental and biological matrices and difficult to separate on the chromatographic column. Derivatization approaches are frequently used to address these challenges. Figure 1-6 summarizes various derivatization techniques that can be implemented in combination with SPME.¹⁵ Some of the techniques, such as direct derivatization in the sample matrix, are analogous to well-established approaches used in solvent extraction. With

the direct technique, the derivatizing agent is first added to the sample vial. The derivatives are then extracted by SPME and introduced into the analytical instrument.

Because of the availability of polar coatings, the extraction efficiency for polar underivatized compounds is frequently sufficient to reach the sensitivity required. Occasionally, however, there are problems associated with the separation of these analytes. Good chromatographic performance and detection can be facilitated by in-coating derivatization following extraction. In addition, selective derivatization to analogues containing high detector response groups will result in enhancement of the sensitivity and selectivity of detection. Derivatization in the GC injector is an analogous approach, but it is performed at high injection port temperatures.

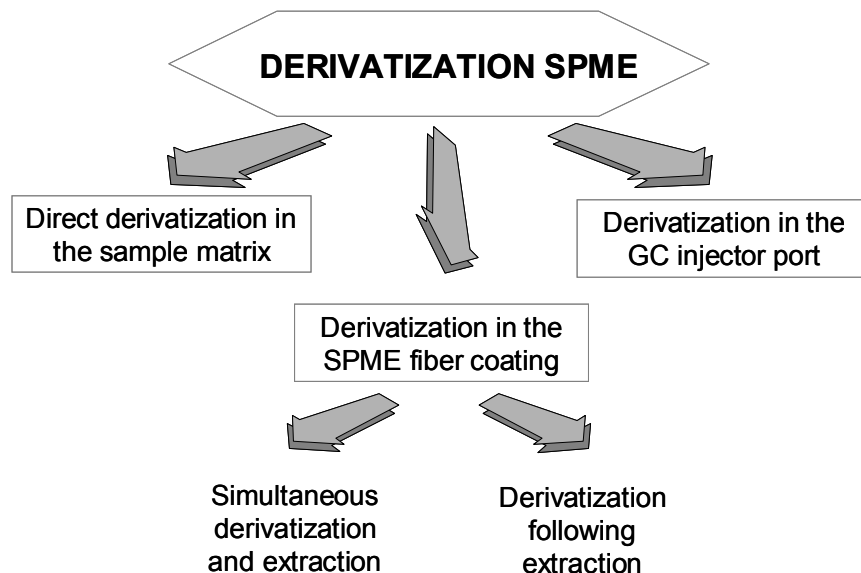


Figure 1-6 SPME derivatization techniques.

The most interesting and potentially very useful technique is simultaneous derivatization and extraction, performed directly in the coating. This approach allows for the high efficiencies and can be used in remote field applications. The simplest way to execute the process is to dope the fiber with a derivatization reagent and subsequently expose it to the sample (Figure 1-7). The analytes are then extracted and simultaneously converted to analogues that possess a high affinity for the coating. This is no longer an equilibrium process, since derivatized analytes are collected in the coating as long as the extraction continues.

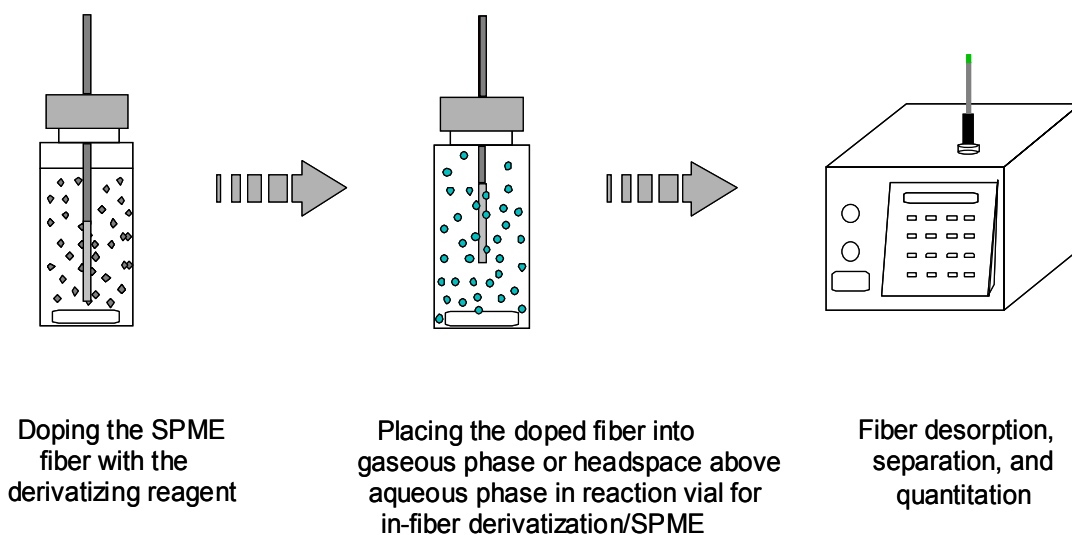


Figure 1-7 In-coating derivatization technique with fiber doping method.

It is emphasized that if the sorbent is almost completely coated with a derivatizing reagent before its exposure to the analyte, a reaction between the approaching gaseous analyte and the sorbed derivatizing reagent is more likely to occur. This is especially true for short exposure times. When the reaction is the rate-limiting step, the reaction rate v

(weight/time) is proportional to the concentration of gaseous analyte (C_0) and the rate constant of the reaction between the derivatization reagent and the analyte¹⁶

$$v = K^* C_0 \qquad \text{Equation 1.7}$$

Therefore, quantitative analyses of an unknown analyte concentration (C_0) is possible using an empirically determined constant K^* and equation 1.7.

This simple and efficient approach is limited to low volatility derivatizing reagents. The approach can be made more general by chemically attaching the reagent directly to the coating. The chemically bound product can then be released from the coating, either by a high temperature in the injector, light illumination, or a change of the applied potential. The feasibility of this approach was recently demonstrated by synthesizing standards bonded to silica-gel, which were released during heating. This approach allowed for solvent-free calibration of the instrument.¹⁷

In addition to using a chemical reagent, electrons can be supplied to produce redox processes in the coating and convert analytes to more favorable derivatives. In this application, the rod and the polymeric film must have good electrical conductivity. A similar principle has been used to extract amines onto a pencil "lead" electrode.¹⁸ The use of conductive polymers, such as polypyrrole, will introduce additional selectivity of the electrochemical processes associated with the coating properties.¹⁹

1.3.5 Calibration Based on Diffusion

1.3.5.1 Diffusion

Diffusion is the transport of a chemical substance in a material system consisting of two or more components, from area of higher concentration in the given phase towards those of lower concentration or, in non-ideal mixtures, of lower activity. The driving force of diffusion is the difference in the chemical potential of the diffusing substance that has the same sign as the difference in its concentrations, in the same phase and at a uniform and constant temperature throughout the system.²⁰

There are two mathematical methods to formulate transport by diffusion.^{21,22} The first, referred to as a *mass transfer model*, relates the net flux J to the occupation density difference between two adjacent subsystems, A and B:

$$J = -\text{constant} \cdot [\text{occupation density in B} - \text{occupation density in A}] \quad \text{Equation 1.8}$$

Fluxes are usually expressed as mass per unit area and per time ($\text{ng cm}^{-2} \text{s}^{-1}$), and the occupation density as mass per volume (ng cm^{-3}). Then the constant (mass transfer coefficient h) in the flux expression must have the dimension of a velocity (cm s^{-1}). Therefore, the mass transfer model takes the form:

$$J = -h (C_B - C_A) \quad \text{Equation 1.9}$$

The second model, the *gradient-flux law*, is considered to be more fundamental. In contrast to the mass transfer model, in which no assumption is made regarding the spatial separation of sub-systems A and B, in the gradient-flux law it is assumed that the sub-system and the distance between them, Δz , become infinitely small. Obviously, the difference in concentration tends toward zero. Yet the ratio of the two differences, concentration over Δz , is equal to the spatial gradient of the occupation density and usually different from zero:

$$J_z = -\text{constant} \frac{d}{dz}(\text{occupation density}) \quad \text{Equation 1.10}$$

where the minus sign indicates that the flux points against the gradient.

One well-known example of the gradient-flux law is Fick's first law, which relates the diffusive flux of a chemical to its concentration gradient and to the molecular diffusion coefficient:

$$J_z = -D \frac{dC}{dz} \quad \text{Equation 1.11}$$

where J_z is the mass flux per unit (cross-sectional) area and per time, D is molecular diffusivity, C is the concentration, and dC/dz is the spatial gradient of C along the Z direction. The molecular diffusivity (or molecular diffusion coefficient) D has the dimension (cm^2s^{-1}), and it depends on the diffusing chemical as well as on the medium through which it moves.

Considering the rectangular element of the volume of thickness $2\delta z$ in the z -direction, in Figure 1-8, the volume element has surface area A , normal to the diffusion flux, and is centred around the point P . δz is very small compared with z and the diffusion flux J_z varies only slightly over the distance $2\delta z$. If J_z is the diffusion flux through the plane BCDE at z ,

then under these conditions the inward flux through the plane JKLM at $z-\delta z$ is $J_z - \left(\frac{\partial J_z}{\partial z}\right)\delta z$.

Similarly, the outward diffusion flux through the plane FGHI at $z+\delta z$ is $J_z + \left(\frac{\partial J_z}{\partial z}\right)\delta z$. The

total rate of accumulation of the diffusing species within the volume element, in units of mass/time, is then:

$$\left[J_z - \left(\frac{\partial J_z}{\partial z} \right) \delta z - J_z - \left(\frac{\partial J_z}{\partial z} \right) \delta z \right] A = -2A \left(\frac{\partial J_z}{\partial z} \right) \delta z \quad \text{Equation 1.12}$$

Since $2A\delta z$ is the volume of the element, so that the time rate of change of concentration within the volume is:

$$\frac{\partial C}{\partial t} = - \frac{\partial J_z}{\partial z} \quad \text{Equation 1.13}$$

by applying Fick's first law of diffusion:

$$\frac{\partial C}{\partial t} = D \frac{\partial^2 C}{\partial z^2} \quad \text{Equation 1.14}$$

Equation 1.14 is often referred to as Fick's second law of diffusion, which states that the local concentration change with time, due to a diffusive transport process, is proportional to the second spatial derivative of the concentration.

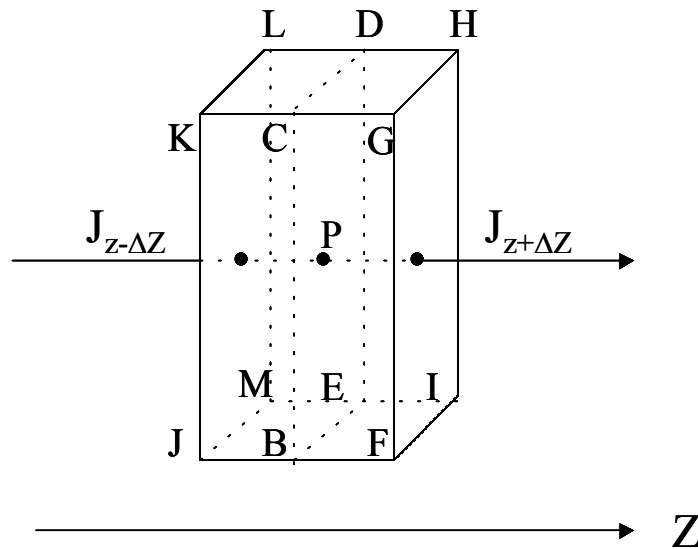


Figure 1-8 The derivation of Fick's Second Law of Diffusion.

As a special case, consider a linear concentration profile along the z-direction $C(z) = a_0 + a_1 z$. Since the second derivative of $C(z)$ of such a profile is zero, diffusion leaves

the concentrations along the z-direction unchanged. In other words, a linear profile is a steady-state solution of equation 1.14.

The relationship between the flux of a property and the spatial gradient of a related property called a gradient-flux law is typical for an entire class of physical processes, in which some physical quantity such as mass or energy or momentum or electrical charge is transported from one region of a system to another. For example, consider a metal bar connecting two heat reservoirs at different temperatures. Heat flows through the bar from the high-temperature reservoir to the low-temperature reservoir; the heat flow is the manifestation of the transport of energy through the bar. Another example is the transport of the electrical charge through a conductor by the application of an electrical potential difference between the ends of the conductor. Mass is transported in the flow of a fluid through a pipe due to the pressure difference between the ends of the pipe.

Table 1.1 Physical processes that obey the gradient-flux law.

Physical process	Law	Equation	Variables
Molecular diffusion	Fick	$J_z = -D \frac{dC}{dz}$	<i>J</i> : Mass flux <i>C</i> : Concentration <i>D</i> : Diffusion coefficient
Conduction of heat	Fourier	$J_z = -\kappa \frac{dT}{dz}$	<i>J</i> : Heat flux <i>T</i> : Temperature κ : Thermal conductivity
Electric conductivity	Ohm	$J_z = -k \frac{dV}{dz}$	<i>J</i> : Electrical current flux <i>V</i> : Voltage <i>k</i> : Electric conductivity

In all cases the flow, defined as the amount of the physical quantity transported in unit time through a unit of area perpendicular to the direction of flow, is proportional to the

gradient of other physical properties such as temperature, pressure, or electrical potential. Table 1.1 lists some physical processes obeying the gradient-flux law.²³

The similarity of molecular diffusion and conduction of heat and electric conductivity is very interesting and important to this work. The former analog provides the possibility of translation of various empirical correlations established for heat transfer to diffusion mass transfer, especially for the cases of ill-defined diffusion zones, such as the analog of heat transfer from bulk to a rod, to mass transfer from bulk to a fiber. Conduction of heat has been extensively studied due to industrial demands. The heat transfer literature is immense, far greater than the mass transfer literature. Mass transfer research may thus benefit from the vast resources of heat transfer research, as will be shown in this thesis.

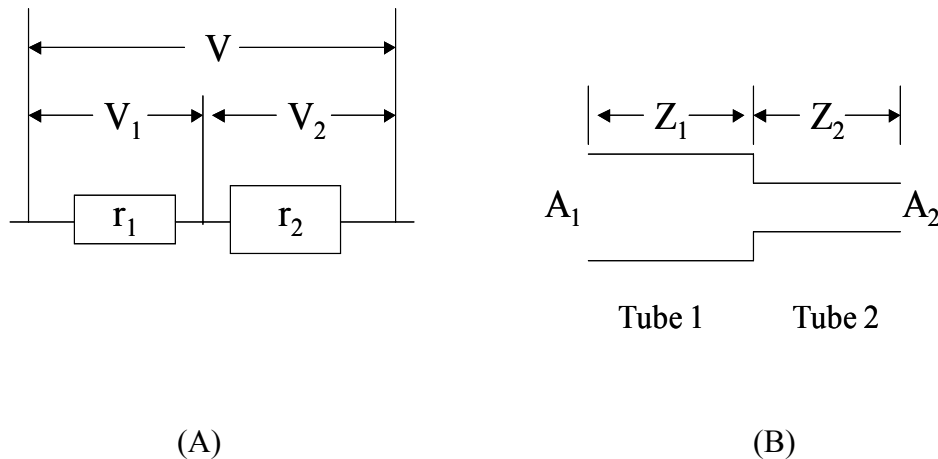


Figure 1-9 (A) Schematic of conduction of electricity through two resistances r_1 and r_2 , and (B) schematic of mass diffusion through two tubes.

The latter analog between molecular diffusion and electric conductivity provides insight for the design of samplers based on diffusion. Figure 1.9 shows the schematic of conduction of electricity through two resistances, r_1 and r_2 , and the schematic of mass diffusion through two tubes.

The current through the two resistances can be expressed as:

$$I = \frac{V_1}{r_1} = \frac{V_2}{r_2} = \frac{V}{r} \quad \text{Equation 1.15}$$

where I is in units of C/s , $r = r_1 + r_2$, and $r_1 = \frac{Z_1}{k_1 A_1}$, $r_2 = \frac{Z_2}{k_2 A_2}$, z_1 and z_2 are the length of the resistances of r_1 and r_2 , respectively, A_1 and A_2 are the cross sectional area of the resistances of r_1 and r_2 , respectively, k_1 and k_2 are the electric conductivity of the resistances of r_1 and r_2 , respectively, V_1 and V_2 are voltage drops along the resistances of r_1 and r_2 , respectively, and total voltage $V = V_1 + V_2$.

Analogously, the mass flow diffusion through tube 1 and tube 2 can be expressed as:

$$\frac{n}{t} = \frac{\Delta C_1}{\left(\frac{Z_1}{D_1 A_1}\right)} = \frac{\Delta C_2}{\left(\frac{Z_2}{D_2 A_2}\right)} = \frac{\Delta C}{\left(\frac{Z}{DA}\right)} \quad \text{Equation 1.16}$$

where n/t is mass flow in units of ng/s , ΔC_1 and ΔC_2 are concentration drops in tube 1 and 2, respectively, z_1 and z_2 are the length of tube 1 and tube 2, respectively, and A_1 and A_2 are the cross section area of tube 1 and tube 2, respectively. Correspondingly, $\frac{Z_1}{D_1 A_1}$ and $\frac{Z_2}{D_2 A_2}$ are the mass transfer resistances in tube 1 and tube 2, and the overall mass transfer resistance is:

$$\left(\frac{Z}{DA}\right) = \frac{Z_1}{DA_1} + \frac{Z_2}{DA_2} \quad \text{Equation 1.17}$$

Equation 1.17 has some important implications. First, the mass transfer resistance is proportional to the diffusion length, and inversely proportional to the diffusion coefficient and the cross sectional area of the diffusion zone. Second, the mass transfer resistance is additive. Further, when one mass transfer resistance is significantly larger than the other one,

the contribution from the small resistance is negligible. In other words, the larger resistance controls the overall mass transfer rate. The mass transfer can be predicted by knowing the larger resistance, and the change of the small resistance does not change the overall mass transfer rate significantly. This conclusion is extremely important for designing passive samplers.

1.3.5.2 Diffusion-Based Rapid SPME

There is a substantial difference between the performance of liquid and solid coatings. With liquid coatings, the analytes partition into the extraction phase, in which the molecules are solvated by the coating molecules. The diffusion coefficient in the liquid coating enables the molecules to penetrate the entire volume of the coating, within a reasonable extraction time if the coating is thin (see Figure 1-10 a). With solid sorbents (Figure 1-10 b), the coating has a glassy or a well-defined crystalline structure, which, if dense, substantially reduces the diffusion coefficients within the structure. Within the time of experiment, therefore, sorption occurs only on the pores of a solid phase and after long extraction times, compounds that exhibit a poor affinity toward the phase are frequently displaced by analytes that more strongly bind or those that are present in the sample at high concentrations. This is due to the limited surface area available for adsorption. If this area is substantially occupied, competition occurs and the equilibrium amount extracted can vary with the concentrations of both the target and other analytes.²⁴ In extraction with liquid phases, partitioning between the sample matrix and extraction phase occurs. Under these conditions, equilibrium extraction amounts vary only if the bulk coating properties are modified by the extracted components; this occurs only when the amount extracted is a

substantial proportion (a few percent) of the extraction phase, resulting in a possible source of non-linearity. This is rarely observed, because extraction/enrichment techniques are typically used for the analysis of trace contaminants.

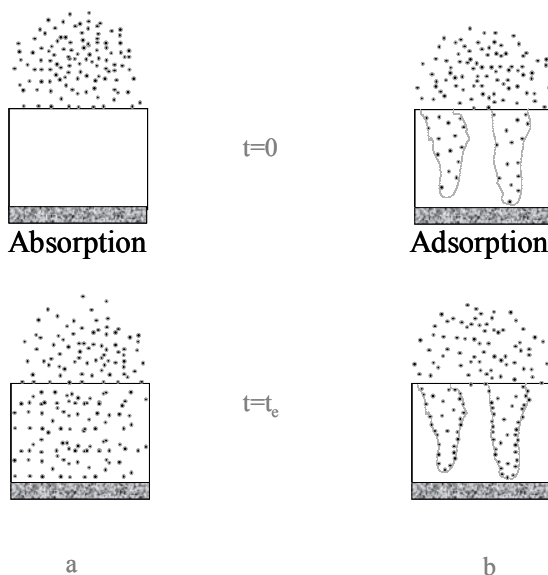


Figure 1-10 Extraction using absorptive (a) and adsorptive (b) extraction phases immediately after exposure of the phase to the sample ($t=0$) and after completion of the extraction ($t=t_e$).

One way to overcome this fundamental limitation of porous coatings in a microextraction application is through the use of an extraction time that is much less than the equilibration time. Thus the total amount of analytes accumulated by the porous coating is substantially less than the saturation value. When such experiments are performed, not only is it critical to precisely control the extraction times, but convection conditions must also be controlled, because they determine the thickness of the diffusion layer. One way of eliminating the need to compensate for differences in convection is to normalize (use consistent) agitation conditions. The short-term exposure measurement has an advantage in that the rate of extraction is defined by the diffusivity of analytes through the boundary layer

of the sample matrix and, thus, the corresponding diffusion coefficients rather than by distribution constants. This situation is illustrated in Figure 1-11 for a cylindrical geometry of the extraction phase dispersed on the supporting rod.

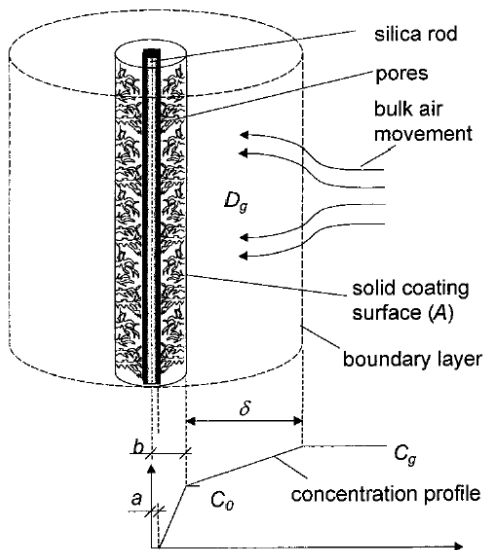


Figure 1-11 Schematic diagram of the diffusion-based calibration model for cylindrical geometry. The terms are defined in the text.

The analyte concentration in the bulk of the matrix can be regarded as constant when a short sampling time is used and there is a constant supply of analyte as a result of convection. The volume of the sample is much greater than the volume of the interface and the extraction process does not affect the bulk sample concentration. In addition, adsorption binding is frequently instantaneous and essentially irreversible. The solid coating can be treated as a “perfect sink“ for analytes. The analyte concentration on the coating surface is far from saturation and can be assumed to be negligible for short sampling times and the relatively low analyte concentrations. The analyte concentration profile can be assumed to be linear from C_g to C_0 .

The function describing the mass of the extracted analyte with the sampling time can be derived²⁵ by the use of the following equation:

$$n(t) = \frac{B_3 A D_g}{\delta} \int_0^t C_g(t) dt \quad \text{Equation 1.18}$$

where n is the mass of analyte extracted (ng) in a sampling time (t), D_g is the gas-phase molecular diffusion coefficient, A is the outer surface area of the sorbent, δ is the thickness of the boundary surrounding the extraction phase, B_3 is a geometric factor, and C_g is the analyte concentration in the bulk of the sample. It can be assumed that the analyte concentration is constant for very short sampling times and, therefore, equation 1.18 can be further reduced to:

$$n(t) = (B_3 D_g A / \delta) C_g t \quad \text{Equation 1.19}$$

It can be seen from equation 1.19 that the mass extracted is proportional to the sampling time, D_g for each analyte, and the bulk sample concentration and inversely proportional to δ . This is consistent with the fact that an analyte with a greater D_g will cross the interface and reach the surface of the coating more quickly. Values of D_g for each analyte can be found in the literature or estimated from physicochemical properties. This relationship enables quantitative analysis. As mentioned above, non-reversible adsorption is assumed. Equation 1.19 can be modified to enable estimation of the concentration of analyte in the sample for rapid sampling with solid sorbents:

$$C_g = n \delta / B_3 D_g A t \quad \text{Equation 1.20}$$

the amount of extracted analyte (n) can be estimated from the detector response.

The thickness of the boundary layer (δ) is a function of the sampling conditions. The most important factors affecting δ are the geometric configuration of the extraction phase, the

sample velocity, temperature, and D_g for each analyte. The effective thickness of the boundary layer can be estimated for the coated fiber geometry by the use of equation 1.21, an empirical equation adapted from the heat transfer theory:⁴

$$\delta = 9.52(b / Re^{0.62} Sc^{0.38}) \quad \text{Equation 1.21}$$

where Re is the Reynolds number $= 2u_s b / \nu$, u_s is the linear sample velocity, ν is the kinematic viscosity of the matrix, b is the outside radius of the fiber coating, and Sc is the Schmidt number $= \nu / D_s$. The effective thickness of the boundary layer in equation 1.21 is a surrogate (or average) estimate and does not take into account changes of the thickness that can occur when the flow separates, when a wake is formed, or when both occur. Equation 1.21 indicates that the thickness of the boundary layer will decrease with increasing linear sample velocity. Similarly, when the sampling temperature (T_s) increases, the kinematic viscosity decreases. Because the kinematic viscosity term is present in the numerator of Re and in the denominator of Sc , the overall effect on δ is small. Reduction of the boundary layer and an increased rate of mass transfer for the analyte can be achieved in two ways—by increasing the sample velocity and by increasing the sample temperature. Increasing the temperature will, however, reduce the efficiency of the solid sorbent (reduce K). As a result, the sorbent coating might not be able to adsorb all of the molecules reaching its surface and it might, therefore, stop behaving as a “perfect sink“ for all of the analytes.

1.3.5.3 Time-Weighted Average Passive Sampling

Consideration of different arrangements of the extraction phase is beneficial. For example, extension of the boundary layer by a protective shield that restricts convection would result in a time-weighted average measurement of the analyte concentration. A variety

of diffusive samplers have been developed based on this principle. One system consists of an externally coated fiber with the extraction phase withdrawn into the needle (Figure 1-12).

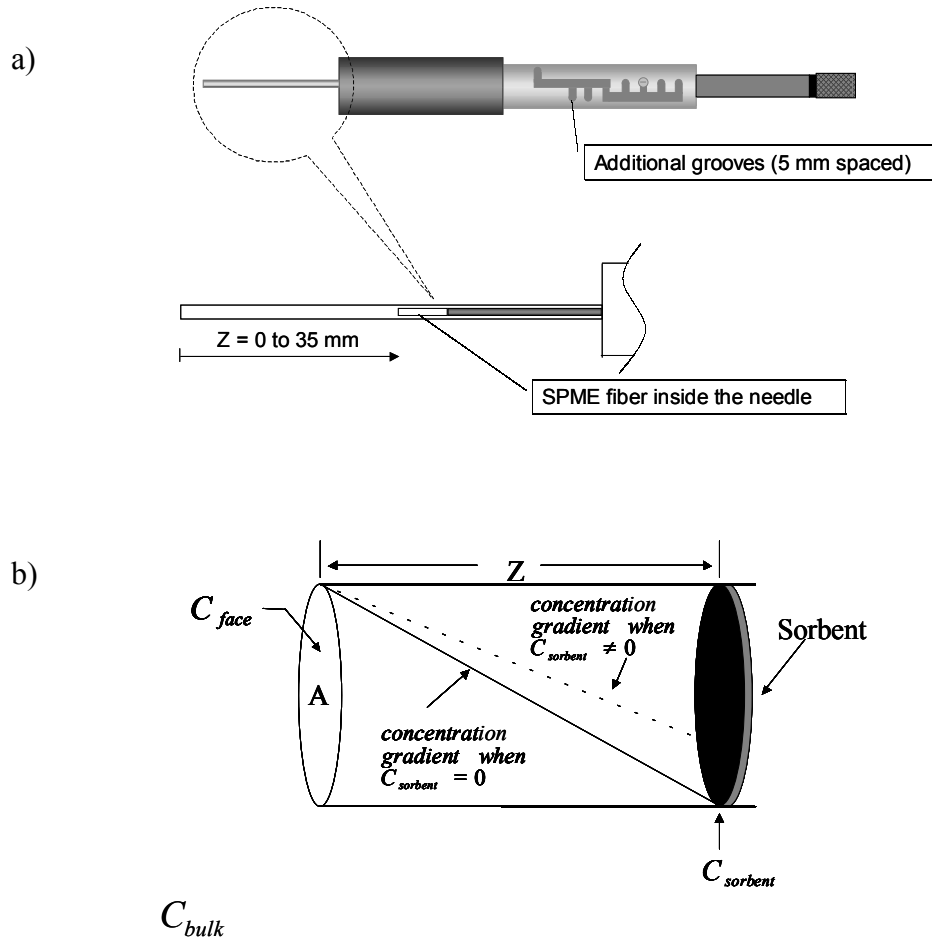


Figure 1-12 Use of SPME for in-needle time-weighted average sampling. a) adaptation of commercial SPME manual extraction holder, b) Schematic.

When the extraction phase in an SPME device is not exposed directly to the sample, but is contained within protective tubing (a needle) without any flow of sample through it, diffusive transfer of analytes occurs via the static sample (gas phase or other matrix) trapped in the needle. This geometric arrangement is a very simple method, capable of generating a response proportional to the integral of the analyte concentration over time and space (when

the needle is moved through space).²⁶ Under these conditions, the only mechanism of analyte transport to the extracting phase is diffusion through the matrix contained in the needle.

The basic process of analyte uptake by the SPME passive sampler can be described by Fick's first law of diffusion (equation 1.11), where J , defined as $\frac{dn}{A dt}$, describes the flux of the analyte:

$$\frac{dn}{A dt} = -D \frac{dc}{dZ} \quad \text{Equation 1.22}$$

where dn is the amount of the analyte passing through a cross-sectional area A during a sampling period dt . dn is proportional to the linear concentration gradient in the sampler (dc/dZ) and the analyte diffusion coefficient D . For a given sampler, both the cross sectional area A and the diffusion path length Z are constant. When sampling reaches the steady state:

$$\frac{dc}{dZ} = \frac{\Delta C}{Z} = \frac{C_{sorbent} - C_{face}}{Z} \quad \text{Equation 1.23}$$

If the sorbent has a large capacity and strong affinity for target analytes, acting as a zero sink, $C_{sorbent}$, the concentration of the analyte at the sorbent/gas interface, is negligible. In these circumstances, equation 1.23 reduces to:

$$\frac{dc}{dZ} = \frac{-C_{face}}{Z} \quad \text{Equation 1.24}$$

If C_{face} , the analyte concentration at the opening, is equal to C_{bulk} (the bulk analyte concentration), which is true when the sampled matrix is well agitated, then:

$$\frac{dc}{dZ} = \frac{-C_{bulk}}{Z} \quad \text{Equation 1.25}$$

Substituting equation 1.25 into equation 1.22, we obtain, after rearrangement:

$$dn = \frac{AD}{Z} C_{bulk} dt \quad \text{Equation 1.26}$$

Because the dimensions of the expression $\frac{AD}{Z}$ are $\text{cm}^3 \text{min}^{-1}$, it is defined as a formal sampling rate R :

$$R = \frac{AD}{Z} \quad \text{Equation 1.27}$$

This definition indicates that the sampling rate, R , is proportional to the cross-sectional area, A , and the analyte diffusion coefficient, D , and inversely proportional to the diffusion path length, Z . Combining equations 1.26 and 1.27 yields equation 1.28:

$$dn = RC_{bulk} dt \quad \text{Equation 1.28}$$

and after integration of both sides over time, equation 1.28 reduces to:

$$n = R \int_{t_1}^{t_2} C_{bulk} dt \quad \text{Equation 1.29}$$

which describes the passive sampler response to a transient concentration of an analyte as a function of time. For a constant analyte concentration, equation 1.29 reduces to:

$$n = RC_{bulk} t \quad \text{Equation 1.30}$$

or

$$R = \frac{n}{C_{bulk} t} \quad \text{Equation 1.31}$$

Equation 1.30 indicates that the rate of uptake of analyte mass by the passive sampler (n/t) is directly proportional the sampling rate of the sampler (R) and the bulk analyte concentration.

According to equation 1.27, the sampling rate, R , will be a constant for a given analyte and passive sampler, and can be determined theoretically. Sometimes, however, it is

difficult to determine R theoretically, especially when the diffusion coefficient is not available. In these circumstances equation 1.31 indicates that an empirical approach can be used — the mass loading, n , is determined during a sampling period, t , at a constant concentration C_{bulk} . When R is determined, it can be used to quantify the unknown analyte concentrations by use of equation 1.32:

$$C_{bulk} = \frac{n}{Rt} \quad \text{Equation 1.32}$$

it is in this way that the SPME device can be used practically as a passive sampler.

It should be emphasized that equation 1.32 is valid only when the amount of analyte extracted on to the sorbent is a small fraction (below the RSD of the measurement, typical 5%) of the equilibrium amount for the lowest concentration in the sample. To extend integration times, the coating can be placed further into the needle (larger Z), the opening can be reduced by placing an additional orifice over the needle (smaller A), or a higher capacity sorbent can be used. The first two solutions will result in low measurement sensitivity. Increasing the sorbent capacity is a more attractive proposition. It can be achieved either by increasing the volume of the coating or by changing its affinity for the analyte. Because increasing the coating volume would require an increase in the size of the device, the optimum approach to increasing the integration time is to use sorbents characterized by large distribution constants. If the matrix filling the needle is something other than the sample matrix, an appropriate diffusion coefficient should be used in equations 1.26 and 1.27.

In the system described, the length of the diffusion channel can be adjusted to ensure that mass transfer in the narrow channel of the needle controls overall mass transfer to the extraction phase, irrespective of the convection conditions.²⁷ This is a very desirable feature of TWA sampling, because the performance of this device is independent of the flow

conditions in the system investigated. This is difficult to ensure for high surface area membrane permeation-based TWA devices, such as, for example, a passive diffusive badge²⁸ and semi-permeable membrane devices.²⁹ For analytes characterized by moderate to high distribution constants, mass transport is controlled by the diffusive transport in the boundary layer. The performance of these devices therefore depends on the convection conditions in the investigated system.³⁰

1.4 Thesis Objective

The overall objective of this thesis is to develop calibration methods for quantitative on-site sampling and sample preparation using SPME. The fundamental base for the calibration focuses on diffusion mass transfer.

1.5 References

¹ Pawliszyn, J. *Anal. Chem.* **2003**, 75, 2543-2558.

² Pawliszyn, J., Ed. *Sampling and Sample Preparation for Field and Laboratory*. Elsevier, Amsterdam. 2002.

³ Buffle, J. and Horvai, G., Ed. *In Situ Monitoring of Aquatic Systems Chemical Analysis and Speciation*. John Wiley & Sons, Ltd., Chichester. 2000.

⁴ Pawliszyn, J. *Solid Phase Microextraction – Theory and Practice*; Wiley – VCH; New York, 1997.

⁵ Arthur, C. L. and Pawliszyn, J. *Anal. Chem.*, **1990**, 62 2145.

-
- ⁶ Pawliszyn, J. (ed.); *Applications of Solid Phase Microextraction*; RSC; Cambridge, UK, 1999.
- ⁷ Müller, L.; Górecki, T. and Pawliszyn, J. *Fresenius J. Anal. Chem.*, **1999**, 364, 610.
- ⁸ Lord, H. L.; Grant, R. P.; Walles, M.; Incedon, B.; Fahie, B.; and Pawliszyn, J. *Anal. Chem.*, **2003**, 75, 5103-5115.
- ⁹ Poerschmann, J.; Kopinke, F-D; and Pawliszyn, J. *Environ. Sci. Technol.*, **1997**, 31, 3629.
- ¹⁰ Mester, Z. and Pawliszyn, J. *Rapid Commun. Mass Spectrom.*, **1999**, 13, 1999.
- ¹¹ Louch, D.; Motlagh, S.; and Pawliszyn, J. *Anal. Chem.*, **1992**, 64, 1187.
- ¹² Martos, P. and Pawliszyn, J. *Anal. Chem.* **1997**, 69, 206.
- ¹³ Zhang, Z. and Pawliszyn, J. *Anal. Chem.* **1995**, 67, 34.
- ¹⁴ Ai, J. *Anal. Chem.* **1997**, 69, 1230.
- ¹⁵ Pan, L. and Pawliszyn, J. *Anal. Chem.*, **1997**, 69, 196.
- ¹⁶ Martos, P. and Pawliszyn, J. *Anal. Chem.*, **1998**, 70, 2311.
- ¹⁷ Konieczka, P.; Wolska, L.; Luboch, E.; Namiesnik, J.; Przyjazny, A.; and Biernat, J. *J. Chromatogr. A*, **1996**, 742, 175.
- ¹⁸ Conte, E.D. and Miller, D.W. *J. High Resolut. Chromatogr.*, **1996**, 19, 294.
- ¹⁹ Wu, J. and Pawliszyn, J. *Anal. Chem.* **2001**, 73, 55.
- ²⁰ Erdey-Gruz, T. *Transport Phenomena in Aqueous Solutions*; John Wiley & Sons, New York, 1974.
- ²¹ Cussler, E.L., *Diffusion: mass transfer in fluid systems*. New York: Cambridge University Press, 1997.
- ²² Schwarzenbach, Rene P., *Environmental Organic Chemistry*, Wiley: New York, 2003.

-
- ²³ Castellan, G. W. *Physical Chemistry*. 2nd Ed. Addison-Wesley Publishing Company, Massachusetts, 1971.
- ²⁴ Ruthven, D. *Principles of Absorption and Adsorption Processes*, Wiley: New York, 1984.
- ²⁵ Carslaw H. and Jaeger, J. *Conduction of Heat in Solid*, Clarendon Press: Oxford, 1986.
- ²⁶ Chai M. and Pawliszyn, J. *Environ. Sci. Technol.*, **1995**, 29, 693.
- ²⁷ Chen Y. and Pawliszyn, J. *Anal. Chem.*, **2003**, 75, 2004.
- ²⁸ Koziel, J. Sampling and Sample Preparation for Indoor Air Analysis. In *Sampling and Sampling Preparation for Field and Laboratory*, J. Pawliszyn, Ed.; Elsevier: Amsterdam, 2002.
- ²⁹ Petty, J.; Orazion, C.; Huckins, J.; Gale, R.; Lebo, J.; Echols, K.; and Cranor, W. J. *Chromatogr. A*, **2000**, 879, 83.
- ³⁰ B. Vrana and G. Schuurmann, *Environ. Sci. Technol.*, **2002**, 36, 290.

Chapter 2 Rapid Solid Phase Microextraction

2.1 Introduction

Exposure of a SPME fiber to an aqueous sample containing volatile organic compounds (VOCs) enables concentration of analytes in a solvent-free environment.¹ Typical quantification utilizes equilibrium-based approach where extractions are completed when equilibrium is achieved between the sorbed analyte in the fiber coating and analyte dissolved in the sample. This type of extraction using SPME fibers, such as polydimethylsiloxane (PDMS), extracting via absorption is well described in the literature.¹ The extracted amount of analyte at equilibrium, n , is related to its concentration in a sample, the volume of the fiber coating, and the fiber/matrix distribution constant, K_{fs} .¹ Estimation of the distribution constant for each analyte may be obtained either from extractions performed on standard solutions of the analyte, from physicochemical properties, from literature, or by calculating chromatographic retention data.² Pre-equilibrium extraction can also be used for quantitative analysis with both liquid and solid SPME coatings.³

With adsorptive coatings, extracted amounts and hence sensitivity (particularly for very volatile organic compounds) are greater when compared to absorptive-type SPME fibers.^{4,5} When using SPME fibers coated with single or mixed porous solid adsorptive coatings such as Carboxen/PDMS (CAR/PDMS) and PDMS/divinylbenzene (PDMS/DVB), the use of equilibrium-based calibration is not practical for high concentrations. This is because of the problems related to limited sorbent coating capacity and competition between analytes for available coating surface and subsequent inter-analyte displacement.^{5,6} These

problems complicate and often preclude quantification, particularly in cases when field or unknown samples are analyzed, with porous SPME fibers.

An alternative approach to quantification is to use very short sampling times for which the coating can be initially assumed to be a zero sink, or perfect sorbent, while the extraction is diffusion-controlled.⁷ Rapid SPME extractions can be modeled using a concept of a boundary layer between the bulk of a sample and the fiber surface, and the mass transfer from boundary layer to the surface of the fiber is controlled via diffusion.^{7,8,9} In cases of short sampling times, the molecular diffusion of analytes across the boundary layer is the extraction-limiting step. The boundary layer thickness (δ) depends on the physical dimensions of the fiber coating, the sample flow conditions, and analyte physicochemical properties. Steady-state flow of a sample around a SPME fiber allows the boundary layer to be maintained, and as a consequence, the extraction process can be calibrated based on diffusion. This model, which uses a very simple and ideal physical process to approximate a complex one, is fundamentally important, and provides a clear picture of rapid SPME extraction.

This rapid extraction approach has been developed and tested for air sampling^{7,8} and applied to rapid water VOCs sampling using PDMS/DVB coatings.⁹ However, there are some limitations with the work mentioned above. It has been shown that analyte displacement during SPME extractions occurred even for short sampling times as small as 1 min when PDMS/DVB coatings were used.⁹ This was likely caused by the limited capacity of the coating. It was postulated that this limitation could be overcome by using SPME coatings with stronger affinities and larger extraction capacities for VOCs, such as CAR/PDMS. However, unpublished data suggested that there was a significant difference

between theoretical and experimental mass uptakes even when CAR/PDMS coatings were used.¹⁰ Then it was questioned whether the use of the empirical equation — equation 6 in reference 9 — to calculate the velocity of the sample flowing around the fiber was appropriate. Since experimental determination of the linear velocity of the sample agitated in a vial proved to be difficult, a flow-through system, where the velocity of the sample is easily controlled and known, has to be used.

In this work, rapid SPME extractions of benzene, toluene, ethylbenzene, and o-xylene (BTEX) from the flow-through system with PDMS/DVB 65 μm and CAR/PDMS 75 μm fibers were tested. Parameters that affect the extraction process, including sampling time, concentration, water velocity, and temperature, were investigated. A new physical model analogous to heat transfer to a circular cylinder in cross flow was used to describe the rapid SPME extraction of VOCs in aqueous samples. A simple empirical correlation to this new model was used to predict the mass transfer coefficient. The new model was also tested for rapid air sampling.

2.2 Theory

When a SPME fiber is exposed to fluid samples, mass transfer from the bulk to the fiber occurs in the same way as heat transfer from bulk to a circular cylinder in cross flow.⁷ Thus, the mass transfer associated with rapid SPME extraction in fluid samples can be described as follows. As shown in Figure 2-1, when a SPME fiber is exposed to a fluid sample whose motion is normal to the axis of the fiber, the fluid is brought to rest at the forward stagnation point from which the boundary layer develops with increasing x under the influence of a favorable pressure gradient. At the separation point, downstream movement is

checked because fluid near the fiber surface lacks sufficient momentum to overcome the pressure gradient. In the meantime, the oncoming fluid also precludes reverse flow upstream. Boundary layer separation thus occurs, and a wake is formed downstream, where flow is highly irregular and can be characterized by vortex formation. Correspondingly, the thickness of the boundary layer (δ) is at a minimum at the forward stagnation point. It increases with the increase of x and reaches its maximum value right after separation point. At the rear of the fiber, where a wake is formed, δ decreases again.

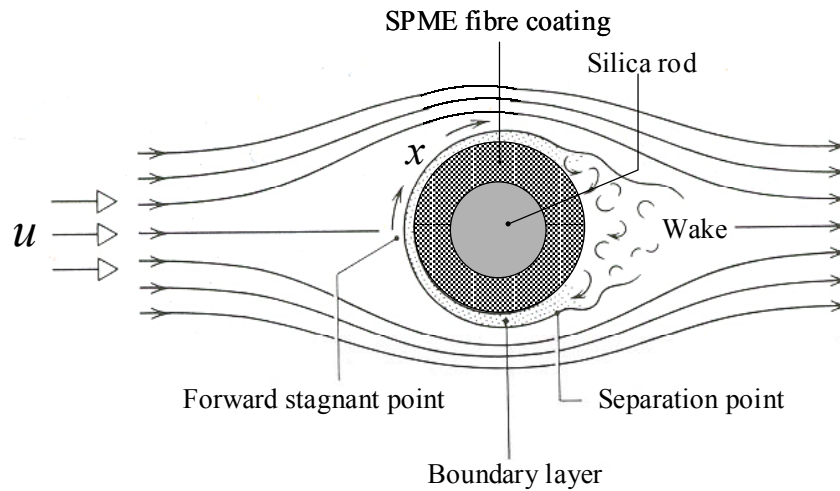


Figure 2-1 Schematic of rapid extraction with a SPME fiber in cross flow.

Although the theoretical description for this process is very complex, empirical correlations with good precision are readily available.¹¹ Often heat transfer can be translated into a mass transfer solution by replacing temperatures with concentrations, heat flux with mass flux and thermal conductivity with molecular diffusion coefficient. According to Hilpert,^{12,13} the average Nusselt number \overline{Nu} can be estimated by the use of equation 2.1 where the Prandtl number is replaced by Schmidt number:

$$\left(\overline{Nu} \equiv \frac{\bar{h}d}{D} \right) = E Re^m Sc^{1/3} \quad \text{Equation 2.1}$$

where \bar{h} is average mass transfer coefficient, d is the outside diameter of the fiber, D is diffusion coefficient, Re is the Reynolds number ($Re = ud/\nu$); u is the linear velocity of the sample, ν is the kinematic viscosity of the matrix media at the extraction temperature, and Sc is the Schmidt number ($Sc = \nu/D$). Constants E and m are dependent on Reynolds number and are listed in table 2.1.^{12,13}

Table 2.1 Constant of equation 2.1 for the fiber in cross flow

Re	E	m
1-4	0.989	0.330
4-40	0.911	0.385
40-4000	0.683	0.466
4000-40,000	0.193	0.618
40,000-250,000	0.027	0.805

When \overline{Nu} is estimated from the empirical correlation, the average mass transfer coefficient \bar{h} is readily calculated from the definition of \overline{Nu} ($\overline{Nu} \equiv \frac{\bar{h}d}{D}$). The amount of extracted analytes dn during sampling period dt can then be calculated by the following equation:

$$dn = \bar{h}A \int_0^t (C_{bulk} - C_{sorbent}) dt \quad \text{Equation 2.2}$$

where A is the surface area of the fiber, C_{bulk} is bulk analyte concentration, and $C_{sorbent}$ is analyte concentration at the interface of the fiber surface and samples of interest. If the sorbent is highly efficient toward target analytes and also is far away from equilibrium, it can

be treated as a 'zero sink'. In other words, $C_{sor bent}$ is assumed to be 0. Under constant bulk analyte concentration, integration of equation 2.3 results in:

$$n = \bar{h}AC_{bulk}t \quad \text{Equation 2.3}$$

Inspection of equation 2.3 shows that the product of $\bar{h}A$ has the units of cm^3/s , which corresponds to the sampling rate used in active and passive sampling while the product of $\bar{h}C_{bulk}$ is the mass flux ($\text{ng}/\text{cm}^2/\text{s}$) towards the fiber.

Rearrangement of equation 2.3 results in:

$$C_{bulk} = \frac{n}{\bar{h}At} \quad \text{Equation 2.4}$$

Equation 2.4 indicates that the concentration of samples can be determined by the mass uptake n onto a SPME fiber during sampling period t when $\bar{h}A$ is known.

2.3 Experimental Section

2.3.1 Chemicals and Supplies

All chemicals were of analytical grade and used as supplied: benzene, toluene, ethylbenzene, and o-xylene (BTEX) were from Sigma-Aldrich (Mississauga, ON, Canada) and HPLC grade methanol was from BDH (Toronto, ON, Canada). The SPME holders, 65 μm PDMS/DVB, and 75 μm CAR/PDMS fibers were obtained from Supelco (Oakville, ON, Canada). The fibers were conditioned at 250°C for 1 h prior to their use. All preparations involving toluene, ethylbenzene, and *p*-xylene (flammable and toxic) and benzene (suspected carcinogen) were carried out in a ventilated fume hood.

2.3.2 Flow-Through System

Figure 2-2 shows the schematic of the flow-through system, which consists of a mixing chamber and a long sampling cylinder with three different diameters (Glass Shop, University of Waterloo, ON, Canada). Generation of standard BTEX aqueous solution is based on the dilution of standard BTEX methanolic solution, which was pre-filled in a 50 mL syringe (Hamilton, Reno, NV) and delivered by a syringe pump (Razel, Stamford, CT), with water (BTEX-free tap water was directly used without purification). A wide range of concentrations of the BTEX aqueous solution can be obtained by varying the concentration of standard BTEX methanolic solution, the delivering rate of the pump, water flow rate, or all. The concentrations of the BTEX aqueous solution can be theoretically calculated by knowing the concentration of standard BTEX methanolic solution, the delivering rate of the pump, and water flow rate. Practically, the concentrations of the standard BTEX aqueous solution were validated by headspace-SPME:¹ 25 mL of the effluent was collected in a 40 mL of vial capped with a phenolic screw cap and PTFE-coated silicone septa (Supelco), a 1” (2.54 cm) PTFE-coated stirring bar (Supelco) was used to agitate the solution at 1200 rpm (model 400S digital magnetic stirrer from VWR Scientific, West Chester, PA), a PDMS 100 μm fiber (Supelco) was used to sample BTEX in the headspace for 2 min followed by introducing the fiber into a GC injector for desorption, separation, and quantification.

The generated standard BTEX aqueous solution then entered the sampling cylinder. The same solution experienced different linear velocities due to the different diameters of each section of the sampling cylinder. The average water linear velocities (u) were calculated by dividing the volumetric flow rate of water by the cross-sectional area of each section of the sampling cylinder. A wide range of linear velocities can be generated depending on the

cross-sectional area of each section of the sampling cylinder and water flow rate. Sampling was performed in each section of the sampling cylinder by piercing through the Thermogreen septum (Supelco) with the fiber needle, then exposing the fiber coating to the standard solution for short times.

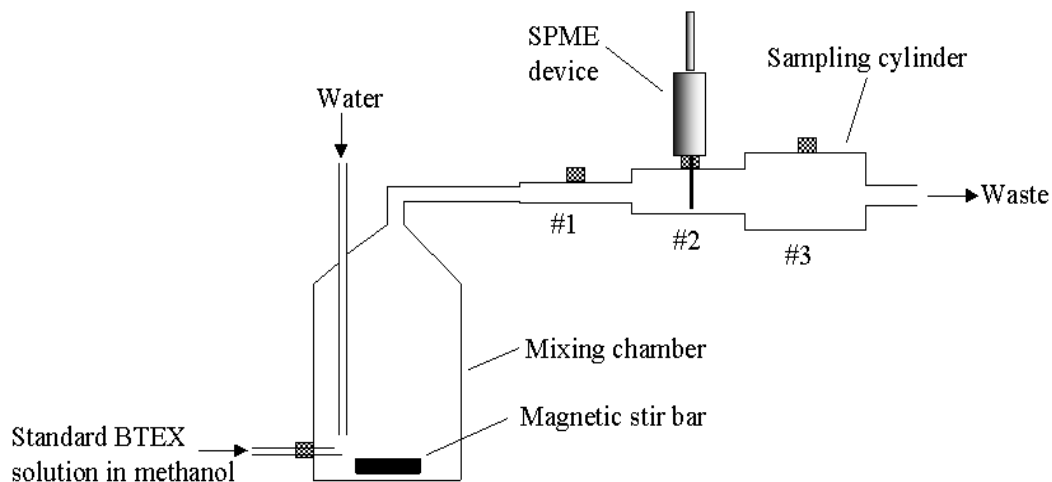


Figure 2-2 Flow-through system for rapid direct sampling of standard aqueous BTEX solution using SPME.

An OmegaluxTM 520 W heating tape (Omega, Stamford, CT) was wrapped around the mixing chamber and connected to an electronic heat control device (Science Shop, University of Waterloo, Ontario, Canada) to provide a controlled temperature environment. An OmegaTM K-type thermocouple and thermometer were used to measure the temperature of the standard aqueous solution. The temperature of the standard solution was controlled at $15 \pm 0.5^\circ\text{C}$.

2.3.3 Monitoring Toluene Concentration in Deionized Water.

Deionized water supplied for chemical laboratories was allowed to pass through the same long sampling cylinder used in the water flow-through system at the average flow rate of 720 mL/min. A CAR/PDMS fiber was exposed directly to the deionized water for 5 min. at section #2 of the sampling cylinder. In the mean time, 25 mL of the deionized water was collected and analyzed by headspace SPME. The temperature of the deionized water was approximately $23\pm 0.5^{\circ}\text{C}$.

2.3.4 Rapid Air Sampling

2.3.4.1 Standard Gas Generator

National Institute of Standards and Technology (NIST) traceable certified permeation tubes (Kin-Tech Laboratories, La Marque, TX, USA) were used for generation BTEX. Ultra-high-purity air at 50 psig was supplied by use of thoroughly cleaned copper tubing and SwagelokTM connectors. The supplied air was also scrubbed by use of a Supelpure HC hydrocarbon trap before entering the standard gas generator. All permeation tubes were placed inside a glass permeation cylinder (KIN-Tech Laboratories, La Marque, TX, USA) and swept with a constant flow of dilution air. The actual airflow rate was verified by use of a primary gas flow standard Mimi-Buck calibrator (A.P. Buck, Orlando, FL, USA). A wide range of concentrations of BTEX was obtained by adjusting both airflow rates and permeation cylinder temperature.

2.3.4.2 Sampling Chamber

Sampling chambers consisted of a 1.5 L glass bulb with several sampling ports plugged with half-hole-type Thermogreen™ septa.⁷ An Omega™ 120 W heating tape was wrapped around the glass bulb to provide a controlled temperature environment. Sampling-chamber temperature was maintained at $25 \pm 0.3^\circ\text{C}$. To investigate the effect of air velocity, a long sampling cylinder with three different diameters (Glass Shop, University of Waterloo, ON, Canada) was installed downstream from the main sampling chamber. The concentrations of BTEX were determined by monitoring the loss of BTEX for a certain time period and air flow rate and were validated by use of both SPME fibers and ORBO charcoal tubes (Supelco) combined with I. H. personal air pumps (A. P. Buck, Orlando, FL) for conventional 1501 NIOSH method.

2.3.5 Indoor Air Sampling

The same long sampling cylinder used for rapid air sampling was utilized to set up the indoor air sampling system (Figure 2-3). Air was drawn through the sampling cylinder by the use of air pump #1 (A. P. Buck), which was constantly operated at 1500 mL/min. NIOSH method 1501 for determination of aromatic hydrocarbons was chosen as the reference method. Air sampling pump #2 was used to draw air at 42 mL/min through the charcoal tube, which was connected to the sampling port of section #1 of the sampling cylinder. A CAR/PDMS fiber with the fiber coating withdrawn into the needle (diffusion path length was 4.6 mm) was deployed at section #3 of the sampling cylinder to determine the time-weighted average (TWA) concentration by passive sampling. Another CAR/PDMS fiber was used to monitor the real time concentration by exposing the fiber coating to the moving air for 2 min

at section #2 of the sampling cylinder from time to time. The whole system was deployed near an organic solvent cabinet in a chemistry laboratory. The approximate sampling temperature was $23\pm 1^\circ\text{C}$, and the relative humidity was 66% (Canadawide Scientific, Ottawa, ON, Canada) during the sampling period.

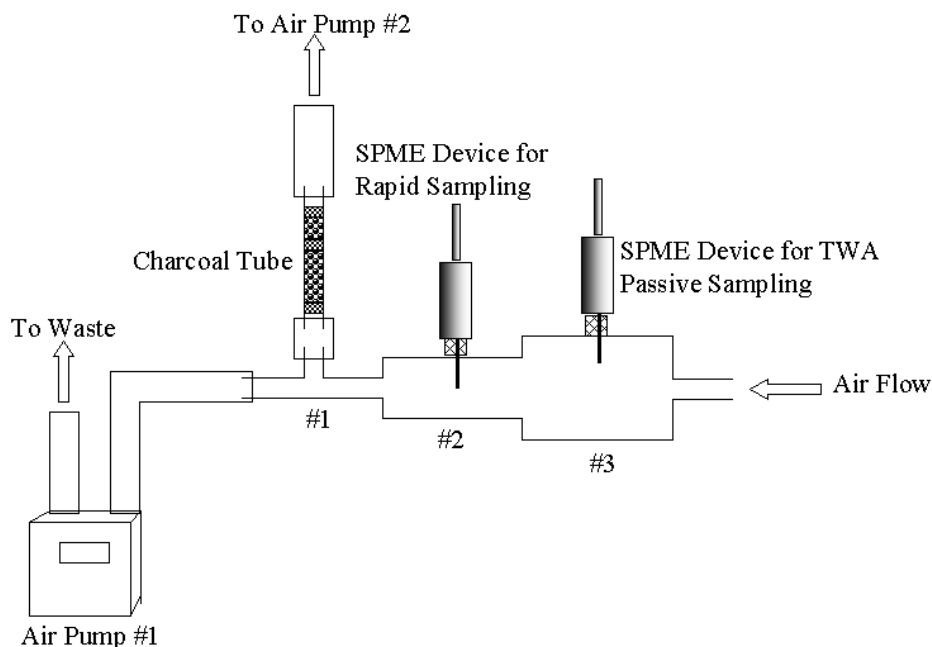


Figure 2-3 Schematic of experimental setup for indoor air sampling.

2.3.6 Gas Chromatography

A Varian star computer-controlled Varian 3400 CX gas chromatograph (Varian Associates, Sunnyvale, CA) equipped with a carbon dioxide cooled septum-equipped programmable injector (SPI) was used for all experiments. A 0.8 mm i.d. SPI insert was coupled to a RTX-5 column (30 m, 0.25 mm i.d., 1.0 μm film thickness) and the column was

coupled to a flame-ionization detector (FID). The injector was maintained at 250°C for PDMS and PDMS/DVB fiber injection and at 300°C for CAR/PDMS fiber injection. For liquid injections the injector temperature was initially 35°C for 0.1 min and then ramped to 250°C at 300°C/min. For SPME fiber and liquid injections the column temperature was maintained at 35°C for 2 min then programmed at 30°C/min to 230°C. The carrier gas (helium) head pressure was set to 25 psig (~ 172 kPa) for both SPME fiber and liquid injection. Detector gas flow rates were 300 mL/min for air and 30 mL/min for nitrogen and hydrogen.

For field sampling, identification of toluene was carried out in a Saturn 3800 GC/2000 ITMS system fitted with a HP-5 column (30 m, 0.25 mm i.d., 0.25 µm film thickness) (Hewlett-Packard, Avondale, PA). Helium as the carrier gas was set to 1 mL/min. The 1079 injector was set to 250°C for PDMS fibers and 300°C for CAR/PDMS fibers. Column temperature program was the same as described above.

The instrument was checked on a daily basis by calibration with SPME extraction of standard BTEX gas mixture by the use of a 100 µm PDMS fiber. Any deviation in area counts greater than 15% required injection of a liquid midpoint calibration standard. If the deviation was proved to be the deviation of response of FID, the instrument was recalibrated with a six-point calibration plot. Peak shape quality, resolution, and retention times were also carefully monitored to ensure all chromatography was within all required specifications.

2.4 Results and Discussion

2.4.1 Extraction Time Profiles for Aqueous Solutions

Extraction time profiles of the standard aqueous solutions of BTEX with varying conditions of linear velocities and concentrations were determined, and two of them are shown in Figure 2-4 and Figure 2-5. It was found that the extracted masses of BTEX increase linearly, without reaching any visible maxima for both CAR/PDMS and PDMS/DVB fibers for all cases. Compared to those results observed previously⁹ when a PDMS/DVB fiber was used to perform the extractions, the extended linear range of sampling time is attributed to the use of lower concentrations of BTEX (in the low range of ppb) that results in lower mass

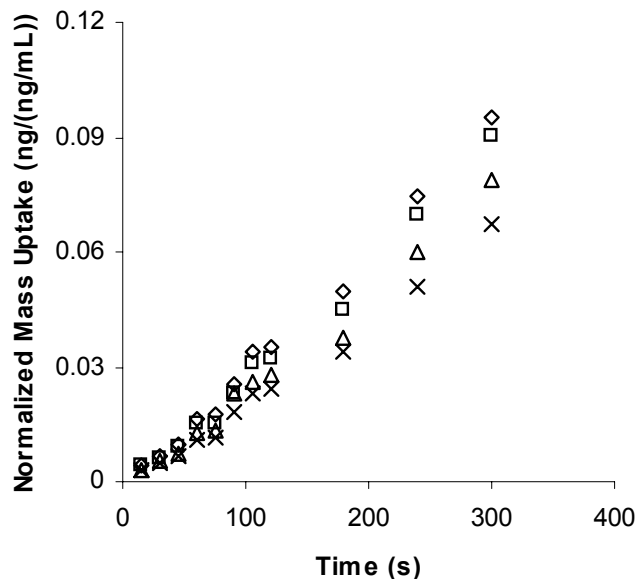


Figure 2-4 Extraction time profiles of BTEX at concentration of 20.8 ng/mL and water velocity of 0.2 cm/s using a 75 μ m CAR/PDMS fiber: benzene, ◇; toluene, □; ethylbenzene, Δ; o-xylene, ×.

uptake under the same sampling conditions, which, in turn, means that more coating surface is available, and displacement is unlikely to occur. Longer sampling times are thus possible with linear mass uptake.

With careful inspection of Figure 2-4, an important result can be recognized. In Figure 2-4, which is obtained by the use of a CAR/PDMS fiber, normalized mass uptake for each BTEX, which is equal to mass uptake of each component of BTEX divided by its bulk concentration, decreases in the order of benzene, toluene, ethylbenzene, and o-xylene at any given sampling moment. In other words, the larger the diffusion coefficient, the larger the normalized mass uptake. This result strongly suggests that the mass transfer of this process is mainly controlled by diffusion.

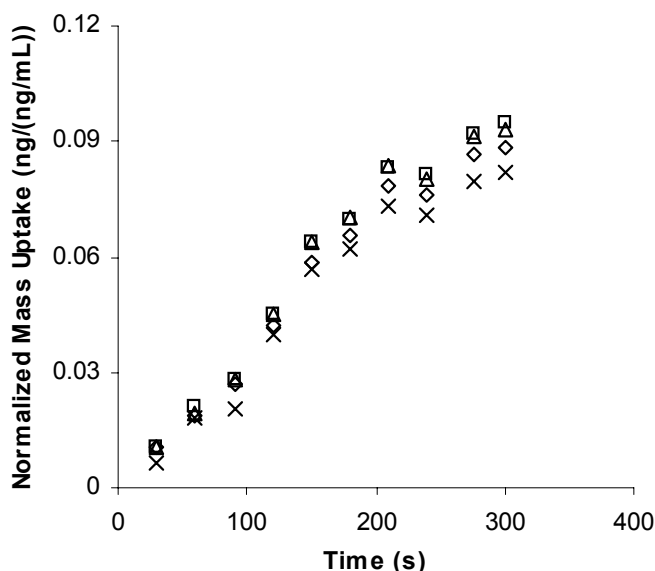


Figure 2-5 Extraction time profiles of BTEX at concentration of 20.8 ng/mL and water velocity of 0.2 cm/s using a 65 μm PDMS/DVB fiber: benzene, \diamond ; toluene, \square ; ethylbenzene, Δ ; o-xylene, \times .

In Figure 2-5 obtained by the use of a PDMS/DVB fiber, however, the normalized mass uptake of benzene is less than those of toluene and ethylbenzene with the increase of

sampling time. Although this result is contrary to those observed above, it is understandable considering the affinity of benzene towards the DVB coating is not very strong. The benzene concentration at the interface of aqueous phase and the coating phase is not negligible, which decreases the mass uptake rate of additional benzene. Referring to equation 2.2, when C_{sorbent} is not zero, mass uptake rate dn/dt decreases.

The CAR/PDMS coating was proved to have stronger affinity and larger capacity towards volatile organic compounds (VOCs).^{4,5,14} This is likely due to the micropores in Carboxen in which capillary condensation likely occurs, a process that favors and enhances extraction of low molecular weight analytes. Stronger affinity ensures that smaller and more volatile molecules can be held for a long time without desorption, while larger capacity ensures that more coating surface are available, and displacement is unlikely to happen. Unless otherwise indicated, all subsequent extractions were carried out with CAR/PDMS fibers.

2.4.2 Effects of Sample Velocity

To evaluate the effect of velocity on the extraction of BTEX from water, 10 to 900 s extractions with sample velocities ranging from 0.2 cm/s to 20.5 cm/s were performed. Normalization of mass uptakes to both concentrations and sampling times results in a variable with units of mL/s. Similar to active and passive sampling, sampling rate is used to represent the normalized mass uptake here. As shown in Figure 2-6, the sampling rates for all BTEX increase as velocity increases. The increase of velocity decreases the thickness of boundary layer, which reduces the resistance to mass transfer, and thus increases the sampling rates. In the lower range of velocity, increase of velocity plays a more significant

effect on the reduction of the thickness of boundary layer, which is reflected by the larger slopes of sampling rates. In the higher range of velocities, a reduced dependence on velocity is observed. The effect of velocity on the sampling rate reflects on the change of Reynolds number Re , and thus Nusselt number \overline{Nu} with the change of velocity. Substituting the definition of Reynolds number Re into equation 2.1 leads to:

$$\overline{Nu} = E \left(\frac{ud}{v} \right)^m Sc^{1/3} \quad \text{Equation 2.5}$$

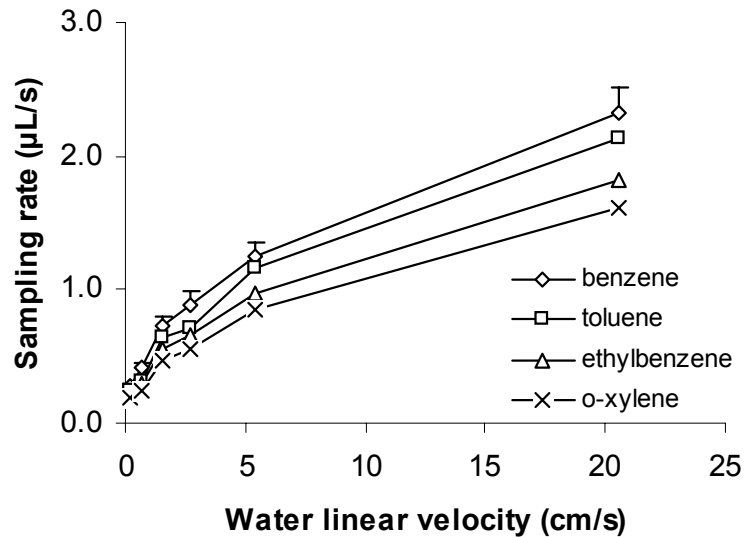


Figure 2-6 Effects of water velocity on the adsorption of BTEX onto the 75 µm CAR/PDMS fiber for various sampling times and concentrations. Only error bars signifying +1 standard deviation from the mean of the sampling rate of benzene for various sampling times and concentrations are displayed for better view. Relative experimental errors of other compounds are comparable to those of benzene.

Because the constant E is in the range of 0.9 to 1, and the constant m is in the range of 0.3 to 0.4 for the entire experimental conditions, the implication of this equation is that the

change of Nusselt number \overline{Nu} with velocity u is not linear. In other words, there is no linear relationship between sampling rate and velocity. According to equation 2.5, Nusselt number \overline{Nu} increases rapidly with the increase of velocity in the range of low velocities, while the increase slows down progressively in the range of high velocities, which agrees well with experimental results, except for those obtained at the velocity of 20.5 cm/s where the experimental results are larger than expected. The reason is that the fiber is vibrating when water velocity is higher than about 11 cm/s, so higher sampling rate results from faster relative movement between the fiber and water. The shaking of fibers at high velocities of samples might put a limit to the use of SPME for rapid sampling of liquid samples. The alternative is the development of stiffer, less flexible SPME fibers.

2.4.3 Mass Uptake Rate Versus Analyte Concentration

Extractions of BTEX at four concentrations with extraction times ranging from 10 to 300 s and water velocity of 0.7 cm/s were performed. For simplification, benzene is used as the example. However, the general description and results are applicable to other BTEX components. Without any exception, mass uptake increases linearly with sampling time. For each concentration, mass uptakes are normalized to sampling times. The average of the mass uptake rates is then plotted against its concentration. The expected linear relationship between mass uptake rate and concentration is demonstrated ($R^2 = 0.995$). The important implication of this result is that the concentration of benzene at the interface of aqueous phase and Carboxen coating can be treated as zero, so the mass uptake rate can response linearly to the bulk concentration, as suggested by equation 2.3. Unlike exhaustive sampling and equilibrium sampling methods, linear mass uptake to both sampling time and analyte

concentration is crucial for the rapid SPME sampling method. To ensure this, feasible strategies include, first, the flow of samples and therefore the boundary layer mass transfer condition must be maintained constant; second, the sorbent must be a ‘zero sink’ to target analytes, which ensures C_{sorbent} is zero; third, sampling time should be optimized to analyte concentrations and sample velocities. An empirical solution to the last strategy is that sampling time should be in the range for which the amount of extracted analyte is larger than the limit of quantification and smaller than 5~10% of the equilibrium amount. The former criterion is self-evident, but the latter is often overlooked.

Adsorption of analytes on a solid sorbent is always accompanied with desorption of analytes from the sorbent. The distribution coefficient K is defined as the ratio of analyte concentration at the surface of the sorbent over analyte bulk concentration under equilibrium conditions. A sorbent with stronger affinity possesses a larger distribution coefficient K . For rapid sampling with SPME, equilibrium between bulk analytes and analytes on the sorbent is not reached. However, quick equilibrium can be assumed between analytes at the interface of sample matrix and the sorbent and those on the sorbent. A sorbent with larger K value and small amount of analyte on its surface (small surface concentration) ensures C_{sorbent} is negligible. When the amount of extracted analyte is larger than 5~10% of its equilibrium amount, C_{sorbent} can rarely be neglected, especially for long sampling times. To avoid extracting too much analytes, short sampling times, small sample velocities, or both can be used and vice versa.

To experimentally test the ‘zero sink’ effect, CAR/PDMS and PDMS/DVB fibers were used to extract standard BTEX gaseous mixture for 15 s, then the BTEX loaded fibers were exposed to BTEX-free water with velocities varying from 0.2 to 11 cm/s for 5 min. It

was found that there is no significant losses of BTEX from CAR/PDMS fibers, while the percentages of the amount of benzene remaining on the PDMS/DVB fiber decreased from 93% to 67%. These results demonstrated that CAR/PDMS fibers were ‘zero sink’ to BTEX, while PDMS/DVB fibers could not be ‘zero sink’ to benzene. These results also support the experimental results in the section of ‘Extraction Time Profiles for Aqueous Solutions’ of this chapter.

2.4.4 Validation of the Theoretical Model

The model (model 1) proposed for rapid water sampling⁹ was used to predict the mass uptake for rapid water sampling in this study. It was found that model 1 underestimated the amount of extracted analytes (Figure 2-7). The reason is ascribed to the model itself that is translated from heat conduction through a solid cylinder.⁷ The uniform boundary layer is rarely formed when a SPME fiber is exposed to a fluid for which motion is normal to the axis of the fiber. In addition, the calculation of the thickness of the boundary layer still depends on an empirical equation, which introduces additional errors. To improve the accuracy of prediction, the model described in the theoretical part (model 2) was used. Since the complexity of this process, theoretical calculation of the thickness of the boundary layer (δ) around the fiber is not possible, and an empirical correlation to estimate \overline{Nu} , and then \bar{h} has to be used. Compared to model 2, model 1 describes an idealized physical mass transfer process, and thus is more fundamentally important. However, model 2 is proved to be more ‘practical’ and accurate. Figure 2-7 shows the experimental mass uptakes, the same data set as shown in Figure 2-4, and theoretical mass uptakes, predicted by model 1 and model 2. It is obvious that model 2 predicts the mass uptakes more accurately.

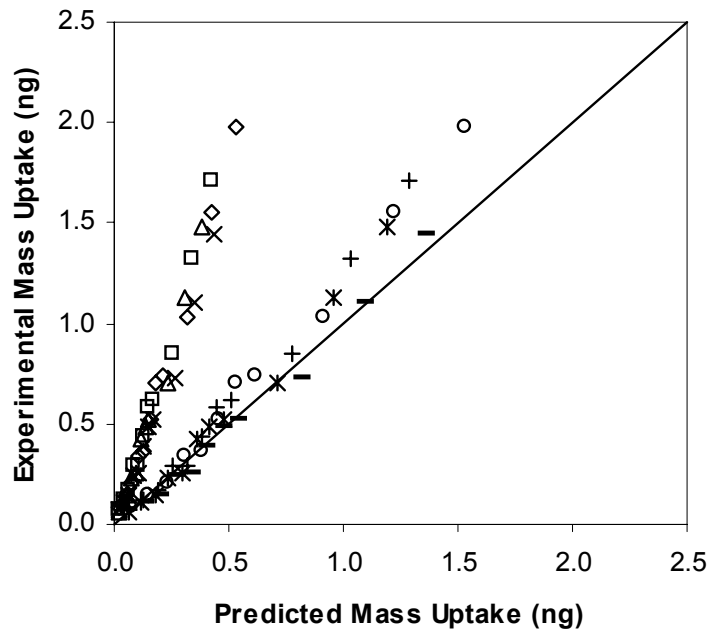


Figure 2-7 Validation of rapid SPME extraction of standard aqueous BTEX solution at concentration of 20.8 ng/mL and water velocity of 0.2 cm/s using model 1: benzene, \diamond ; toluene, \square ; ethylbenzene, Δ ; o-xylene, \times ; and model 2: benzene, \circ , $y = 1.31x - 0.07$, $R^2 = 0.993$; toluene, $+$, $y = 1.33x - 0.07$, $R^2 = 0.989$; ethylbenzene, $*$, $y = 1.24x - 0.06$, $R^2 = 0.987$; o-xylene, $-$, $y = 1.06x - 0.05$, $R^2 = 0.991$.

The validation of model 2 for direct rapid sampling with SPME was completed in experiments with extraction times varying from 10 to 900 s, BTEX concentrations from 2.8 to 20.8 ng/mL, and water velocities from 0.2 to 5.4 cm/s. The experimental mass uptakes, obtained under various conditions, are plotted against mass uptakes predicted by model 2 ((Figure 2-8), where benzene is used as the example). Significant correlation exists between experimental and theoretical mass uptakes, which indicates the viability of model 2 for description of rapid sampling with SPME in aqueous samples. However, experimental mass uptakes are generally larger than predicted mass uptakes for most cases. The possible reason is the roughness of the fiber coating surface causing additional turbulence and therefore the reduction of the boundary layer thickness where convection occurs.

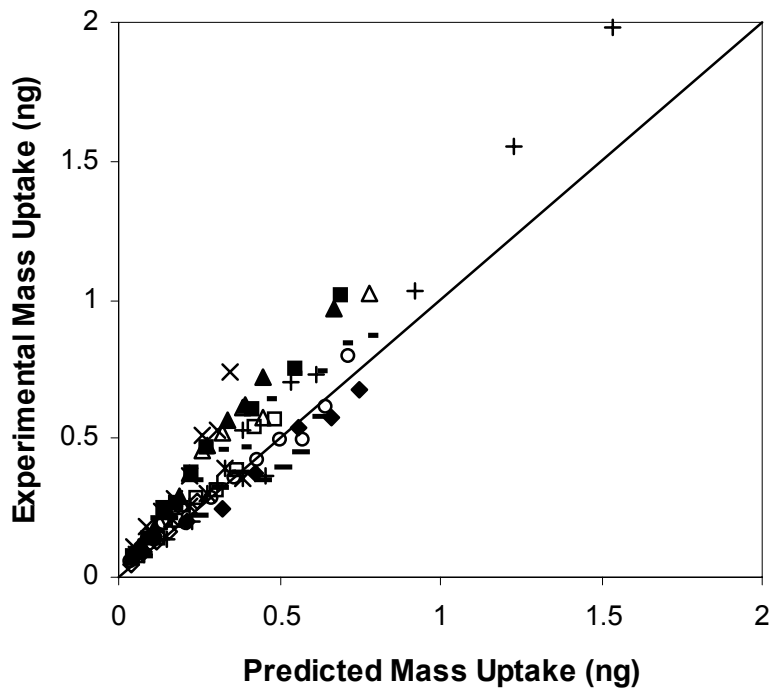


Figure 2-8 Validation of rapid SPME extraction of standard aqueous BTEX solution at various sampling times, concentrations, and water velocities using model 2 (equation 2.3, benzene as the example). Only parts of data are presented because of limit of the space. 2.8 ng/ml, 0.7 cm/s, —; 2.8 ng/ml, 2.7 cm/s, ◆; 4.9 ng/ml, 0.2 cm/s, ○; 4.9 ng/ml, 0.7 cm/s, *; 4.9 ng/ml, 1.5 cm/s, ▲; 4.9 ng/ml, 2.7 cm/s, ×; 4.9 ng/ml, 5.4 cm/s, ■; 11.0 ng/ml, 0.2 cm/s, ◇; 11.0 ng/ml, 0.7 cm/s, □; 11.0 ng/ml, 2.7 cm/s, Δ; 20.8 ng/ml, 0.2 cm/s, +; 20.8 ng/ml, 0.7 cm/s, -.

These results also suggest that the empirical equation 6 in the reference 9 tends to overestimate the sample velocity. The overall effect of combining model 1, which underestimates the mass uptake, and equation 6 in the reference 9, which overestimates the velocity of sample, leads to good prediction of rapid SPME water sampling for some conditions. Without the flow-through system for which the velocity of the sample is known and controlled, it is difficult to define this problem.

2.4.5 Effect of Water Temperature

The temperature effect on traditional SPME equilibrium extraction using a liquid coating, e.g. PDMS, has been well studied.¹ Increase in temperature results in decrease of the distribution coefficient, thus decreasing the amount of extracted analyte. On the other hand, an increase in temperature shortens the time required to reach equilibrium. Optimization of both temperature and sampling time can be done according to the requirements of application.

For rapid SPME extraction using a solid coating, the effect of temperature can be divided into two parts— (1) the effect on the distribution coefficient and (2) the effect on the diffusion coefficient. No matter what the temperature is, once the SPME coating is a ‘zero sink’ for target analytes, the effect of temperature on the distribution coefficient is negligible for the rapid SPME extraction. Carboxen coating was shown to be a ‘zero sink’ for most VOCs even with temperatures up to 35°C for TWA air sampling.¹⁴ Hence for typical field water sampling for which temperature rarely exceeds 35°C, the effect of temperature on the distribution coefficient can be neglected.

The relationship between temperature and diffusion coefficient can be approximated as:¹⁵

$$D \propto T$$

Equation 2.6

Because the diffusion coefficient also appears in the denominator of the definition of Schmidt number, which partially counteracts the effect of diffusion coefficient, the overall effect of temperature on sampling rate is less than that of temperature on the diffusion coefficient alone. Further calculation indicates that a 10-deg variation of temperature at ~293 K causes approximately 3% change in sampling rate. Considering that this change of

sampling rate is less than experimental error (5%~15%), the effect of temperature is negligible if the temperatures do not differ too much.

The change in temperature also changes the properties of water, which is reflected on the change of the kinematic viscosity ν . However, the kinematic viscosity ν appears in the denominator of the definition of Reynolds number Re and in the numerator of the definition of the Schmidt number Sc , so the overall effect of the change of the kinematic viscosity of water on the Nusselt number \overline{Nu} is not large.

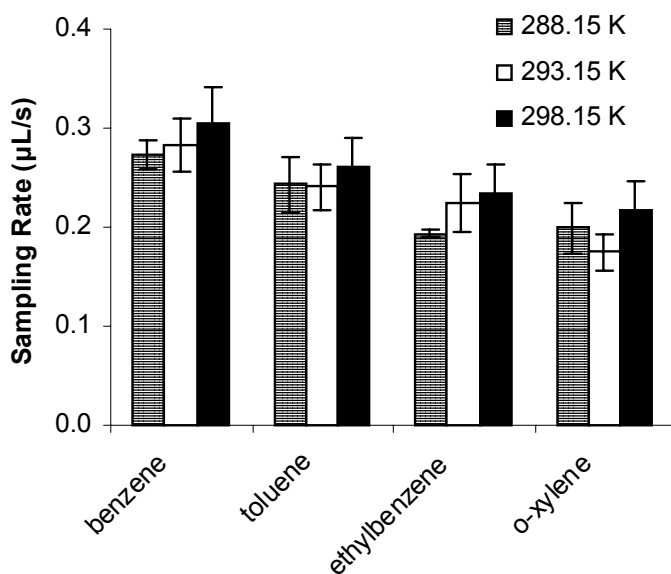


Figure 2-9 Effect of temperature on the adsorption of BTEX onto the 75 µm CAR/PDMS fiber.

Experimental assessment of the overall effect of temperature on rapid SPME sampling was performed at three temperatures, namely 15, 20, and 25°C, and the results are shown in Figure 2-9, which indicates temperature does not affect sampling rate significantly.

2.4.6 Monitoring Toluene Concentration in Deionized Water

Because resin material was used in the purification system to generate deionized water, toluene was suspected to exist in the deionized water. The monitoring began at 12:15 P.M. and ended at 8:00 P.M. in a working day during which rapid SPME and headspace SPME were performed simultaneously at 30 min intervals.

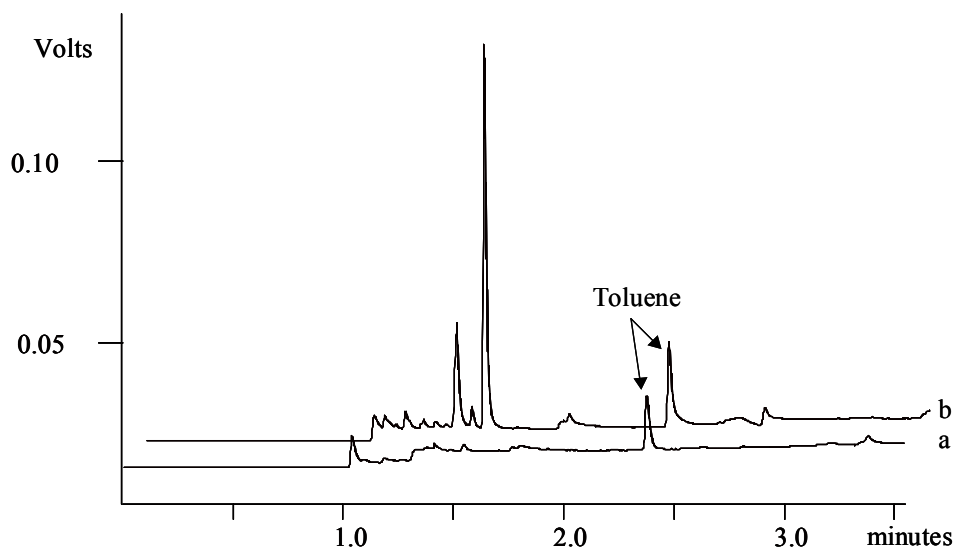


Figure 2-10 Chromatograms obtained from monitoring toluene concentration in deionized water by a) headspace SPME and b) rapid SPME.

Figure 2-10 shows two typical chromatograms obtained by rapid SPME in aqueous phase and headspace SPME. It is obvious that the sensitivities of both methods toward toluene are comparable under the experimental conditions. However, the amount of toluene

extracted by rapid SPME can be increased by increasing water linear velocity and/or sampling time. Two other polar compounds were suspected to exist in the deionized water as indicated by the two large peaks eluted before toluene from the chromatogram of rapid SPME. They can be barely observed from the chromatogram of headspace SPME, because PDMS coating cannot extract volatile polar compounds very efficiently. The identification of toluene was confirmed by standard addition and GC/MS.

The concentrations of toluene determined by rapid SPME were estimated from equation 2.4. The resulting concentration profiles of toluene obtained by both methods are shown in Figure 2-11, which indicates that there was a significant amount of toluene in the deionized water, and the concentrations of toluene were relatively stable during the monitoring period, ranging from 1.0 ng/mL to 1.5 ng/mL. In addition, both concentration profiles are essentially comparable, because the relative deviations are largely within 15%, and the largest relative deviation is 22%. This means that the rapid SPME method (model 2) is very reliable.

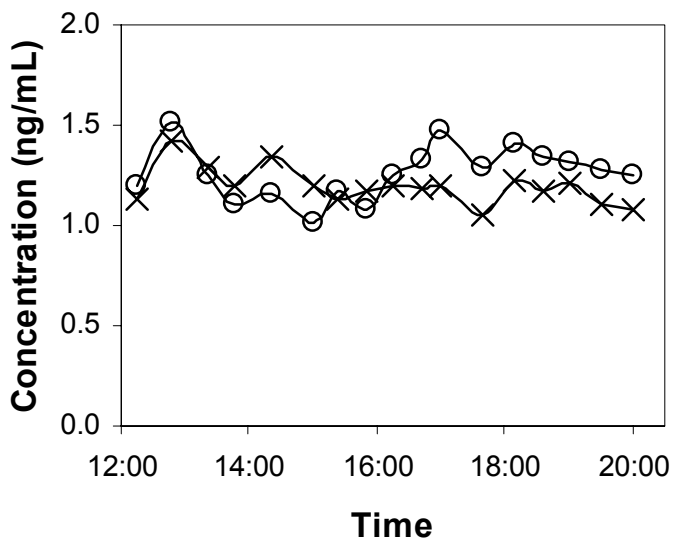


Figure 2-11 Concentration profiles of toluene in the deionized water determined by rapid SPME (o) and headspace SPME (x).

2.4.7 Rapid Air Sampling

To test the applicability of model 2 for air sampling, rapid extractions of standard BTEX gas mixture were performed. The concentrations of BTEX were 0.64, 0.57, 0.10, and 0.12 ng/mL, respectively. The investigated air velocities were 2.8 and 0.3 cm/s and are smaller than the critical velocity (~ 10 cm/s) for which the effects of the boundary layer thickness are negligible.⁷ A 75 μm CAR/PDMS fiber was used to extract BTEX, and the time of extraction varied from 5 to 120 s. The experimental mass uptakes were compared with theoretically predicted mass uptakes (Figure 2-12). Similar results were obtained when air velocity was 0.3 cm/s. Obviously, model 2 is suitable for rapid air sampling.

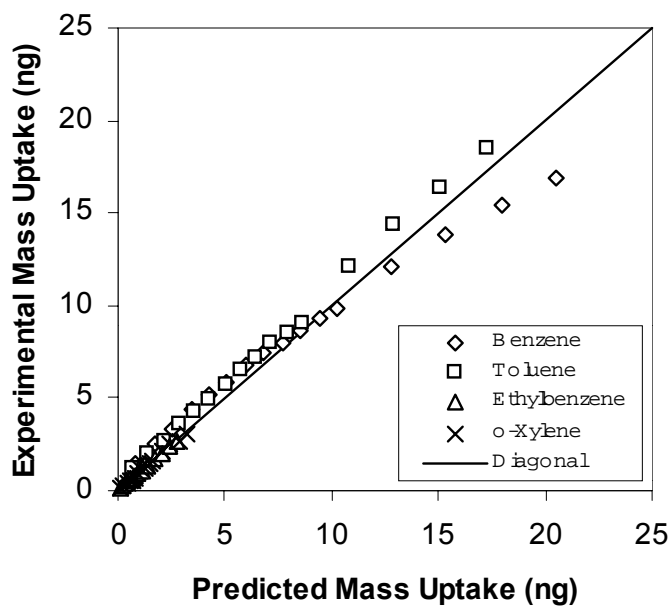


Figure 2-12 Comparison of experimental and predicted mass uptakes of BTEX for rapid air sampling using a CAR/PMS fiber. Air velocity is 2.8 cm/s.

To investigate the difference of model 1⁷ and model 2 for describing rapid air sampling, model 1 was also used to predict the mass uptakes for this experiment. It was found that the mass uptakes predicted by model 1 were only ~5% larger than those predicted by model 2. Further theoretical calculations indicated that the difference of mass uptakes predicted by both models was less than 30% when the air velocity is in the range of 0.2 cm/s to 10 cm/s. This suggests that both models can be used for rapid air sampling, though, overall, model 2 is still more accurate.

However, there is a question as to why model 1 can describe rapid air sampling much more accurately than rapid water sampling. The reason is probably that the boundary layer thickness around the SPME fiber is much larger in air than in water under the same bulk velocity (about 30 times larger).¹ Small deviation of the calculation from the boundary layer thickness does not cause large relative errors for rapid air sampling, while the same deviation may cause very large errors for rapid water sampling where the boundary layer thickness becomes much smaller.

2.4.8 Indoor Air Sampling

It is well known that rapid sampling is sensitive to concentration variation. Rapid SPME sampling can be done within several minutes or even several seconds. Quantitative techniques are not readily available to validate the results obtained from rapid SPME sampling because sampling times are restricted to several seconds or minutes except some real time techniques developed for specific compounds. However, standard methods for long term air monitoring or TWA sampling are available. The idea to validate quantitative analysis with rapid SPME sampling is to perform a large number of rapid SPME sampling

over a long time period, then the TWA concentration can be calculated using the following equation:¹⁶

$$\bar{C} = \frac{\sum_i C_i t_i}{\sum_i t_i} \quad \text{Equation 2.7}$$

where \bar{C} is the TWA concentration and C_i is the concentration observed at sampling period t_i . The TWA concentration determined by this way is compared with the result obtained by a standard method that, in this case, is NIOSH 1501. Since TWA passive sampling using SPME possesses a number of merits, such as absence of solvent, reusable format, insensitivity to convection conditions, etc.,¹⁴ TWA passive sampling using SPME was performed at the same sampling period.

The indoor air sampling in a chemical laboratory was carried out from 10:25 A.M. to 6:00 P.M. in a working day. Three sampling methods, i.e., rapid SPME, TWA SPME, and the charcoal tube sampling were essentially performed in the same sample simultaneously. Toluene was chosen as the target analyte. The adsorption of toluene onto the inner walls of the sampling cylinder is assumed to be negligible due to its high volatility. In addition, the amount of toluene extracted by rapid SPME sampling and SPME TWA passive sampling carried out in the upstream of the moving air was negligible. Figure 2-13 shows the concentration time profiles of toluene during the sampling period. The concentrations from rapid SPME sampling were estimated using equation 2.4. The corresponding TWA concentration was calculated from equation 2.7. It was ~20% larger than the TWA concentration determined by SPME passive sampling, while the latter was ~20 % larger than the TWA concentration obtained by NIOSH 1501. The discrepancy is probably due to the following reasons. First, as suggested by equation 2.7, the more rapid sampling performed,

the more accurate the TWA concentration will be. Second, loss of toluene may occur during the desorption process using CS₂ (backup charcoal was analyzed, and no breakthrough was observed). Nevertheless, the difference is not large. It is believed that any results larger than that of NIOSH 1501 and smaller than that of SPME grab sampling are reasonable and acceptable.

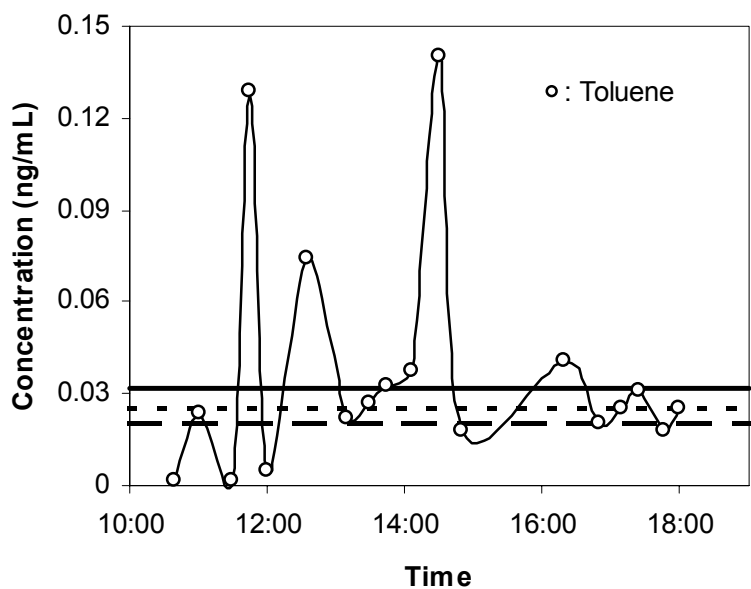


Figure 2-13 Concentration profile of toluene determined from rapid SPME sampling in a chemistry laboratory. o : Rapid SPME sampling; — : TWA concentration calculated from rapid SPME sampling using equation 2.7; - - - : TWA concentration determined by SPME passive sampling; — — — : TWA concentration determined by the NIOSH method 1501.

The design of this system (Figure 2-3) is useful and versatile for field rapid SPME sampling. First, it can be used for water sampling when air pumps are replaced with water pumps. Second, the linear velocities of samples are only related to the inner diameter of the sampling cylinder and pumping rate of the pump #1. In other words, the linear velocities of samples can be controlled within a range to which rapid SPME analysis is applicable. Thus,

this system is applicable to both stagnant and turbulent samples, e.g. lake water, or river water. The rapid SPME requires controlled sample flow. The proposed rapid SPME sampling system can ensure that the critical velocity for air sampling⁷ is not exceeded and can also minimize or eliminate vibrations of SPME fibers in aqueous samples at high velocities.

Finally, it is interesting to note that all of the three methods used for the indoor air sampling do not need calibration once the response factor of the detector is known. The NIOSH 1501 method is based on exhaustive extraction, while rapid SPME sampling and SPME TWA passive sampling are diffusion-based.

2.5 Conclusion

A new mass transfer model translated from heat transfer to a circular cylinder in cross flow was proposed to quantitatively describe rapid and direct extraction of BTEX with SPME. This new model still emphasizes that mass transfer from the bulk of samples to the fiber is mainly controlled by diffusion. It was demonstrated in this study that the sampling rate increases with the increase of the diffusion coefficient. To quantify rapid water and air sampling with SPME, an empirical correlation to the new model was used. The amount of extracted mass predicted by the new model compares well with experimental mass uptakes. The main advantage of this method is that quantification is diffusion-based, which means no calibration curves or internal standards are needed, because necessary constants, e.g., diffusion coefficient, can be found in literature, or can be reliably estimated from empirical equations. Such characteristics make this method especially suitable for on-site analysis, where construction of calibration curves or addition of internal standards proves to be very difficult.

It should be emphasized that the sorbent must be a ‘zero sink’ to target analytes during entire sampling period when using this technique. Parameters affecting the ‘zero sink’ effect include sorbent affinity and capacity, the amount of extracted mass, sampling time, temperature, and other variables. The use of a sorbent with strong affinity and large capacity, such as CAR/PDMS, limiting the amount of extracted mass less than 5~10% of equilibrium amount, and low temperature have positive effects on ‘zero sink’.

Coupled to a portable/fast GC for separation and detection of analytes, the use of very short extraction times with SPME has a great potential for field use, especially when on-site decision must be made. However, quantitative extractions require samples with a flowing medium. The sample velocity must be known and controlled, requiring additional equipments. Future work will concentrate on developing a rapid SPME or other extraction techniques that are independent of sample velocities, which is the research presented in Chapter 3.

2.6 References

¹ Pawliszyn, J. *Solid Phase Microextraction – Theory and Practice*; Wiley – VCH; New York, 1997.

² Martos, P.A.; Saraullo, A.; Pawliszyn, J. *Anal. Chem.*, **1997**, *69*, 402-408.

³ Ai, J. “Quantitation by SPME before Reaching a Partition Equilibrium”, *in* Pawliszyn, J. (ed.); *Applications of Solid Phase Microextraction*; RSC; Cambridge, UK, 1999; Chapter 2, pp. 23–37.

-
- ⁴ Mani, V. “Properties of Commercial SPME Coatings”, in Pawliszyn, J. (ed.); *Applications of Solid Phase Microextraction*; RSC; Cambridge, UK, 1999; Chapter 5, pp. 63–67.
- ⁵ Górecki, T. “Solid versus Liquid Coatings”, in J. Pawliszyn (ed.); *Applications of Solid Phase Microextraction*; RSC; Cambridge, UK, 1999, Chapter 7, pp. 92–108.
- ⁶ Górecki, T.; Yu, X. and Pawliszyn, J. *Analyst* **1999**, *124*, 643.
- ⁷ Koziel, J.; Jia, M. and Pawliszyn, J. *J. Anal. Chem.* **2000**, *72*, 5178.
- ⁸ Augusto, F.; Koziel, J. and Pawliszyn, J. *J. Anal. Chem.*, **2001**, *73*, 481.
- ⁹ Sukola, K.; Koziel, J.; Augusto, F. and Pawliszyn, J. *J. Anal. Chem.*; **2001**, *73*, 13.
- ¹⁰ Sukola, K.; Koziel, J.; Augusto, F. and Pawliszyn, J. “Diffusion-based calibration for fast SPME analysis of VOCs in aqueous samples with Carboxen/PDMS coating”, unpublished work.
- ¹¹ Morgan, V. T. “The Overall Convective Heat transfer from Smooth Circular Cylinders”, in Jr., T. F. Irvine; Hartnett, J. P. (ed.); *Advances in Heat Transfer*, Vol. 11, Academic Press, New York, 1975.
- ¹² Hilpert, R. *Forsch. Geb. Ingenieurwes.* **1933**, *4*, 215.
- ¹³ Knudsen, J.G.; Katz, D. L. *Fluid Dynamics and Heat Transfer*, McGraw-Hill, New York, 1958.
- ¹⁴ Chen, Y. and Pawliszyn, J. *J. Anal. Chem.* **2003**, *75*, 2004.
- ¹⁵ Bonoli, L. and Witherspoon, P.A. *J. Phys. Chem.* **1968**, *72*, 2532.
- ¹⁶ Martos, P. A. and Pawliszyn, J. *J. Anal. Chem.* **1999**, *71*, 1513.

Chapter 3 Standards on A Fiber

3.1 Introduction

SPME was developed to address the need for rapid sampling and sample preparation, both in the laboratory and on-site, where the investigated system is located.¹ To date, the most well-established and widely used quantification method using SPME is the equilibrium extraction method, where a fiber, coated with a liquid polymeric film, is exposed to a sample matrix until an equilibrium is reached. The extracted amount of analyte, n , is linearly proportional to the initial concentration of the analyte in the sample matrix, C_0 , according to equation 3.1:¹

$$n = \frac{KV_f V_s}{V_s + KV_f} C_0 \quad \text{Equation 3.1}$$

where K is the distribution coefficient, V_f is the volume of the fiber coating, and V_s is the volume of sample matrix. The advantage of the equilibrium extraction method for field sampling is significant. The volume of the field sample matrix, such as indoor air, ambient air, lake water, and river water, is very large. The product of K and V_f is essentially negligible compared to V_s . Thus, equation 3.1 can be simplified to:

$$n = KV_f C_0 \quad \text{Equation 3.2}$$

since the distribution constant can be obtained from literature, from an extraction performed on a standard solution of the analyte, or by calculating the chromatographic retention.² Quantification for on-site analysis is possible without considering the sample volume. This method has been applied for field air sampling^{2,3,4} and field water sampling.^{5,6}

However, the equilibrium extraction method is not readily applicable for fibers with porous solid coatings. The extracted amount of analyte onto a porous solid coating under equilibrium could be non-linear with the initial concentration of the analyte in the sample matrix, at a high concentration range.⁷ Pre-equilibrium extraction must be used for quantitative analysis with porous solid coatings, especially for field analysis, and several methods have been proposed to date.^{8,9} The first theoretical model⁸ for the calibration was formulated based on the diffusion through the boundary layer between the sampled air and the SPME coating. The mass of the extracted analyte with sampling time can be derived using the analogy of heat transfer in a cylinder with a constant axial supply of heat. This model, which uses a very simple and ideal physical process to approximate a complex one, is fundamentally important, and provides a clear picture of rapid SPME extraction. The second mass transfer model⁹ was translated from the heat-transfer from bulk to a circular cylinder in cross-flow. The average mass-transfer coefficient is calculated by knowing the average Nusselt number that is correlated with the Reynolds number and the Schmidt number by an empirical equation. This new model was found to be more practical, accurate, and applicable to both air and water sampling. The main advantage of these methods is that quantification is diffusion-based. In other words, no calibration curves or internal standards are needed. This is a very desirable feature, especially for field sampling. However, quantification requires a constant flow of the sample matrix. The sample velocity must be known and controlled. In cases that the sample velocity is changing, and/or it is difficult, if not impossible, to determine or control the sample velocity, on-site analysis using these methods is challenging.

Internal standardization and standard addition are important calibration approaches that are very effective when quantifying target analytes in complex matrices. They

compensate for additional capacity or activity of the sample matrix. However, such approaches require delivery of the standard. This is incompatible in some sampling situations, such as with on-site or *in-vivo* investigations. This approach is also not practical for conventional exhaustive extraction techniques, since the extraction parameters are designed to facilitate complete removal of the analytes from the matrix. However, in microextraction a substantial portion of the analytes remains in the matrix during the extraction and after the equilibrium is reached. This suggests that the standard could be added to the investigated system together with the extraction phase.

“Stepwise SPME” was thus developed for field sampling/sample preparation, in which an internal standard was preloaded onto a fiber for calibrating the extraction of hydrocarbons in the field air, and monitoring the loss of extracted analytes during the transportation and storage of samplers.¹⁰ In “Stepwise SPME”, a Carboxen fiber, a ‘zero sink’ for both the internal standard and the target analytes, was used, which minimized the loss of the internal standard during short sampling durations. Therefore, no information about the convection conditions of the sample matrix could be obtained. In this work, when a standard loaded fiber was exposed to an agitated sample matrix, intended loss of the standard was used as a convection “indicator”. The kinetics of the desorption process was studied, and used to calibrate the extraction of hydrocarbons.

3.2 Theory

When a SPME liquid coating fiber that is preloaded with an analyte is exposed to an agitated sample matrix, desorption of the analyte from the fiber occurs. The desorbed analyte further diffuses through the boundary layer, between the fiber surface and the bulk of sample

matrix, into the bulk of sample matrix (Figure 3-1). When the diffusion reaches a steady state, this process follows Fick's first law of diffusion:

$$J \equiv \frac{1}{A} \frac{dq}{dt} = -D_f \frac{dC^f}{dx} = -D_s \frac{dC^s}{dx} \quad \text{Equation 3.3}$$

where J is the mass flux of the analyte from the fiber to the sample matrix, A is the surface area of the fiber, dq is the amount of the analyte desorbed from the fiber during time period dt , D_f and D_s are diffusion coefficients of the analyte in the fiber coating and in the sample matrix, respectively, and C^f and C^s are concentrations of the analyte in the fiber coating and in the boundary layer, respectively.

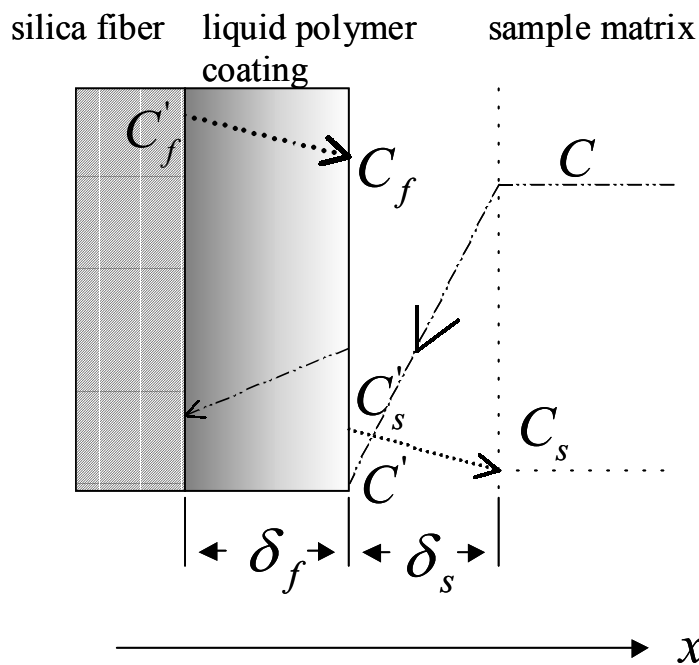


Figure 3-1 Schematic of the calibration of the extraction of hydrocarbons by the desorption of a standard from a SPME fiber coated with a liquid polymeric coating to an aqueous solution. A steady state of diffusion is assumed when the aqueous solution is agitated constantly. A linear concentration gradient is assumed in both the polymer and the boundary layers.

A linear concentration gradient in the fiber coating and boundary layer is assumed:

$$\frac{1}{A} \frac{dq}{dt} = -\frac{D_f}{\delta_f} (C_f - C'_f) = -\frac{D_s}{\delta_s} (C_s - C'_s) \quad \text{Equation 3.4}$$

where δ_f and δ_s are the thickness of the fiber coating and the boundary layer, respectively, C_f is the concentration of the analyte in the coating at the interface of the fiber coating and the boundary layer, C'_f is the concentration of the analyte in the coating at the interface of the fiber coating and the fused silica, C_s is the concentration of the analyte in the bulk of the sample matrix, and C'_s is the concentration of the analyte in the boundary layer at the interface of the fiber coating and the boundary layer. The mass transfer coefficient of the analyte in the fiber coating h_f and that in the boundary layer h_s are defined as $h_f = \frac{D_f}{\delta_f}$ and

$$h_s = \frac{D_s}{\delta_s} \text{ and}$$

$$\frac{1}{A} \frac{dq}{dt} = -h_f (C_f - C'_f) = -h_s (C_s - C'_s) \quad \text{Equation 3.5}$$

It is assumed that a quick partition equilibrium exists at the interface of the fiber coating and the boundary layer:

$$K = \frac{C_f}{C'_s} \Rightarrow C'_s = \frac{C_f}{K} \quad \text{Equation 3.6}$$

K is the distribution coefficient of the analyte between the fiber coating and the sample matrix. In the bulk of aqueous solution:

$$C_s = \frac{q}{V_s} \quad \text{Equation 3.7}$$

where V_s is the sample volume. Substitution of equations 3.6 and 3.7 into equation 3.5 results in:

$$-h_f(C_f - C'_f) = -h_s\left(\frac{q}{V_s} - \frac{C_f}{K}\right) \Rightarrow C_f - C'_f = \frac{h_s\left(\frac{q}{V_s} - \frac{C_f}{K}\right)}{h_f} \quad \text{Equation 3.8}$$

A linear concentration gradient is assumed in the polymer layer:

$$q_0 - q = V_f \frac{C_f + C'_f}{2} \Rightarrow C_f + C'_f = \frac{2(q_0 - q)}{V_f} \quad \text{Equation 3.9}$$

where q_0 is the amount of the analyte initially loaded onto the fiber coating before exposure of the fiber to the sample matrix, V_f is the volume of the fiber coating.

Equation 3.8 + equation 3.9:

$$2C_f = \frac{h_s\left(\frac{q}{V_s} - \frac{C_f}{K}\right)}{h_f} + \frac{2(q_0 - q)}{V_f} \Rightarrow C_f = \frac{K[h_s V_f q + 2(q_0 - q)h_f V_s]}{V_s V_f (2h_f K + h_s)} \quad \text{Equation 3.10}$$

Substitution of equation 3.10 into the right side of equation 3.8:

$$C_f - C'_f = \frac{h_s}{h_f} \left[\frac{q}{V_s} - \frac{[h_s V_f q + 2(q_0 - q)h_f V_s]}{V_s V_f (2h_f K + h_s)} \right] = \frac{2q(KV_f h_s + V_s h_s)}{2h_f KV_s V_f + h_s V_s V_f} - \frac{2q_0 h_s}{2h_f KV_f + h_s V_f}$$

Equation 3.11

Substitution of equation 3.11 into equation 3.5:

$$\frac{1}{A} \frac{dq}{dt} = -h_f \left[\frac{2q(KV_f h_s + V_s h_s)}{2h_f KV_s V_f + h_s V_s V_f} - \frac{2q_0 h_s}{2h_f KV_f + h_s V_f} \right] \quad \text{Equation 3.12}$$

Let:

$$a = \frac{2Ah_f(KV_f h_s + V_s h_s)}{2h_f KV_s V_f + h_s V_s V_f} \quad \text{Equation 3.13}$$

$$b = \frac{2q_0 Ah_s h_f}{2h_f KV_f + h_s V_f} \quad \text{Equation 3.14}$$

Then equation 3.12 is simplified as:

$$q' + aq = b \quad \text{Equation 3.15}$$

The general solution to equation 3.15 is:

$$q \exp \int a dt = \int b (\exp \int a dt) dt + Z \quad \text{Equation 3.16}$$

$$q \exp(at) = \frac{b}{a} (\exp(at) - 1) + Z \quad \text{Equation 3.17}$$

The boundary condition to equation 3.17 is: $t=0, q=0$.

Then $Z=0$. Equation 3.17 becomes:

$$q = \frac{b}{a} [1 - \exp(-at)] \quad \text{Equation 3.18}$$

Equation 3.13 divided by equation 3.14:

$$\frac{b}{a} = \frac{V_s}{KV_f + V_s} q_0 \quad \text{Equation 3.19}$$

Substitution of equation 3.19 into equation 3.18:

$$q = q_0 [1 - \exp(-at)] \frac{V_s}{KV_f + V_s} \quad \text{Equation 3.20}$$

If $V_s \geq KV_f$, as in field sampling, for example, equation 3.20 can be simplified to:

$$q = q_0 [1 - \exp(-at)] \quad \text{Equation 3.21}$$

Let $Q = q_0 - q$, and Q is the amount of the analyte remaining on the fiber coating after exposure of the fiber to the sample matrix for sampling time t . Then:

$$Q = q_0 \exp(-at) \quad \text{Equation 3.22}$$

Equation 3.20 or equation 3.22, in which parameter a is defined in equation 3.13, describes the kinetics of desorption of an analyte from a liquid coating fiber.

3.3 Experimental Section

3.3.1 Chemicals, Supplies, and Standard Gases

All chemicals were of analytical grade. Benzene, toluene, ethylbenzene, and o-xylene (BTEX) were purchased from Sigma-Aldrich (Mississauga, ON, Canada). HPLC grade methanol was purchased from BDH (Toronto, ON, Canada), and naphthalene, acenaphthene, and fluorene were purchased from Supelco (Oakville, ON, Canada). Deuterated toluene (d -8) was purchased from Cambridge Isotope Laboratories (Andover, MA, U.S.A.). The SPME holders and 100 μm polydimethylsiloxane (PDMS) fibers were obtained from Supelco. The fibers were conditioned at 250°C for 1 h prior to their use. All preparations involving toluene, ethylbenzene, and p -xylene (flammable and toxic), benzene (suspected carcinogen), naphthalene, acenaphthene, and fluorene (suspected carcinogen) were carried out in a ventilated fume hood.

The system for generating the standard BTEX gas mixture has been described in Chapter 2 of this thesis^{11,12} and briefly described here. The generation of the standard BTEX gas mixture was based on the permeation of BTEX through polymer tubes (KIN-Tech Laboratories, La Marque, TX), which were swept with a constant flow of dilution air. A wide range of concentrations of BTEX was obtained by adjusting both the airflow rate and the incubation temperature of the polymer tubes. To investigate the effect of the air velocity, a long sampling cylinder with three different diameters (Glass Shop, University of Waterloo, ON, Canada) was installed downstream from the main sampling chamber.

3.3.2 Flow-Through System

The flow-through system has been described in Chapter 2 of this thesis.⁹ In this study, it was used for three purposes. First, only water with controlled and known velocities was generated to study the desorption of BTEX from fibers into agitated water. Second, a standard BTEX aqueous solution was flowed at a controlled and known velocity to study absorption of BTEX onto fibers from the flowing standard BTEX aqueous solution. Third, a standard polycyclic aromatic hydrocarbon (PAH) aqueous solution was flowed at a controlled and known velocity to study the effect of water velocity on the calibration using a standard. The concentrations of standard BTEX and PAHs aqueous solution were monitored and validated using headspace SPME.^{1,9}

3.3.3 Gas Chromatography

A Varian star computer-controlled Varian 3400 CX gas chromatograph (Varian Associate, Sunnyvale, CA) equipped with a carbon dioxide cooled septum-equipped programmable injector (SPI) was used for the BTEX analysis. A 0.8 mm i.d. SPI insert was coupled to a RTX-5 column (30 m, 0.25 mm i.d., 1.0 μ m film thickness) and the column was coupled to a flame-ionization detector (FID). The injector was maintained at 250°C for the PDMS fiber injection. The column temperature was maintained at 35°C for 2 min and then programmed at 30°C/min to a maximum of 230°C. The carrier gas (helium) head pressure was set to 25 psig (~ 172 kPa). Detector gas flow rates were set at 300 mL/min for air and 30 mL/min for nitrogen and hydrogen.

A Saturn 3800 GC/2000 ITMS system fitted with a HP-5 column (30 m, 0.25 mm i.d., 0.25 μ m film thickness) (Hewlett-Packard, Avondale, PA) was used for the analysis of deuterated toluene and PAHs. Helium, as the carrier gas, was set to 1 mL/min. The 1079 injector was set to 250°C for deuterated toluene and 270°C for PAHs, and a desorption time of 1 min for deuterated toluene and 10 min for PAHs. For the analysis of deuterated toluene, the column temperature was maintained at 45°C for 2 min and then programmed at 20°C/min to a maximum of 180°C. For the analysis of PAHs, the GC split valve was set to open after 5 min of insertion. The column temperature was maintained at 45°C for 2 min and then programmed at 20°C/min to a maximum of 280°C, and held for 5 min. The MS system was operated in the electron ionization (EI) mode, and tuned to perfluorotributylamine (PFTBA). A mass scan from 40 to 300 amu was acquired, and the base peak of each compound was selected and integrated.

3.4 Results and Discussion

3.4.1 Desorption

It is inferred from equation 3.20 to equation 3.22 that the amount of an analyte remaining on the fiber decreases exponentially with time during a desorption process. The desorption rate is determined by the parameter a , which is defined in equation 3.13 and is determined by the mass transfer coefficients, the distribution coefficient, the physical dimensions of the sample matrix and the SPME polymer film. Factors that affect the parameter a are discussed later.

To validate the theoretical description of the desorption of analytes from a SPME fiber (equation 3.20 to equation 3.22), a 100 μm PDMS fiber (100 μm PDMS fibers were used throughout the experiments, unless specified otherwise) was used to extract a BTEX standard gas mixture for 2 min, and the BTEX loaded fiber was then exposed to the flow-through system to determine the desorption time profile. Figure 3-2 illustrates one of the desorption time profiles where $\ln(Q)$ is used as the y-axis, because $\ln(Q)$ changes with desorption time linearly and the slope is $-a$, according to equation 3.22. For all BTEX components, the linear correlation coefficients (R^2) are better than 0.99, which demonstrates that equation 3.20 to equation 3.22 are suitable to describe the kinetics of the SPME desorption process.

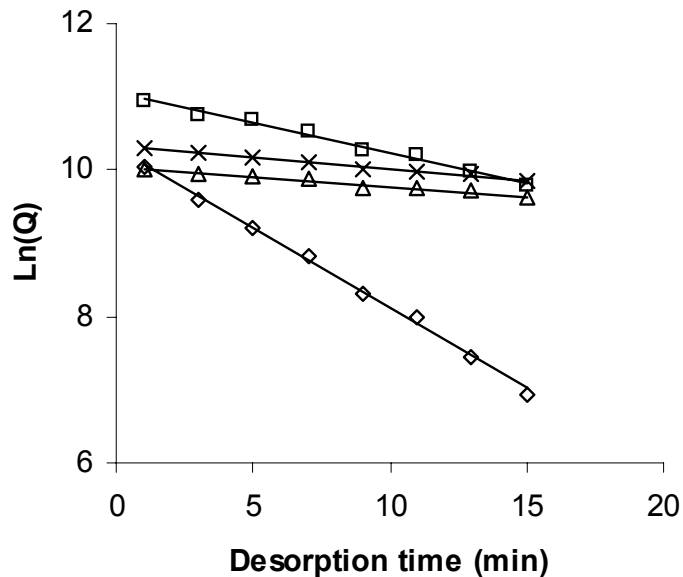


Figure 3-2 Desorption time profiles of benzene (\diamond), toluene (\square), ethylbenzene (Δ), and o-xylene (\times). Desorption of BTEX from a 100 μm PDMS fiber into water at a rate of 0.25 cm/s (at 25°C).

The slope ($-a$) in Figure 3-2 for BTEX decreases, in order for benzene, toluene, o-xylene, and ethylbenzene, which is consistent with the order of the absorption rate. This trend implies similarity between the desorption and absorption, which deserves further investigation.

3.4.2 Absorption Versus Desorption

Absorption of an analyte onto a SPME liquid coating fiber is theoretically described with equation 3.23:¹³

$$n = n_0 [1 - \exp(-at)] \quad \text{Equation 3.23}$$

where n is the amount of the extracted analyte, and n_0 is the amount of analyte extracted onto a fiber at equilibrium.

Equation 3.23 shares the same format as equation 3.21 for the desorption of an analyte from a SPME liquid coating fiber. The constant a in equation 3.23 for the absorption has the same definition as constant a in equation 3.21 for the desorption. In other words, the value of constant a , for the same analyte, should be the same for both the absorption and the desorption of the analyte, under the same experimental conditions (sample bulk velocity and temperature). This implies the isotropy of the absorption and the desorption of an analyte onto and from a SPME fiber, which can be demonstrated by rearranging equation 3.22 (desorption) into:

$$\frac{Q}{q_0} = \exp(-at) \quad \text{Equation 3.24}$$

and rearranging equation 3.23 (absorption) into:

$$\frac{n}{n_0} = 1 - \exp(-at) \quad \text{Equation 3.25}$$

the left side of equation 3.24 represents the fraction of the analyte remaining on the fiber after desorption time t , while the left side of equation 3.25 represents the fraction of the analyte absorbed on the fiber after absorption time t . When constant a has the same value for the absorption and the desorption, the sum of $\frac{Q}{q_0}$ (desorption) and $\frac{n}{n_0}$ (absorption) should be 1 at any desorption/absorption time.

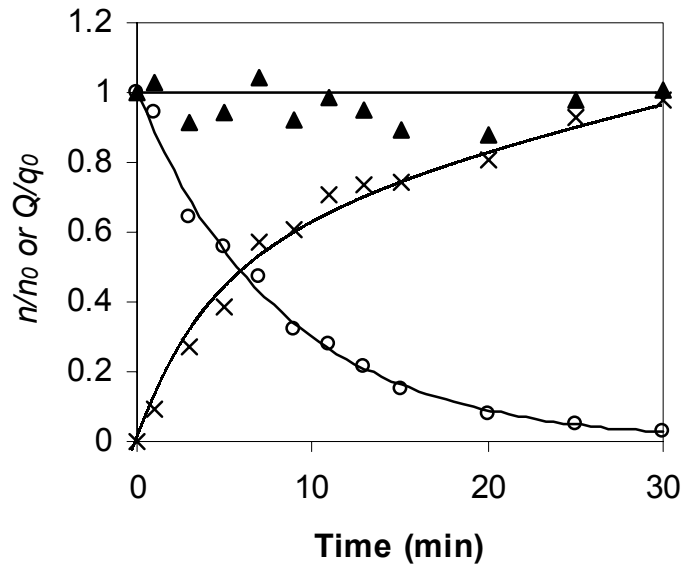


Figure 3-3 The isotropy of absorption and desorption in SPME. Simultaneous absorption of toluene (x) and desorption of deuterated toluene (*d*-8) (o) onto and from a 100 μm PDMS fiber from and into water at a rate of 0.25 cm/s (at 25°C). (\blacktriangle) represents of the sum of $\frac{Q}{q_0}$ and $\frac{n}{n_0}$.

Two experiments were carried out to validate the above conclusion. The first experiment involved the simultaneous determination of the desorption time profile of deuterated toluene (*d*-8) and the absorption time profile of toluene. A PDMS fiber was loaded with deuterated toluene, and the fiber was then exposed to a flowing standard BTEX aqueous solution for different experimental times. Figure 3-3 presents the values of $\frac{Q}{q_0}$

calculated from the resulting desorption time profile, the values of $\frac{n}{n_0}$ calculated from the

resulting absorption time profile, and the sum of $\frac{Q}{q_0}$ and $\frac{n}{n_0}$. Although the sum of $\frac{Q}{q_0}$ and

$\frac{n}{n_0}$ at any time is close to 1, it appears that the sum of $\frac{Q}{q_0}$ and $\frac{n}{n_0}$ is smaller than 1. This is

ascribed to the slight difference of physicochemical properties between deuterated toluene and toluene. This assumption is supported by the fact that the chromatographic peak of deuterated toluene does not completely overlap with that of toluene. Deuterated toluene is eluted prior to toluene by roughly 3 s. The constant a of deuterated toluene was also about 10% larger than that of toluene. As will be demonstrated, the difference could be corrected by knowing the difference of physicochemical properties between standards and target analytes.

The second experiment involved the separate determination of the absorption time profiles and the desorption time profiles of BTEX. The absorption time profiles were determined by exposing a PDMS fiber to a flowing standard BTEX aqueous solution for different experimental times. The desorption time profiles were determined by exposing a BTEX loaded PDMS fiber to flowing water (at the same velocity and temperature as for the determination of the absorption time profile) for different times. The sums of $\frac{Q}{q_0}$ (desorption) and $\frac{n}{n_0}$ (absorption) for all BTEX components are equal to 1 within 5% experimental error. The absorption constant a for each component of BTEX is equal to its desorption constant a , within 5%.

The aforementioned BTEX experiments proved the isotropy of the absorption and the desorption of an analyte onto and from a SPME fiber. Further implication is that by knowing the behavior of either the absorption or the desorption, the opposite one will also be understood. The application of this conclusion is clear. To determine the concentration of an analyte in a sample matrix, a certain amount of isotropically labeled analog is extracted onto a SPME liquid coating fiber. Then, the fiber is exposed to the sample matrix for a certain

time period, during which a part of the isotopically labeled analog is desorbed from the fiber and a certain amount of the analyte is absorbed onto the fiber. Constant a can be obtained using equation 3.22, by knowing the initial amount (q_0) of the isotopically labeled analog loaded onto the fiber, the sampling time t , and the amount (Q) of the isotopically labeled analog remaining on the fiber after sampling time t . As mentioned above, this constant a also characterizes the dynamic mass uptake process of the analyte onto the fiber. Utilizing the known constant a , n , and equation 3.23, in which n_0 is expressed as $\frac{KV_fV_s}{KV_f+V_s}C_0$ (equation 3.1), the concentration of the analyte (C_0) can be determined. The estimated concentration of toluene by the use of deuterated toluene in the first experiment was within 10% deviation from the concentration determined by headspace SPME. It is expected that the deviation would be smaller if an other type of isotopically labeled toluene was used, with more similar physicochemical properties to toluene.

When the agitation condition of the sample matrix and the concentration of the analyte are constant during a sampling period, it is possible to determine the analyte concentration without a standard, by exposing a fiber to the sample matrix for different times, even if the agitation condition of the sample matrix is unknown and an equilibrium is not reached. However, when the agitation condition of the sample matrix and/or the concentration of the analyte change(s) during a sampling period, a standard has to be used to determine the analyte concentration. This is because the determination of the initial amount of the standard loaded onto a fiber (q_0) is separate from the sampling period. Exposure of the fiber to a sample matrix just one time is enough to determine the constant a , while it requires at least two exposures of the fiber to a sample matrix, for different times, to determine the

constant a without a standard, and the agitation condition of the sample matrix and the concentration of the analyte must be constant during the entire sampling period.

3.4.3 Calibration of Rate of Absorption using Rate of Desorption

In equation 3.22, the parameter a , which is defined in equation 3.13, is a constant that is a measure of how quick a desorption equilibrium can be reached. It is determined by the mass transfer coefficients, the distribution constant, the physical dimensions of the sample matrix and the fiber coating. Analysis of how these factors affect parameter a would be helpful for a better understanding of the mass transfer process associated with the desorption or the absorption of an analyte from or onto a SPME fiber.

The numerator and denominator of the right side of equation 3.13 are divided by the sample volume V_s and the mass transfer coefficient h_f :

$$a = \frac{2Ah_s \left(\frac{KV_f}{V_s} + 1 \right)}{2KV_f + \frac{h_s V_f}{h_f}} \quad \text{Equation 3.26}$$

When V_s is far larger than KV_f , such as during field sampling, equation 3.26 can be simplified to:

$$a = \frac{2Ah_s}{2KV_f + \frac{h_s V_f}{h_f}} = \frac{2Ah_s}{(2K + \frac{h_s}{h_f})V_f} = \frac{2A}{\left(\frac{2K}{h_s} + \frac{1}{h_f} \right)V_f} \quad \text{Equation 3.27}$$

where $\frac{K}{h_s}$ and $\frac{1}{h_f}$ represent relative mass transfer resistance in the boundary layer and in the fiber coating, respectively.

When $\frac{K}{h_s}$ is far smaller than $\frac{1}{h_f}$, such as during the air sampling of volatile organic compounds (VOCs), or during the water sampling of VOCs with perfect agitation (small K and large h_s), the overall mass transfer resistance is contained within the fiber coating. In other words, the diffusion in the fiber coating controls the overall mass transfer rate. A change in the agitation conditions of the sample matrix does not affect mass transfer rate for either the absorption or the desorption. Figure 3-4 illustrates the desorption of o-xylene from a PDMS fiber into clean air, with a linear velocity ranging from 0.02 to 37 cm/s. No significant difference for the desorption rate was found, which is similar to the absorption of o-xylene onto a PDMS fiber under the same conditions. Thus it is not necessary to utilize a standard to calibrate the effect of agitation under these conditions. Since the equilibrium time is very short when $\frac{K}{h_s}$ is far smaller than $\frac{1}{h_f}$, an equilibrium extraction is generally used for quantification.

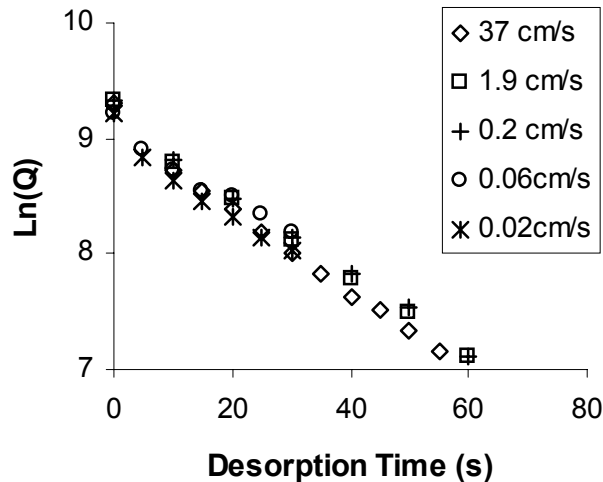


Figure 3-4 Desorption of o-xylene from a 100 μm PDMS fiber into clean air at various flow velocities (at 25°C).

Rearranging equation 3.27 yields to equation 3.28,

$$h_f = \frac{aV_f}{2A} \quad \text{Equation 3.28}$$

The mass transfer coefficient h_f in the coating can be determined with constant a . Since h_f is defined as D_f/δ_f , where δ_f is the thickness of the coating, it is thus possible to estimate the diffusion coefficient D_f of the analyte in the polymeric coating. The diffusion coefficient D_f of o-xylene was found to be $(1.15 \pm 0.08) \times 10^{-6}$ cm²/s from the above experiments, which is in the estimated range of the diffusion coefficient of VOCs in PDMS.¹ The procedure described herein to estimate the diffusion coefficient in liquid polymer coatings using SPME is very simple, and has a number of advantages. First, the only parameter that must be determined experimentally is constant a , and the determination process is quite simple. It involves exposure of a fiber to a standard gas, or an analyte-loaded fiber to clean air, for different experimental times. Constant a can then be determined from the absorption or the desorption time profile without any calibration. Second, the geometries of the fibers are well defined and their physical dimensions are guaranteed by the fiber manufacturers. Therefore, the estimation of the diffusion coefficient using SPME is very fast and simple.

When $\frac{K}{h_s}$ is comparable to $\frac{1}{h_f}$, such as during the water sampling of VOCs with practical agitation, or during the air sampling of semi VOCs with weak agitation, both the diffusion in the boundary layer and the diffusion in the coating contribute to the overall mass transfer rate. This is the most complicated experimental situation possible, where a change of the agitation conditions only “partially” changes the overall mass transfer rate. Although no

simple theoretical solution could be found, calibration of the effect of the agitation condition using a standard (such as an isotopically labeled analog) is a practical experimental tool.

When $\frac{K}{h_s}$ is far larger than $\frac{1}{h_f}$, such as during the water sampling of VOCs and semi-VOCs with weak agitation, or during sampling using a porous solid coating fiber, diffusion in the boundary layer controls the overall mass transfer rate. In this case, the rearrangement of equation 3.27 results in:

$$h_s = \frac{aKV_f}{A} \quad \text{Equation 3.29}$$

The mass transfer coefficient in the boundary layer can be estimated from constant a , if K is known. Not only can the mass transfer coefficient estimated from equation 3.29 be used to characterize the absorption process under the same conditions, but also it can be used to estimate the effective thickness of the boundary layer (δ).

It can therefore be concluded that the use of an isotopically labeled analog as a standard is a feasible solution for the calibration of the convection effect, for those conditions in which the diffusion in the boundary layer partially or completely control the overall mass transfer rate. However, there are disadvantages to this method. First, the isotopically labeled analog of the target analyte may not always be available. Second, each target analyte requires its own isotopically labeled analog. When the number of target analytes increases, the requirement for corresponding isotopically labeled analogs increases the expense and difficulty of analysis.

A more universal solution is that only one standard is loaded onto the fiber, and the mass transfer coefficients or constant a of target analytes are extrapolated from that of the standard, based on the diffusion mass transfer. During the desorption/absorption of VOCs

with weak agitation, and semi VOCs into/from water with practical agitation, diffusion in the boundary layer controls the overall mass transfer. If the diffusion coefficient of the standard is different from that of the target analyte, their mass transfer coefficients are different. In an aqueous solution, the diffusion coefficients of most organic compounds are in the range of $\sim 10^{-5}$ cm²/s. If the molecular size of the standard does not differ greatly from that of the target compound, their diffusion coefficients and their mass transfer coefficients do not differ greatly. h_s , estimated from equation 3.29, can be used to roughly characterize the absorption of the target analyte for fast screening purposes.

To further describe the absorption of the target analyte by the use of a standard, the mass transfer coefficient of the target analyte can be reliably extrapolated from the mass transfer coefficient of the standard. As suggested by various mass transfer correlations, the mass transfer coefficient varies with the diffusion coefficient to the 0.5 to 0.7 power,¹⁴ and the midpoint 0.6 is used in these studies. In other words, $\left(\frac{D}{D_s}\right)^{0.6}$ is used as a correction factor.

$$h = \left(\frac{D}{D_s}\right)^{0.6} h_s \quad \text{Equation 3.30}$$

where D is the diffusion coefficient of target analyte in the sample matrix, h is the mass transfer coefficient of the target analyte in the boundary layer.

Once h is known, the mass uptake (n) or the concentration of the target analyte (C) can be easily estimated from equation 3.31 or equation 3.32 if the fiber coating acts as a 'zero sink' towards the target analyte, i.e. $C' = 0$ (Figure 3-1):

$$n = AhCt \quad \text{Equation 3.31}$$

$$C=n/(Aht)$$

$$\text{Equation 3.32}$$

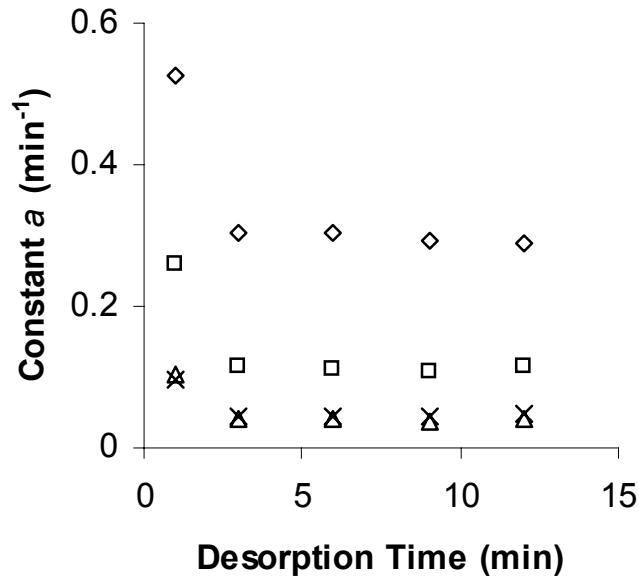


Figure 3-5 Desorption time profile of constant a : desorption of benzene (\diamond), toluene (\square), ethylbenzene (Δ), and o-xylene (\times) from a 100 μm PDMS fiber into water at a rate of 0.25 cm/s (at 25°C).

To validate the proposed method, a BTEX mixture was used as the standard. One advantage to loading several standards with different volatilities on a fiber at the initial validation stage is that helps to understand the desorption process and helps to optimize the experiments. Figure 3-5 presents one of the constant a time profiles obtained with the exposure of a PDMS fiber, preloaded with BTEX, in pure water for different times under various agitation conditions. The initial values of constant a are high, but they level off quickly. This reflects the unsteady mass flux at the beginning of the desorption, and the steady mass flux is reached when constant a does not change with time. Figure 3-5 also shows that the constant a decreases with the increase of the distribution coefficient K . The

larger the distribution coefficient, the longer the equilibrium time, and this agrees with Figure 3-5.

However, the effect of the diffusion in the boundary layer on the overall mass transfer rate can not be directly derived from constant a , unless the mass transfer coefficient can be estimated from constant a , especially with different agitation conditions, as shown in Figure 3-6. For this case, the overall mass transfer resistance is assumed to be contained within the diffusion in the boundary layer and the mass transfer coefficient h_s is estimated from equation 3.29. The mass transfer coefficients h_s of BTEX increases as the water agitation is increased. However, the mass transfer coefficients h_s of benzene are smaller than those of toluene, ethylbenzene, and o-xylene. With the increase of the water velocity, the difference between the mass transfer coefficients h_s of benzene and those of toluene, ethylbenzene, and o-xylene increases, while the mass transfer coefficients h_s of toluene, ethylbenzene, and o-xylene are still similar to each other. It is therefore suggested that the use of equation 3.29 to estimate the h_s of benzene is not appropriate under the experimental conditions used in this study. Referring to equation 3.27, the ratio of h_s over h_f must be significantly smaller than the distribution coefficient K when equation 3.29 is used to estimate h_s . Under the experimental agitation conditions, h_s/h_f is estimated to be about 10.¹³ If the distribution coefficient K is smaller than 100, h_s is underestimated by the use of equation 3.29 (the distribution coefficient K of benzene is about 53 at 25°C). This suggests that the use of a standard with a large K , especially under vigorous agitation, or the use of a porous fiber coating, where the overall mass transfer is exclusively contained within the boundary layer within the experimental period, could improve the accuracy of the method.

Various empirical correlations suggest that the mass transfer coefficient varies with the 0.7 power of the fluid linear velocity.¹⁴ Data presented in Figure 3-6 demonstrate that the power was 0.69, 0.69, and 0.71 for toluene, ethylbenzene, and o-xylene, respectively, which indicates that the calculation of the mass transfer coefficient h_s from equation 3.29, with the use of constant a , is reliable for toluene, ethylbenzene, and o-xylene under the experimental conditions used in this study.

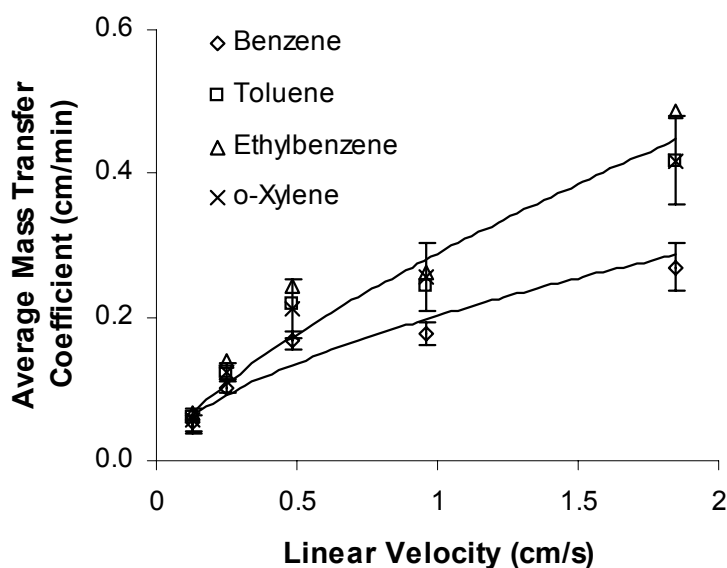


Figure 3-6 The dependence of mass transfer coefficient on the linear velocity of water. Error bars signify ± 1 standard deviation from the mean of the mass transfer coefficient of benzene and o-xylene. Relative experimental errors of toluene and ethylbenzene are comparable to those of o-xylene.

The next validation was completed by exposing a BTEX loaded PDMS fiber to a PAH standard aqueous solution for different times under various agitation conditions. The mass transfer coefficients (h) of the PAHs in the boundary layer were estimated from equation 3.30. PDMS coating is assumed to be a ‘zero sink’ for PAHs for short sampling periods, due to its high affinity toward PAHs.¹⁵ The predicted mass uptakes (n) of PAHs

were estimated from equation 3.31. Figure 3-7 illustrates the comparison of the predicted mass uptake with the experimental mass uptake (only the results of fluorene are shown, while the results of the other PAHs used in the experiments, and the results for other agitation conditions, exhibit similar trends to those presented in Figure 3-7). The mass uptake predicted by the use of benzene is significantly smaller than the experimental mass uptake, because the mass transfer coefficient is underestimated. When toluene, ethylbenzene, or o-xylene was used as the standard, the predicted mass uptake of fluorene agrees with the experimental mass uptake well, which demonstrates the feasibility of the proposed method.

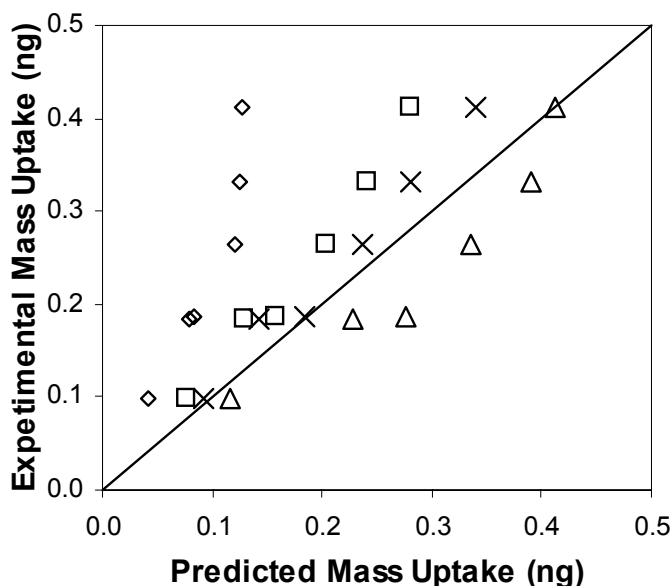


Figure 3-7 Validation of the calibration of uptake of PAHs (fluorene as the example) onto a 100 μm PDMS fiber by the use of desorption of a standard from the same fiber into a standard PAHs aqueous solution of 0.27 cm/s at 25°C. Experimental mass uptake vs. predicted mass uptake with benzene (◇), toluene (□), ethylbenzene (Δ), and o-xylene (x) as the standard.

For the experiments presented herein, the flow direction of the sample matrix was perpendicular to the axis of the fiber. However, it is not critical to the method that the flow

direction of the sample matrix is perpendicular to the axis of the fiber. When the orientation of the flow direction of the sample matrix and the axis of the fiber changes, the thickness of the boundary layer and its distribution along the fiber change, resulting in changes to the mass transfer resistance in the boundary layer. But the change exerts the same influence on the absorption and the desorption, simultaneously. In other words, the isotropy of the absorption and the desorption of the analyte is independent of the orientation of the flow direction of the sample matrix and the axis of the fiber. Figure 3-8 demonstrates that when the axis of the fiber is perpendicular, at 45 degree, or parallel to the flow direction of the sample matrix, the mass uptake of fluorene can still be reliably predicted by the use of a standard (o-xylene in this case). This is an advantage of methods utilizing internal standards which is normally difficult to achieve.

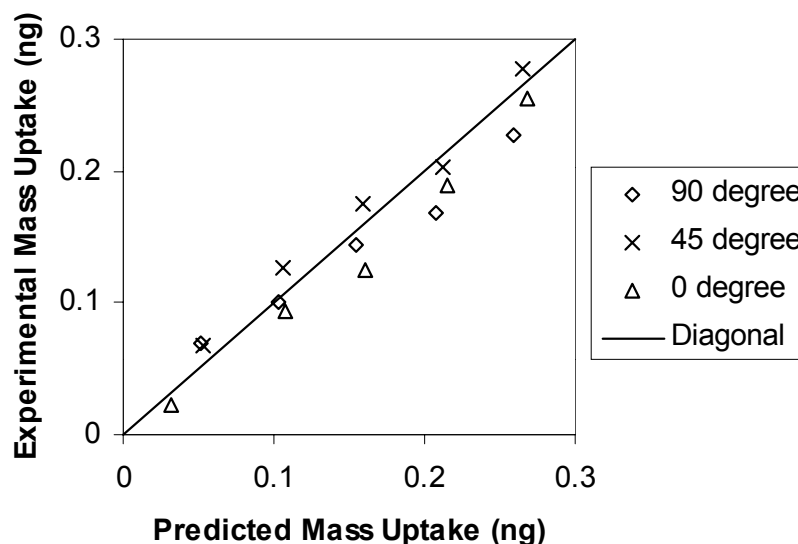


Figure 3-8 Calibration of the uptake of PAHs (fluorene as the example) onto a 100 μm PDMS fiber by the desorption of o-xylene from the same fiber into a standard PAHs aqueous solution at a rate of 1.2 cm/s (at 25°C), when the axis of the fiber is in different orientations to the flow direction of the standard solution.

From this discussion, it is proposed that the calibration is also independent of the geometry of the extraction phase, which allows the use of specially designed extraction phases for some challenging applications, such as *in-vivo* analysis.

3.4.4 Effect of Extraction Temperature

If the physical dimensions of the fiber do not change within the experimental temperatures, the effect of temperature on the calibration is focused on the change of the mass transfer coefficient with temperature. Mass transfer coefficient h is defined as D/δ . By studying the effect of temperature on D and δ , the effect of temperature on the mass transfer coefficient will be straightforward, and has been qualitatively discussed in the literature.⁹ In this study, the effect of the extraction temperature is addressed in a different way.

According to equation 3.29, the mass transfer coefficient is dependent on both the distribution coefficient K and the time constant a .

3.4.4.1 The Temperature Dependence of Distribution Coefficient K

The distribution coefficient decreases with the increase of temperature because the partition of analytes from water onto the PDMS is an exothermic process. The relationship between the distribution coefficient and temperature is:¹

$$K = K_0 \exp \frac{-\Delta H}{R} \left(\frac{1}{T} - \frac{1}{T_0} \right) \quad \text{Equation 3.33}$$

where K_0 is the distribution coefficient when both the fiber and the sample are at temperature T_0 , ΔH is the molar change in enthalpy of the analyte when it moves from the sample matrix to the fiber coating, and R is the gas constant.

However, equation 3.33 is often used for qualitative discussion of the temperature effect, due to the lack of ΔH . It is therefore necessary to determine the quantitative relationship between the distribution coefficient and temperature experimentally.

Table 3.1 summarizes the distribution coefficients of BTEX at temperatures from 12.3 to 28.3°C, determined with the flow-through system. The distribution coefficients decreased with the increase of temperature, which conforms to the theoretical prediction. K for BTEX at 22 °C are 58, 185, 584, and 465, which agree well with those reported in the references,¹ i.e. 58, 189, 566, and 485, respectively. $\ln K$ was correlated with $1/T$, and the slope was used to calculate ΔH . It was found that the average ΔH for BTEX were 10100, 10100, 10500, and 12400 J/mol within the experimental temperature range, respectively. Although ΔH is dependent on temperature, it does not change a great deal under a normal experimental temperature range, such as from 5 to 40°C. It is thus possible to extrapolate the distribution coefficients of BTEX at other temperatures with the use of the average ΔH and equation 3.33. The uncertainty within the experimental temperature range is about 5-10%. It is expected that the uncertainty outside the experimental temperature range will be larger than 5-10%.

Table 3.1 Distribution coefficients of BTEX between the PDMS coating* and water at various temperatures.

Temperature (K)	Distribution Coefficient K			
	Benzene	Toluene	Ethylbenzene	o-Xylene
285.45	62±4	204±11	647±35	525±26
288.45	61±5	201±5	633±36	520±31
291.45	61±5	192±14	608±42	485±34
295.75	58±6	185±16	584±51	465±39
298.35	53±4	171±11	546±52	429±35
301.45	50±7	164±22	507±68	399±54

* 100 μm PDMS fiber coating

3.4.4.2 The Temperature Dependence of Time Constant a

As mentioned previously, the time constant a is a measure of how fast a desorption/absorption equilibrium can be reached, and is determined by the mass transfer coefficients, the distribution coefficient, the physical dimensions of the sample matrix and the fiber coating. Therefore, the temperature effect on the time constant a is quite complicated, as suggested by equation 3.13.

To simplify the discussion, equation 3.29 is rearranged to:

$$a = \frac{Ah_s}{KV_f} \quad \text{Equation 3.34}$$

Assuming that the volume and surface area of the fiber do not change during normal experimental conditions, the change of temperature affects the time constant a in two respects. First, the diffusion coefficient and the mass transfer coefficient increase as the

experimental temperature increases. Second, the distribution coefficient decreases as the experimental temperature increases. The overall temperature effect is that the time constant a increases as the experimental temperature increases, and the effect is more significant than the temperature effect on the mass transfer coefficient. Figure 3-9 demonstrates that the higher the temperature, the shorter the equilibration time.

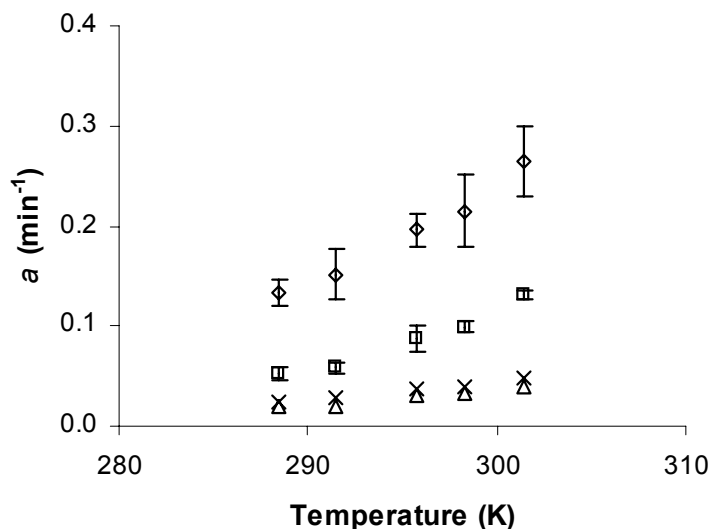


Figure 3-9 The temperature dependence of constant a . Desorption of benzene (◇), toluene (□), ethylbenzene (Δ), and o-xylene (x) from a 100 μm PDMS fiber into water at a rate of 0.25 cm/s at various temperatures. Relative experimental errors of ethylbenzene and o-xylene are comparable to those of toluene.

After the temperature effects on the distribution coefficient K and time constant a have been determined, the temperature dependence of the mass transfer coefficient can be obtained by the combination of the two effects. With the increase of temperature, the mass transfer coefficient increases with the increase of a , but the increase is partially offset by the decrease of the distribution coefficient. Figure 3-10 illustrates the overall temperature effect

on the mass transfer coefficient. As expected, the mass transfer coefficient increases with the increase of temperature. In other words, the mass desorb/uptake rate increases with the increase of temperature, under the same agitation conditions.

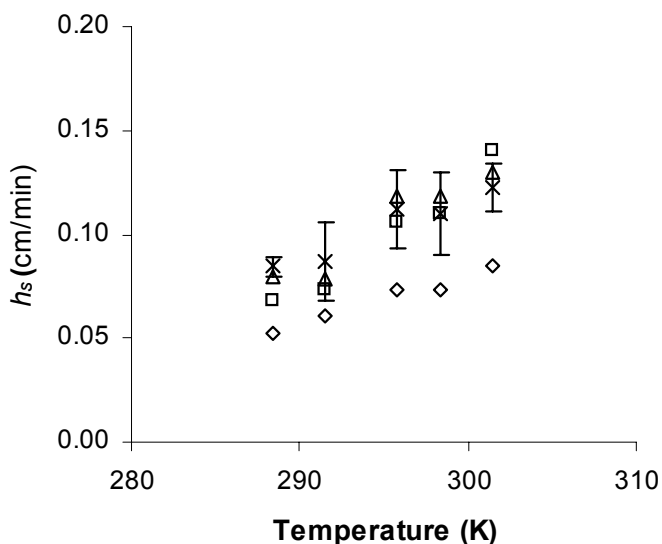
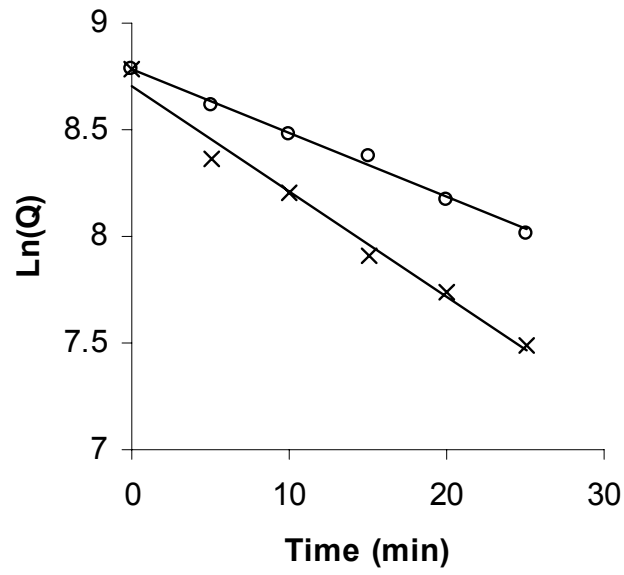


Figure 3-10 The temperature dependence of the mass transfer coefficient. Desorption of benzene (\diamond), toluene (\square), ethylbenzene (Δ), and o-xylene (\times) from a 100 μm PDMS fiber into water at a rate of 0.25 cm/s at various temperatures. Error bars signify ± 1 standard deviation from the mean of the mass transfer coefficient of o-xylene. Relative experimental errors of other compounds are comparable to those of o-xylene.

When a BTEX-loaded PDMS fiber was exposed to a flowing standard PAH aqueous solution at two different temperatures (15 and 25°C), the increase of the desorption rate of BTEX from the fiber (o-xylene, as shown in Figure 3-11 (A)) and the increase of the uptake rate of PAHs (fluorene, as shown in Figure 3-11 (B)) were observed simultaneously. In other words, temperature affects both the absorption and the desorption processes in the same way. It is thus understandable that the uptake of PAHs could be reliably predicted by the use of a standard.

(A)



(B)

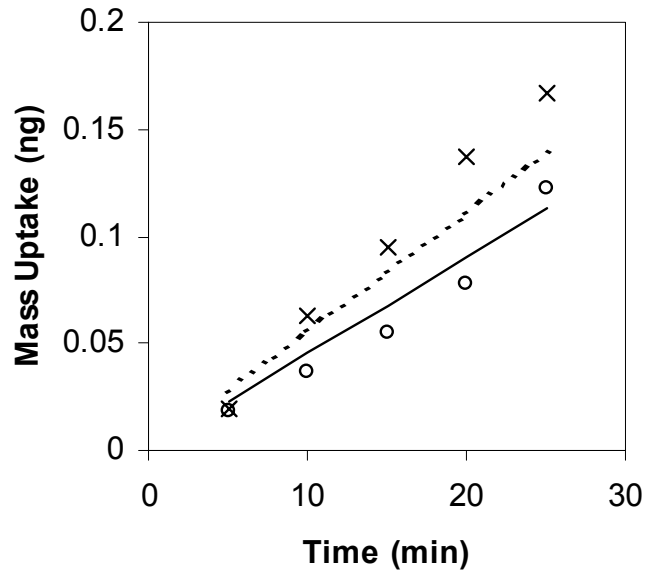


Figure 3-11 Calibration of uptake of PAHs (fluorene as the example) onto a 100 μm PDMS fiber by the desorption of o-xylene from the same fiber into a standard PAHs aqueous solution at a rate of 0.25 cm/s (at 15°C (o) and 25°C (x)). (A) Desorption time profile of o-xylene. (B) Mass uptake profile of fluorene. —: prediction for 15°C; ---: prediction for 25°C.

3.5 Conclusion

The isotropy of absorption and desorption in SPME allows for the calibration of absorption using desorption. This is especially important for the calibration of on-site, *in-situ*, or *in-vivo* analysis, because the control of the agitation condition of the matrix is sometimes difficult, and direct spiking of standards into the matrix is typically not possible in these cases. However, in this study, successful calibration was accomplished by introducing standards together with the extraction phase, while investigating kinetics of the absorption/desorption process. Since the mass transfer rate is controlled by the diffusion in the boundary and/or in the extraction phase in most of the pre-equilibrium absorption/desorption, desorption of the standards can be used to determine the mass transfer rate, which can be used for the calibration of the absorption of the target analytes.

In the most advanced approach, the standard can be added to balance the analyte loss from the matrix during the extraction, to minimize the impact of the extraction of the analyte from the investigated system. This objective is accomplished by adding the same amount of the standard as that of the analyte removed from the matrix, and the isotropically labeled analog of the target analyte can be chosen as the standard. In addition, this approach can provide insights into the physicochemical partitioning and adsorption phenomena among sample matrix components.

The standard in the extraction phase calibration can be applied in any microextraction or steady state approach, including SPME, micro liquid phase extraction (MLPE), membrane extraction, or headspace extraction. In SPME, the standard can be used to dope the solid/polymeric extraction phase and in MLPE, the standard would be present in the liquid

extraction phase. In membrane extraction, the standard would be present in the stripping phase, and, in headspace extraction, the standard would be present in the gaseous headspace.

3.6 References

-
- ¹ Pawliszyn, J. *Solid Phase Microextraction – Theory and Practice*; Wiley–VCH; New York, 1997.
 - ² Martos, P.A.; Saraullo, A. and Pawliszyn, J. *Anal. Chem.*, **1997**, 69, 402.
 - ³ Chai, M. and Pawliszyn, J. *Environ. Sci. Technol.*, 1995, 29, 693.
 - ⁴ Martos, P.A. and Pawliszyn, J. *Anal. Chem.*, **1997**, 69, 206.
 - ⁵ Potter, D.W. and Pawliszyn, J. *Environ. Sci. Technol.* **1994**, 28, 298.
 - ⁶ Grote, C.; Levsen, K. The Application of SPME in Water Analysis. In *in* Pawliszyn, J. (ed.); *Applications of Solid Phase Microextraction*; RSC; Cambridge, UK, 1999; Chapter 12, pp. 169–187.
 - ⁷ Górecki, T. Solid versus Liquid Coatings, *in* J. Pawliszyn (ed.); *Applications of Solid Phase Microextraction*; RSC; Cambridge, UK, 1999, Chapter 7, pp. 92–108.
 - ⁸ Koziel, J.; Jia, M. and Pawliszyn, J. *Anal. Chem.* **2000**, 72, 5178.
 - ⁹ Chen, Y.; Koziel, J.A. and Pawliszyn, J. *Anal. Chem.* **2003**, 75, 6488.
 - ¹⁰ Xiong, G.; Chen, Y. and Pawliszyn, J. *J. Chromatogr. A.* **2003**, 999, 43.
 - ¹¹ Koziel, J. A.; Jia, M.; Khaled, A.; Noah, J. and Pawliszyn, J. *Anal. Chim. Acta* **1999**, 400, 153.
 - ¹² Koziel, J. A.; Martos, P.A. and Pawliszyn, J. *J. Chromatogr. A* **2004**, 1025, 3.
 - ¹³ Ai, J. *Anal. Chem.* **1997**, 69, 1230.

¹⁴ Cussler, E.L., Diffusion: mass transfer in fluid systems. New York: Cambridge University Press, 1997.

¹⁵ Shurmer, B. and Pawliszyn, J. *Anal. Chem.*, **2000**, 72, 3660.

Chapter 4 Time-Weighted Average Passive Sampling

4.1 Introduction

In 1970, to protect workers who might be exposed to airborne pollutants for eight hours per day, forty hours per week, for a working lifetime, from adverse effect the Occupational Safety and Health Administration (OSHA) established limit values specifying maximum allowable employee exposure levels to approximately 400 substances, on a TWA concentration basis, for eight hours exposure. OSHA now is in the process of promulgating expanded standards for employee exposure to toxic substances. Accompanying these proposed standards are requirements for monitoring of employee long-term exposure. This can be achieved in two ways.¹ One is to take many grab samples during the period of interest then average the concentrations for the total sampling time. The average analyte concentration can be determined by use of equation 4.1:

$$\bar{C} = \frac{C_1t_1 + C_2t_2 + C_3t_3 + \dots + C_nt_n}{t_1 + t_2 + t_3 + \dots + t_n} = \frac{\sum_{i=1}^n C_i t_i}{\sum_{i=1}^n t_i} \quad \text{Equation 4.1}$$

where \bar{C} is the TWA concentration and C_i is the analyte concentration observed for time period t_i . Alternatively, for convenience and cost, only one sample is acquired if the mass loading of the analyte of interest is directly proportional to the gaseous analyte concentration for the entire time period of interest. The latter method is highly recommended, because of its simplicity and cost-effectiveness and because it obviates the need to acquire a large number of samples to describe the TWA concentration.

Two general strategies — active or passive sampling — can be used to achieve the latter. Active sampling methods utilize pumps to draw air at a constant mass flow rate through a solid or liquid collecting medium which extracts the target analytes of interest.² Although active sampling methods are generally believed to be more accurate, and many standard methods are based on them, they do suffer from disadvantages when used for TWA sampling. In TWA sampling of whole air samples the sampling systems and interfaces to gas chromatographic equipment are costly and can require substantial maintenance. Sorbent beds, in turn, cannot be re-used and typically require chemical desorption with toxic eluents. Sampling of analytes into a liquid medium with bubblers is not very practical, because it is difficult to maintain the sampling device in a vertical position when worn by individuals while they are performing their daily work activities. The use of pumps also has significant drawbacks, e.g. relatively high unit cost, need for periodic replacement, because of their relatively short service time, limitation of sampling time by battery lifetime, and workers' resistance to wearing active devices throughout the whole working day, owing to their bulk, weight, and the noise generated by the pumps.³

To obviate the need for air sampling pumps truly quantitative passive sampling, which is based on molecular diffusion, was first introduced in 1973.⁴ Since then much effort has been devoted to the development of new types and applications of passive samplers. Although there is great variety in the details of implementation of the different types of passive sampler, all share a common characteristic — the presence of a barrier between the medium sampled and the collecting medium. The barrier defines the rate at which analyte molecules at a given concentration can be collected, which is crucial for quantitative

analysis. In practice, the barrier usually falls into one of two categories — diffusion or permeation — which form the basis for the most general classification of passive samplers.

However, most passive sampling devices currently available still require use of highly toxic solvents as the collecting medium or for chemical desorption, are not reusable, and are not amenable to automation. There are some types of dosimeter used for passive sampling can be thermally desorbed, but special accessory equipment is needed which requires some maintenance; in addition, cryofocus is usually needed.⁵

SPME is a solvent-free technique that combines sampling and sample preparation in a single step.⁶ Since its inception SPME has been used to sample a considerable number of waterborne and airborne analytes.⁷

Preliminary investigations have provided strong evidence that the SPME device can be used as a passive sampler. Martos *et al.* used PDMS fibers for passive sampling of a wide range of hydrocarbons and found that this fiber coating does not act as a zero sink for volatile compounds.⁸ Khaled *et al.* used both PDMS and PDMS/DVB fibers for passive sampling of normal alkanes from C₅ to C₁₅. Good results were obtained from sampling of organic compounds of medium volatility with PDMS/DVB fibers, but not for compounds of higher or lower volatility because of either weak affinity or adsorption on the needle.⁹

In this work a modified SPME device is shown to be a viable passive sampler without the drawbacks of conventional passive sampling systems, and a comprehensive study of TWA passive sampling with an SPME device was started by testing three fibers — 100 µm polydimethylsiloxane (PDMS-100), 65 µm polydimethylsiloxane/divinylbenzene (PDMS/DVB-65) and 75 µm CarboxenTM/Polydimethylsiloxane (CAR/PDMS-75) — for the three prerequisites of passive sampling — ‘zero sink’, face velocity, and response time. This

was followed by the validation of diffusion-based calibration and a study of the effects of environmental conditions, e.g. temperature, pressure, and relative humidity, on TWA passive sampling with a SPME device. Finally, a SPME device was used for field sampling and the results were compared with those obtained by use of NIOSH method 1501. This systematic study has demonstrated the viability of the SPME device as a tool for TWA passive sampling of VOCs in air.

4.2 Theory

Detailed description of theory for TWA passive with a SPME device can be found in Chapter 1, section 1.3.5.3.

4.3 Experimental Section

4.3.1 Chemicals

n-Pentane, *n*-hexane, *n*-heptane, *n*-octane, *n*-nonane, *n*-decane, *n*-undecane, carbon disulfide, and toluene were purchased from Sigma–Aldrich (Mississauga, ON, Canada).

4.3.2 Materials

All SPME fibers and holders, ORBO™-32 tubes, gas purifiers, Teflon™ tubing, syringes, Thermogreen™ septa, gas sampling bulbs, and vials were purchased from Supelco (Oakville, ON, Canada). Six additional grooves were made on the barrel of the SPME holder with 5 mm spaced and 3 additional holes were made on the plunger of the SPME holder

which are 0.5, 1 and 3 cm away from original one, the modification was allowed to precisely control the diffusion path length from 0.3 to 3.5 cm. Deactivated needles are from Restek (Bellefonte, PA, USA). The timer was purchased from VWR (Mississauga, ON, Canada). Ultra-high-purity hydrogen, nitrogen, oxygen, and helium were purchased from Praxair (Waterloo, ON, Canada). Personal air pumps and the mini-Buck calibrator were purchased from A.P. Buck (Orlando, FL, USA). Ultra-pure air for the standard gas generator and for flame ionization detection was supplied by a Whatman zero air generator (model 76-803).

4.3.3 Standard Gas Generator

The standard gas generator has been described in Chapter 2, section 2.3.4.1.

4.3.4 Sampling Chamber

The sampling chambers have been described in Chapter 2, section 2.3.4.2.

To generate a standard gas with different levels of relative humidity, an in-line impinger trap (Supelco) was installed. A digital humidity meter (Canadawide Scientific, Ottawa, ON, Canada) was used to measure the relative humidity. Relative humidity of different levels was obtained by maintaining the water level in the impinger trap at different height.

Ozone was generated by a homemade generator constructed by the electronic science shop (University of Waterloo, ON, Canada), and mixed with standard gas before entering the sampling chamber. The concentration of ozone can be controlled by adjusting either the

voltage of discharge electrodes or flow-rate of oxygen and was measured by Dräger tubes (Dräger Sicherheitstechnik GmbH, Germany).

4.3.5 Instrumentation and Methods for SPME and Liquid Injections

A Varian star computer-controlled Varian 3400 CX gas chromatograph equipped with a carbon dioxide cooled septum-equipped programmable injector (SPI) was used for all experiments. A 0.8 mm i.d. SPI insert was coupled to a RTX-5 column (30 m, 0.25 mm i.d., 1.0 μm film thickness) and the column was coupled to a flame-ionization detector (FID). The injector was maintained at 250°C for PDMS-100 and PDMS/DVB-65 fiber injection and at 300°C for CAR/PDMS-75 fiber injection. For liquid injections the injector temperature was initially 35°C for 0.1 min and then ramped to 250°C at 300°C min^{-1} . For SPME fiber and liquid injections the column temperature was maintained at 35°C for 2 min then programmed at 30°C min^{-1} to 230°C that was held for 5 min. The carrier gas (helium) head pressure was set to 20 psig (~ 138 kPa) for both SPME fiber and liquid injection except for CAR/PDMS-75 fiber injection, for which it was 30 psig (~ 207 kPa). Detector gas flow rates were 300 mL min^{-1} for air and 30 mL min^{-1} for nitrogen and hydrogen.

The instrument was checked on a daily basis by calibration with a liquid midpoint calibration standard. Any deviation in area counts greater than 15% required re-injection of that standard; if then the deviation was still greater than 15% the instrument was recalibrated with a six-point calibration plot. Peak shape quality, resolution, and retention times were also carefully monitored to ensure all chromatography was within all required specifications.

4.3.6 Field TWA Sampling with SPME using A CAR/PDMS-75 Fiber

NIOSH method 1501 for determination of hydrocarbons in air was chosen as the reference method. A mass-flow-controlled air-sampling pump was used to draw air through charcoal tubes at a known flow rate from 50 to 100 mL min⁻¹. The analytes were then desorbed with 1 mL carbon disulfide in a PTFE-capped 2 mL vial.

For TWA sampling with SPME eight CAR/PDMS-75 fibers were conditioned at 250°C for 1 h then retracted and sealed with narrow-bore solid TeflonTM caps. Six were used for sampling and the other two as blanks.

All samples were analyzed on a Varian 3400 GC with a carbon dioxide cooled SPI and coupled with MS. The conditions for fiber and liquid injection were as described for GC–FID. The initial column temperature was 35°C. This was maintained for 3 min for SPME and 1 min for liquid injection, and then ramped at 10°C min⁻¹ to 250°C, which was held for 5 min. All SPME with CAR/PDMS-75 and active charcoal tube samples were analyzed immediately after acquisition. The approximate sampling temperature was 296 K during the sampling period.

4.4 Results and Discussion

4.4.1 Three Prerequisites

4.4.1.1 Zero Sink

To achieve successful TWA passive sampling three basic prerequisites must be satisfied.^{10,11,12,13} The first is that the sorbent of a passive sampler should be a ‘zero sink’ for

the target analytes, i.e. $C_{\text{sorbent}}=0$ (Figure 1-12). This ensures that when an analyte is sorbed the rate of mass loading of additional analyte is not affected.

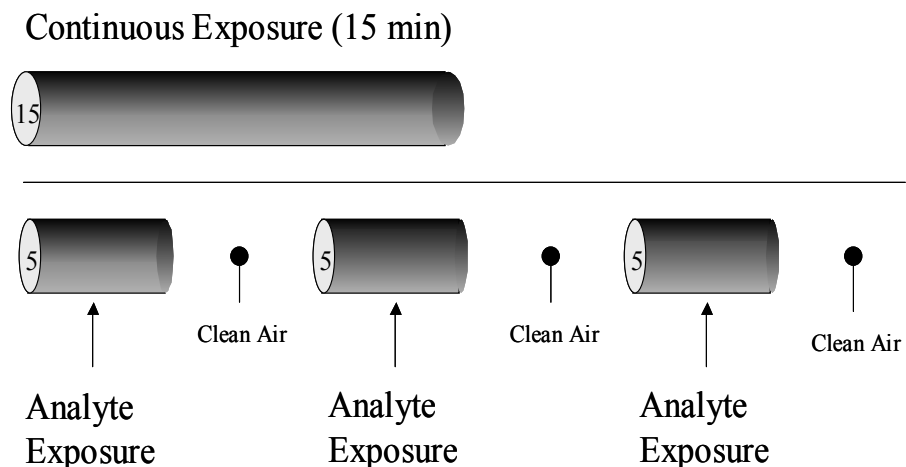


Figure 4-1 Continuous (15 min) and intermittent (15 min total) retracted-fiber exposure to the standard gas with a total of 15 min exposure to clean air.

The 'zero sink' effect for the SPME device was tested by use of an empirical approach based on intermittent and continuous exposure to the test gas.⁸ The concept is that a strong sorbent will retain the analytes during the time analyte concentrations vary from high to low. Figure 4-1 depicts the retracted-fiber exposure patterns for both continuous and intermittent exposure to the standard gas. For continuous exposure the retracted fiber is continuously exposed to the standard gas for 15 min. For intermittent exposure the retracted fiber is exposed to the standard gas for 5 min, then to clean air for 5 min, and then to the standard gas, etc., for 15 min total exposure to standard gas and 15 min exposure to clean air. The mass of analyte sorbed on the sorbent should therefore be the same for each exposure routine. The results from this study are shown in Figure 4-2. In this study, PDMS-100,

PDMS/DVB-65, and CAR/PDMS-75 fibers were used for passive sampling of *n*-alkanes from *n*-pentane to *n*-undecane — volatile alkanes with a broad range of boiling points and vapor pressures and pollutants very familiar to environmental scientists.

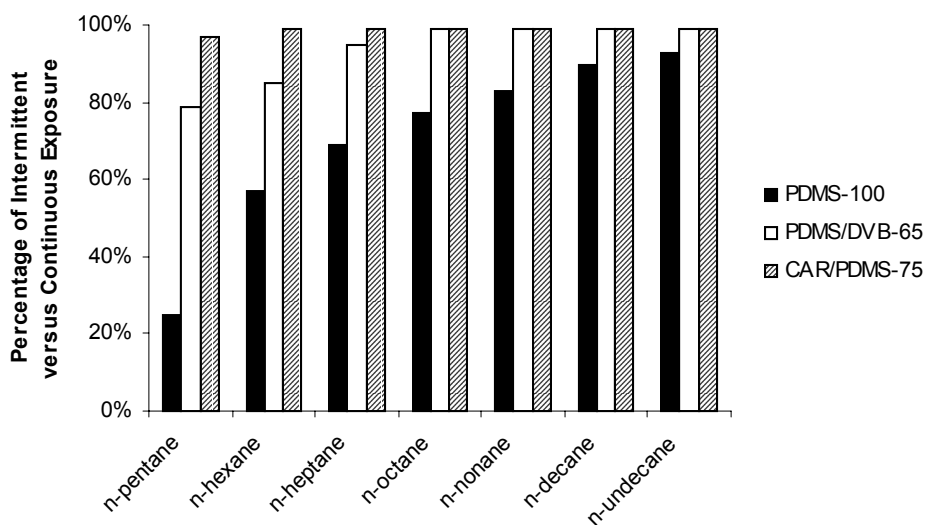


Figure 4-2 Amounts (%) of analytes on PDMS-100, PDMS/DVB-65, and CAR/PDMS-75 fibers after intermittent exposure, relative to the amounts after continuous exposure.

As mentioned earlier, analyte uptake on PDMS is by absorption. So, for low boiling point compounds from *n*-pentane to *n*-nonane with small distribution coefficients sorbed analytes are lost on exposure to clean air because $C_{sorbent}$ cannot be negligible. For high boiling point compounds such as *n*-decane and *n*-undecane with large distribution coefficients $C_{sorbent}$ is quite small — loss of sorbed analytes constitutes approximately 10% of total absorbed analytes during exposure to clean air. This indicates that the PDMS-100 fiber can be used only for TWA passive sampling of high boiling point compounds over short sampling times, because of the weak affinity and small capacity of the PDMS-100 fiber. The PDMS/DVB-65 fiber is a ‘zero sink’ for most of the target analytes, the exceptions being *n*-

pentane and *n*-hexane, whereas the CAR/PDMS-75 fiber is a ‘zero sink’ for all the target compounds, because of the strong affinity and large capacity of Carboxen.

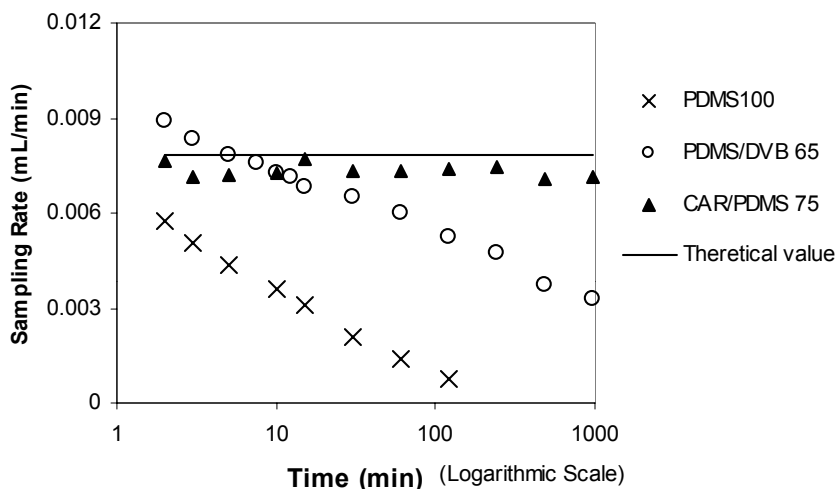


Figure 4-3 Sampling rate determined by TWA passive sampling of *n*-hexane with PDMS-100, PDMS/DVB-65, and CAR/PDMS-75 fibers ($Z=0.48$ cm).

These results were also verified by TWA passive sampling of *n*-hexane with PDMS-100, PDMS/DVB-65, and CAR/PDMS-75 fibers. Figure 4-3 shows the rates of sampling achieved by use of these three fibers. For the PDMS-100 fiber the rate of sampling decreases with increasing sampling time, because the PDMS is not a ‘zero sink’ for *n*-hexane, the sorbed *n*-hexane decreases the mass uptake rate of *n*-hexane to be sorbed. A similar trend is observed for TWA sampling of *n*-hexane by means of the PDMS/DVB-65 fiber, although the observed sampling rate is larger than that obtained by use of the PDMS-100 fiber, because of the greater affinity of PDMS/DVB for *n*-hexane. For the CAR/PDMS-75 fiber the rate of sampling is constant over the entire sampling period and is accurate to approximately 5% of the theoretical prediction. The CAR/PDMS-75 fiber was therefore used for SPME passive

sampling in subsequent experiments. Similar results should be obtained by use of the PDMS/DVB-65 fiber for TWA passive sampling of VOCs of boiling point equal to or higher than that of *n*-heptane.

4.4.1.2 Response Time

The second prerequisite is that a passive sampler must respond proportionally to changing analyte concentration at the face of the device. An important function of any passive sampler is that it is able to integrate high peak concentrations. This function is directly related to the response time of the sampler. A measure of the response time is the average residence time of an analyte within the diffusion zone.¹⁴ Assuming 100% collection efficiency the concentration of analyte at the sorbent surface will be zero. Thus, the average concentration within the diffusion zone is simply $C=C_{face}/2$ and total mass holdup is $n=(C_{face}/2) \cdot ZA$. The residence time can be readily estimated by use of equation 4.2:

$$\text{Response time, } T = \frac{\text{mass holdup}}{\text{mass uptake rate}} = \frac{(C_{face}/2) \cdot ZA}{\frac{DA}{Z} C_{face}} = \frac{Z^2}{2D} \quad \text{Equation 4.2}$$

where Z is the diffusion path length, in cm, and D is the diffusion coefficient, in $\text{cm}^2 \text{s}^{-1}$

For a SPME sampler used to monitor *n*-hexane the calculated response time is found to be approximately 2 and 15 s when the diffusion path length, Z , is equal to 0.5 and 1.5 cm, respectively. The short response time for the SPME sampler enables integration of rapidly changing concentration profiles, which ensures that the sample collected represents a true TWA concentration.

4.4.1.3 Effect of Face Velocity

The third prerequisite is that bulk analyte concentration, C_{bulk} , must equal the analyte concentration at the face of the opening, C_{face} , i.e., $C_{bulk}=C_{face}$. A passive sampler can be expected to sample accurately if all resistance to analyte transport is contained within the stagnant air layer inside the device. As the velocity of air across the sampler surface (face velocity) decreases external resistance to mass transfer associated with convection increases. When this latter resistance becomes a significant fraction of the internal diffusion resistance the mass of analyte collected will become less than that predicted on the basis of Fick's first law of diffusion. This suggests that a minimum air velocity is required and that when this minimum is achieved performance will be velocity-insensitive over a wide range. For a typical passive sampler, a large surface area is required to ensure a large amount of analyte is sampled, to satisfy analytical detection limits.^{14,15} A large surface area, in turn, requires a large face velocity, usually 15 to 50 ft min⁻¹ (~ 4.6-15 m min⁻¹), to ensure that C_{bulk} is equal to C_{face} .¹⁴

SPME takes advantage of thermal desorption, which transfers all the collected analytes into the instruments used for quantification, thus enhancing analytical sensitivity. A SPME sampler, for which the cross-sectional area of the needle is extremely small (8.6×10^{-4} cm²), requires a very small face velocity only. Experimental assessment of velocity-dependence indicated there were no significant effects of using the SPME device at a face velocity as low as 0.6 cm min⁻¹ (Figure 4-4). To explore further the lower limit of face velocity for TWA passive sampling with a SPME device the standard gas was passed through a 1 L gas sampling bulb, until a steady state was reached, then both stopcocks were closed to enclose a virtually static standard gas. TWA passive sampling performed in the gas sampling

bulb showed there was no significant difference between the sampling rates determined with the static standard gas and those obtained by the procedure described above. This is a significant advantage of the SPME device over other passive samplers and means that, in practice, the SPME device can be used for TWA passive sampling without considering the face velocity problem, which must be taken seriously when deploying other passive samplers.

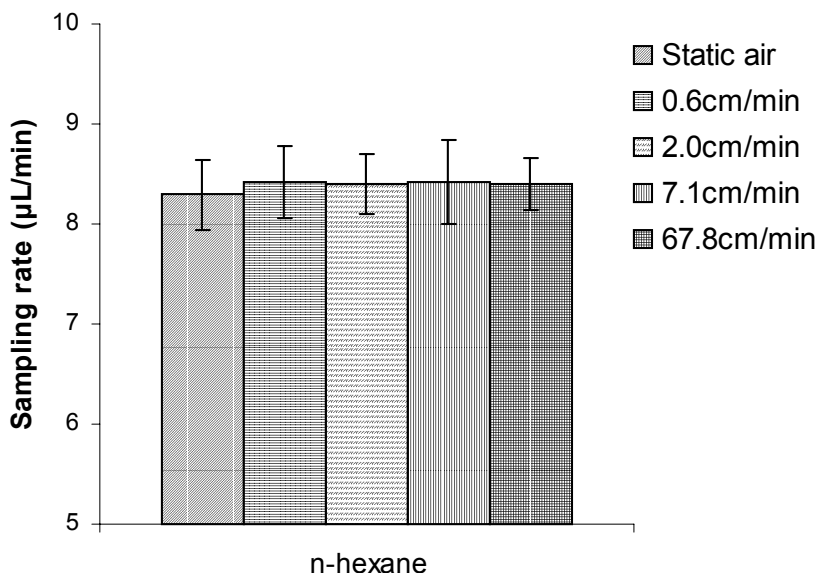


Figure 4-4 Relationship between face velocity and sampling rate ($Z=0.45$ cm).

4.4.2 TWA Passive Sampling with The CAR/PDMS-75 Fiber

Figure 4-5 depicts results from TWA passive sampling of *n*-alkanes with a retracted CAR/PDMS-75 fiber ($Z=1.47$ cm). In the figure the sampling volume/normalized mass uptake is used as the Y-axis, so the slopes of these lines are the sampling rates. From *n*-pentane to *n*-undecane the diffusion coefficient decreases with increasing molecular weight and Figure 4-5 shows that the sampling rate decreases with decreasing diffusion coefficient, which conforms to Fick's first law of diffusion.

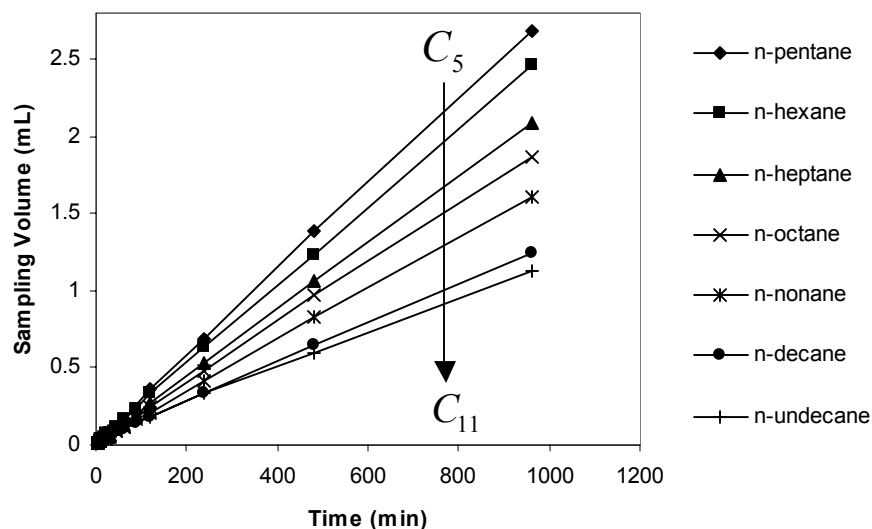


Figure 4-5 TWA passive sampling of *n*-alkanes with a CAR/PDMS-75 fiber ($Z=1.47$ cm).

Rearrangement of the definition of sampling rate R results in:

$$\frac{R}{D} = \frac{A}{Z} \quad \text{Equation 4.3}$$

Equation 4.3 indicates that the R/D ratio depends on the physical dimensions of the sampler only, in other words, R/D is independent of the target analytes. Figure 4-6 shows theoretical and experimental values of R/D for each target analyte. It is obvious that experimental results for low boiling point compounds, from *n*-pentane to *n*-nonane, agree very well with the theoretical value. For high boiling point compounds, however, e.g. *n*-decane and *n*-undecane, not only are the experimental results larger than the theoretical values, but also the standard deviations of the experimental results are quite large, probably because of adsorption of the compounds on the needle; this can be eliminated by use of deactivated needle.

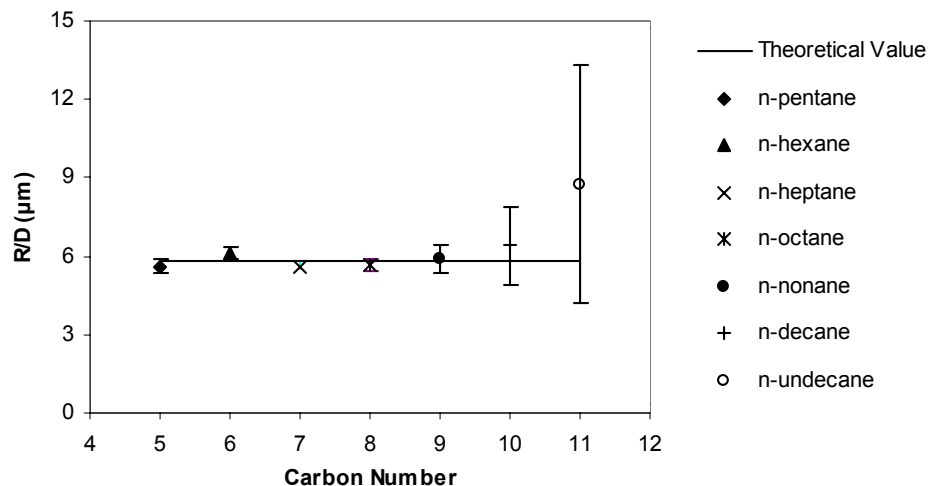


Figure 4-6 Plot of the dependence of experimental and theoretical R/D on the carbon number of each analyte for the CAR/PDMS-75 fiber ($Z=1.47$ cm).

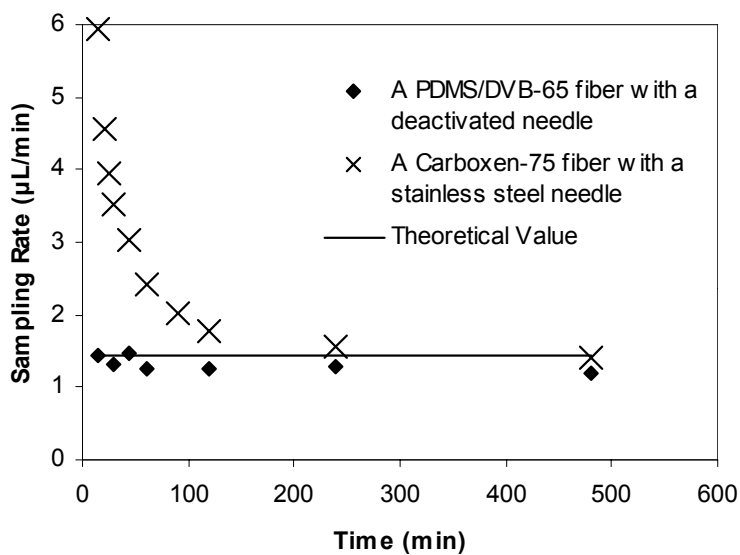


Figure 4-7 Comparison of the sampling rates determined by use of a PDMS/DVB-65 fiber with a deactivated needle and a Carboxen-75 fiber with a stainless steel needle ($Z=1.50$ cm).

Figure 4-7 depicts results obtained from TWA passive sampling of *n*-undecane with a PDMS/DVB-65 fiber with a deactivated needle and a Carboxen-75 fiber with a stainless steel needle. Sampling rates determined by the deactivated needle fiber for sampling times from 15 min to 8 h are consistent with theoretical values and are highly reproducible (RSD=10.6%), while those obtained with the stainless steel needle fiber were significantly higher than the theoretical values for the first two hours sampling when the amount of *n*-undecane extracted by the coating is small and the amount of *n*-undecane adsorbed on the stainless steel needle is the main component of the total amount of *n*-undecane introduced into a GC injector. To ensure a constant sampling rate for TWA passive sampling of compounds of high boiling point with SPME, the use of a deactivated needle fiber is recommended. These results are promising and demonstrate that analyte uptake by an SPME fiber is well described by Fick's first law of diffusion, i.e. the SPME device can be used as a TWA passive sampler.

Although TWA passive sampling with SPME has the same advantages as conventional SPME sampling — solvent-free, re-usable, etc. —there is one advantage specific to TWA passive sampling by SPME. The diffusion path length can be increased or decreased easily. According to the definition of sampling rate, *R* is inversely proportional to the diffusion path length. Therefore, for *R*₁ determined at *Z*₁, moving the fiber coating to *Z*₂ proportionally changes the sampling rate. Equation 4.4 shows the effect of changing the diffusion path length from *Z*₁ to *Z*₂ and indicates that sampling can occur at *Z*₂ whereas calibration can be performed at *Z*₁.

$$\frac{R_1}{R_2} = \frac{Z_2}{Z_1} \qquad \text{Equation 4.4}$$

Figure 4-8 shows the experimental results obtained from TWA sampling of *n*-hexane with a CAR/PDMS-75 fiber at different diffusion path lengths from 0.45 to 3.47 cm. The linear correlation coefficient ($R^2=0.9978$) and negligible intercept ($b=0.0003$) indicate there is a very good linear relationship between R and the reciprocal of Z . This is a significant characteristic of TWA sampling by use of SPME. The resulting implication is that a longer diffusion path, corresponding to a lower sampling rate, can be used to accommodate high concentrations or long sampling times whereas a shorter diffusion path, corresponding to a higher sampling rate, can be used to accommodate low concentrations or short sampling times.

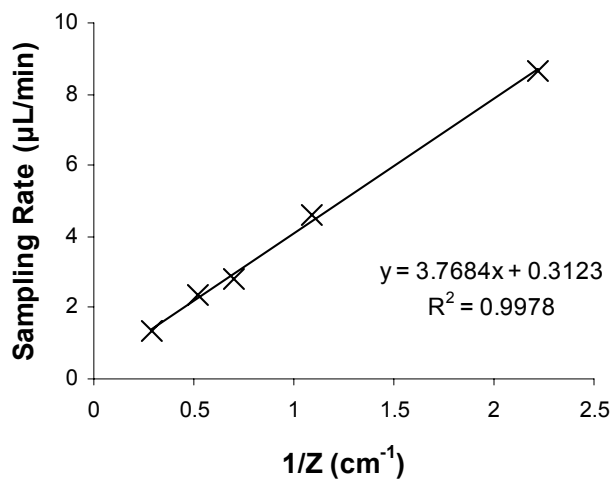


Figure 4-8 Relationship between sampling rate and diffusion path length.

4.4.3 Sensitivity to Ambient Conditions

Before deploying SPME devices for field sampling, laboratory studies were conducted to determine the effects of the temperatures, pressures, humidity, and ozone levels likely to be encountered in practical use.

4.4.3.1 Effects of Temperature and Pressure

The effects of temperature and pressure on passive sampling can be predicted theoretically.^{16,17} First, the mass loading n is proportional to the diffusion coefficient D and the concentration C (weight/volume):

$$n \propto (D \times C) \quad \text{Equation 4.5}$$

Second, D is proportional to $T^{3/2}$ and inversely proportional to P (total pressure):

$$D \propto \left(\frac{T^{3/2}}{P} \right) \quad \text{Equation 4.6}$$

Third, C is proportional to p_i (partial pressure) and inversely proportional to T :

$$C \propto (p_i / T) \quad \text{Equation 4.7}$$

Combining equations 4.5, 4.6, and 4.7 yields equation 4.8. For a closed system, the ratio $\left(\frac{p_i}{P} \right)$ is equal to the mole fraction of the analyte. So equation 4.8 indicates that change in pressure does not affect mass loading rate, and mass loading is proportional to the square root of the absolute temperature:

$$n \propto \left[T^{1/2} \times \left(\frac{p_i}{P} \right) \right] \quad \text{Equation 4.8}$$

This relationship indicates that a ten-degree variation of temperature at approximately 298 K causes only ~ 1% change of mass loading, which is completely independent of pressure.

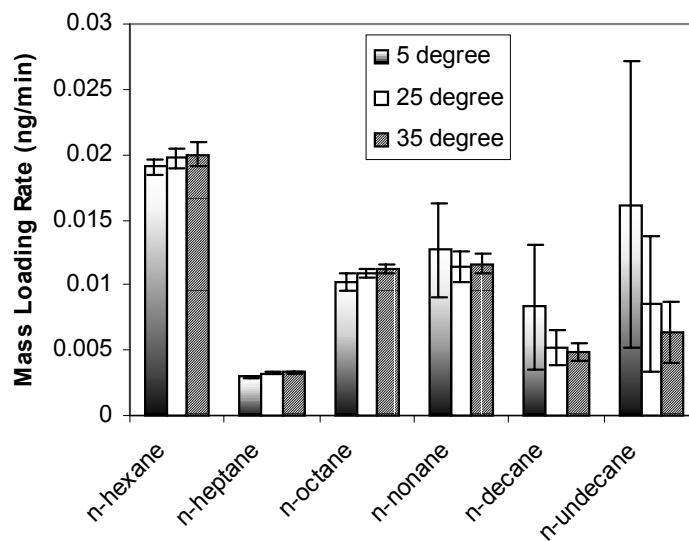


Figure 4-9 Effect of temperature on mass loading rate.

Experimental measurements of the temperature-dependence of mass loading were conducted at 5, 25, and 35°C. Figure 4-9 shows the mass loading rates for alkanes at different temperatures. From these it can be concluded that for low boiling point compounds (*n*-hexane to *n*-octane) the mass loading rate increases slightly with increasing temperature, in agreement with theoretical prediction (above). For high boiling point compounds, however, especially *n*-decane and *n*-undecane, the mass loading rate decreases with increasing temperature. This seemingly contradictory result can be easily understood by considering the effect of reduced needle adsorption with increasing temperature. The sampling rates for *n*-decane and *n*-undecane at 35°C, $(2.16 \pm 0.28) \times 10^{-3}$ and $(2.16 \pm 0.80) \times 10^{-3}$ mL min⁻¹, respectively, are close to the theoretical values (1.85×10^{-3} and 1.74×10^{-3} mL min⁻¹).

4.4.3.2 Effect of Humidity

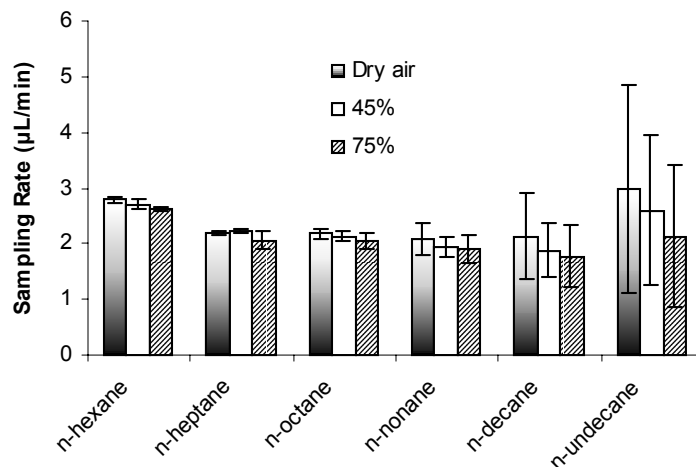


Figure 4-10 Effect of relative humidity on TWA passive sampling of *n*-alkanes with a CAR/PDMS-75 fiber ($Z=1.44$ cm).

The effect of humidity was tested for TWA passive sampling of *n*-alkanes with the CAR/PDMS-75 fiber at three different levels of relative humidity (dry air, 45%, and 75%) at 22°C (Figure 4-10). It is apparent that with increasing relative humidity the sampling rate decreases slightly. There is, however, no significant difference among the sampling rates at these three different levels. Possible reasons are, first, that Carboxen is a hydrophobic sorbent, so there is little adsorption of water molecules, and, second, Carboxen is far from saturation during TWA sampling (typically no more than 5% of equilibrium for an analyte mass loaded during TWA passive sampling can be accepted), so the effect of competition between water and analyte molecules for sorbent surface is not large.

4.4.3.3 Effect of Ozone

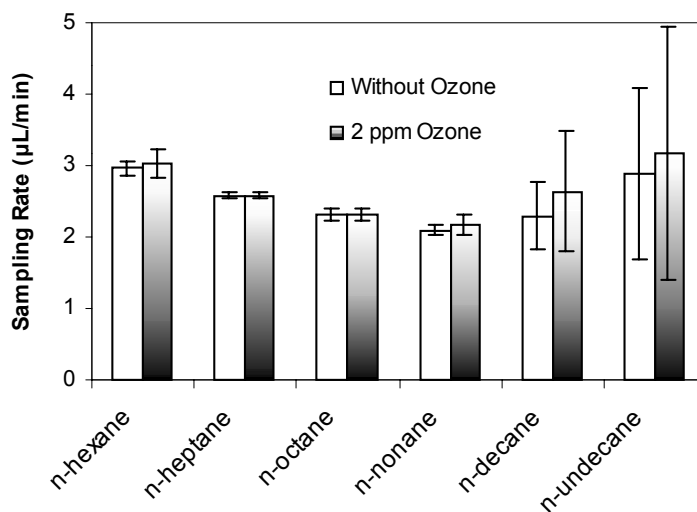


Figure 4-11 Effect of ozone on TWA sampling of *n*-alkanes with a CAR/PDMS-75 fiber ($Z=1.42$ cm).

Ozone is the most insidious and ubiquitous air pollutant affecting ecological systems and causing health problems for humans and animals. Its strong oxidizing effect is partially responsible for the depletion of forests and crops.^{18,19} It would be useful for long-term air monitoring to consider the effect of ozone on the stability of target compounds and on the performance of samplers. The study was performed by comparing TWA passive sampling in the presence of 2 ppm ozone and in the absence of the gas. It was found that although ozone does not affect sampling (Figure 4-11) at high concentrations (several thousand ppm) ozone reacts with *n*-alkanes and might damage fibers.

4.4.4 Storage Stability

The storage stability of the CAR/PDMS-75 fiber for *n*-alkanes (C₆–C₁₁) was tested in two ways.¹¹ First, a CAR/PDMS-75 fiber was used for passive sampling, for 30 min, of a standard gas containing *n*-alkanes; the fiber with the coating retracted was then exposed, for 8 h, to clean air at the same flow rate as the standard gas. No significant loss was observed for any of the analytes. Second, three CAR/PDMS-75 fibers were used for passive sampling, for 8 h, of a standard gas containing *n*-alkanes. One of the fibers was analyzed immediately after sampling whereas the others were sealed with narrow-bore solid Teflon™ caps, and stored at normal laboratory temperature (22°C). Another CAR/PDMS-75 fiber was used as blank. No significant change of mass adsorbed was observed after storage for two weeks.

4.4.5 Field TWA Sampling

Indoor and outdoor air was analyzed in an office, a solvent laboratory, an instrument laboratory, a store, a basement, and a gas station for periods from 90 min to 7 days to determine the TWA concentration of toluene. The reason for choosing toluene as target analyte was its ubiquity, high toxicity, high volatility, and ease of identification.

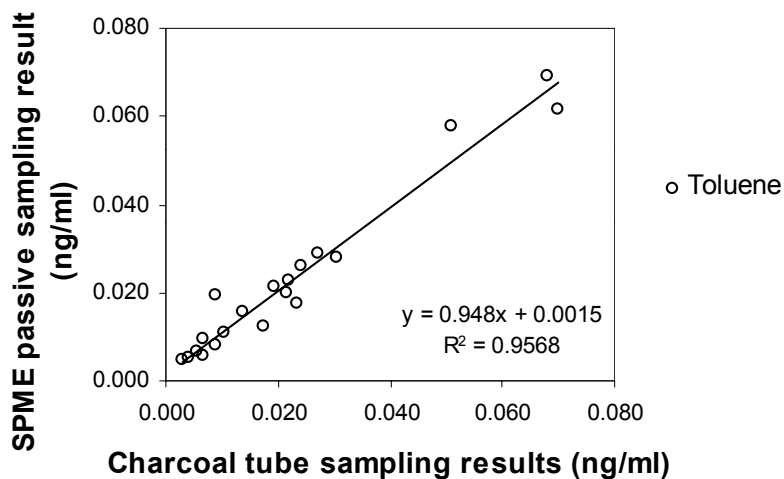


Figure 4-12 Field testing. Comparison of results from use of a charcoal tube (NIOSH method1501) and SPME with a CAR/PDMS-75 fiber.

The results obtained from the field study for determination of the TWA concentration of toluene by use of SPME with CAR/PDMS-75 and by use of active charcoal tubes are presented in Figure 4-12; significant correlation ($R^2=0.96$, 20 samples) without significant bias was found for results from the SPME device and from charcoal tubes. Standard deviations for the SPME device varied from 6 to 15%.

4.5 Conclusion

A modified SPME device was tested for use as a passive sampler to determine the TWA concentration of VOCs in air. It was shown that the SPME device satisfied all three prerequisites for successful passive sampling, i.e. ‘zero sink’, short response time, and insensitivity to face velocity. It is worth noting that the SPME device can be used for TWA passive sampling without considering face velocity, because of the extremely small diameter

of the needle. There was good agreement between theoretical predictions and experimental results for TWA passive sampling with the SPME device. In addition to all the advantages of conventional SPME sampling — flexibility, possibility of re-use, solvent-free operation, and easy automation, etc. — one advantage specific to TWA passive sampling with the SPME device is that the position of the SPME sorbent can be easily adjusted, i.e. the diffusion path length can be easily increased or decreased. The SPME device can therefore be used for TWA sampling over a large range of analyte concentrations and/or with different sampling times, depending on mass-detection requirements. Effects of environmental conditions — temperature, pressure, humidity, and ozone levels — were studied. Mass loading rate was affected only slightly by temperature, and was independent of pressure and of ozone levels. One important result is that adsorption of high boiling point compounds on the needle is alleviated by increasing the temperature, and can be eliminated by using a deactivated needle. The latter is preferred because of the convenience of operation. Experimental results indicated that relative humidity does not significantly affect mass loading rates as long as the SPME fiber is far from saturation (usually less than 5% of the equilibrium amount). In field sampling, it was demonstrated that the overall accuracy of the SPME device is similar to that of the charcoal tube method.

The SPME device has been shown to be a successful passive sampler for determination of the TWA concentration of VOCs. The sampling time could be further increased by attaching other pieces of tubing of different diameters and lengths to the needle. Future work should include the design of a new user-friendly device that would encourage acceptance of this technology, and application of the same principle for passive water sampling.

4.6 References

-
- ¹ Marty, J.; Jalifer-Merlon, E.; in: J. Nriagu (Ed.), *Gaseous Pollutants, Characterization and Cycling*, Wiley, New York, 1992.
- ² *The Industrial Environment-Its Evaluation and Control*, U.S. Department of Health and Human Services, Public Health Service, Center for Disease Control, National Institute for Occupational Safety and Health, 1973.
- ³ Namiesnik, J.; Zygmunt, B. and Kozdron-Zabiegala, B. *Pol. J. Environ. Stud.* **1994**, 3, 5.
- ⁴ Palmes, E.D. and Gunnison, A.F. *Am. Ind. Hyg. Assoc. J.* **1973**, 34, 78.
- ⁵ Brown, R.H.; Charlton, J. and Saunders, K.J. *Am. Ind. Hyg. Assoc. J.* **1981**, 42, 865.
- ⁶ Pawliszyn, J. *Solid Phase Microextraction—Theory and Practice*, Wiley-VCH; New York, 1997.
- ⁷ Pawliszyn, J. (ed.); *Applications of Solid Phase Microextraction*; RSC; Cambridge, UK, 1999.
- ⁸ Martos, P. A. and Pawliszyn, J. *Anal. Chem.* **1999**, 71, 1513.
- ⁹ Khaled, A. and Pawliszyn, J. *J. Chromatogr. A*, **2000**, 892, 455.
- ¹⁰ Namiesnik, J.; Gorecki, T. and Kozlowski, E. *Sci. Total Environ.* **1984**, 38, 225.
- ¹¹ Brown, R.H.; Harvey, R.P.; Purnell, C.J. and Saunders, K.J. *Am. Ind. Hyg. Assoc. J.* **1984**, 45, 67.
- ¹² Lautenberger, W.J.; Kring, E.V. and Morello, J.A. *Am. Ind. Hyg. Assoc. J.* **1980**, 41, 737.
- ¹³ Hearl, F. J. and Manning, M. P. *Am. Ind. Hyg. Assoc. J.*, **1980**, 41, 778.
- ¹⁴ Tompkins, F. C. and Goldsmith, R. L. *Am. Ind. Hyg. Assoc. J.*, **1977**, 38, 371.
- ¹⁵ Persoff, P. and Hodgson, A. T. *Am. Ind. Hyg. Assoc. J.*, **1985**, 46, 648.
- ¹⁶ Rose, V.E. and Perkins, J.L. *Am. Ind. Hyg. Assoc. J.*, **1982**, 43, 605.

¹⁷ Kring, E.V.; Lautenberger, W.J.; Baker, W.B.; Douglas, J.J. and Hoffman, R.A. *Am. Ind. Hyg. Assoc. J.*, **1981**, 42, 373.

¹⁸ Lippmann, M. *J. Air. Waste. Manage. Assoc.* **1989**, 39, 672.

¹⁹ Cecinato, A.; Palo, V. Di and Possanzini, M. *Fresenius J. Anal. Chem.* **2001**, 369, 652.

Chapter 5 A New SPME Field Sampler

5.1 Introduction

The application of SPME to date is principally within the laboratory.¹ The increasing need for fast screening, environmental and personal monitoring, clinical investigations, and *in-vivo* sampling are now driving SPME applications for field use.² Coupled to a portable GC, on-site analysis using SPME is feasible, with the advantage of eliminating the need to store and transport samples and/or samplers. This option for sampling on-site provides the capability for real-time decision making, when remediation is immediately required.^{3,4} In cases when on-site analysis is not possible, SPME is a simple and elegant sampling/sample preparation technique for field applications. SPME devices are small, which is crucial for deployment, storage, and transportation. No solvent is involved, meeting the requirement of “green chemistry”. Sampling and sample preparation are combined into a single step, which allows for a simple and fast sampling/sample preparation process.

The evolution of SPME theories is also moving rapidly towards field sampling. The basic sampling/sample preparation of SPME, developed to date, allows for possible rapid, short-term, and long-term/TWA field sampling.^{5,6,7} A variety of SPME fibers are commercially available, providing a large selection for different applications. Liquid coatings are generally used for the equilibrium extraction of volatile organic compounds (VOCs) via absorption. In the case of field sampling, equation 5.1 can be used to describe the amount of extracted analyte (n) and its concentration (C_0) in the sample.¹

$$n = K_{fs} V_f C_0$$

Equation 5.1

where K_{fs} is the distribution coefficient, V_f is the volume of fiber coating. One of the advantages of this method is that the sample volume does not need to be known, because the sample volume is generally very large. Solid porous coatings extract analytes by adsorption. The use of equation 5.1 for a solid porous coating is limited to low analyte concentrations, due to the limited coating surface area where the adsorption of analytes can occur. At high analyte concentrations, inter-analyte displacement complicates and often precludes quantification, particularly in cases when field or unknown samples are analyzed with porous SPME fibers.⁸ An alternative approach to quantification is to use very short sampling times for which the coating can be initially assumed to be a zero sink, or perfect sorbent, while the extraction is diffusion-controlled.^{5,7} When fibers are withdrawn inside the needle, solid porous fibers find their application for long-term/TWA sampling.⁶

To apply SPME for field sampling, several SPME field samplers have been developed, such as the Supelco field sampler, the SPME field sampler with a two-leaf closure, the disposable SPME field sampler with a Teflon cap, and the gas-tight valve syringe modified for SPME field applications.⁹ Field applications of these devices have also been conducted. However, none of these devices integrates the preservation of samples, ease of deployment, storage, and transportation. Supelco field samplers utilize a septum to seal the needle. The loose pegs used for setting the position of the needle and the fiber during exposure can be easily lost. The storage capacity of the two-leaf sampler is largely dependent on the quality of the seal between the two leaves of the closure. The Teflon-capped sampler utilizes a separate Teflon cap that is also easily lost. The gas-tight valve syringe sampler is not rugged.

The purpose of this study is to design, build, and test a new field SPME sampler that can protect fibers during sampling, storage, and transportation, while preserving the integrity of the samples, and is a more user-friendly and easy format for deployment and automation.

5.2 Experimental Section

5.2.1 Standard Gas Generator

The standard gas generator has been described in Chapter 2, section 2.3.4.1.

5.2.2 Sampling Chamber

The sampling chambers have been described in Chapter 2, section 2.3.4.2.

5.2.3 Gas Chromatography

A Varian star computer-controlled Varian 3400 CX gas chromatograph (Varian Associate, Sunnyvale, CA) equipped with a carbon dioxide cooled septum-equipped programmable injector (SPI) was used for all of the experiments. A 0.8 mm i.d. SPI insert was coupled to a RTX-5 column (30 m, 0.25 mm i.d., 1.0 μm film thickness) and the column was coupled to a flame-ionization detector (FID). The injector was maintained at 250°C for the PDMS and the PDMS/DVB fiber injection and at 300°C for the CAR/PDMS fiber injection. For liquid injections, the injector temperature was initially 35°C for 0.1 min and then ramped to 250°C at 300°C/min. For the SPME fiber and the liquid injections, the column temperature was maintained at 35°C for 2 min and then programmed at 30°C/min to

230°C. The carrier gas (helium) head pressure was set to 25 psig (~ 172 kPa) for both the SPME fiber and the liquid injection. Detector gas flow rates were 300 mL/min for air and 30 mL/min for nitrogen and hydrogen.

The experiments to test the cross contamination were carried out with a Saturn 3800 GC/2000 ITMS system fitted with a HP-5 column (30 m, 0.25 mm i.d., 0.25 µm film thickness) (Hewlett-Packard, Avondale, PA). Helium as the carrier gas was set to 1 mL/min. The 1079 injector was set to 250°C. The column temperature was maintained at 60°C for 1 min and then programmed at 10°C/min to 250°C and held for 5 min.

The instrument was checked on a daily basis by calibration with a SPME extraction of a standard BTEX gas mixture with a 100 µm PDMS fiber. Any deviation in the area counts greater than 15% required an injection of a liquid mid-point calibration standard. If the deviation was shown to be due to the response of the FID, the instrument was recalibrated with a six-point calibration plot. Peak shape quality, resolution, and retention times were also carefully monitored to ensure all chromatography was within the required specifications.

5.3 Results and Discussion

5.3.1 The SPME Field Sampler

The new field sampler was designed so that a commercialized fiber assembly can be used, making the sampler more universal and achieving inter-fiber reproducibility. The first requirement to design a field sampler is that the fiber needle must be sealed. Based on a previous study,⁹ Teflon was chosen as the material to seal the needle. Teflon is soft and provides good sealing of the needle. It also is an inert material that minimizes adsorption of

analytes released from the fibers and contamination from the environment. The Teflon cap should be attached to the SPME field sampler because a loose cap could be easily lost and would be difficult to find in the field. The cap should be easily replaceable if it becomes worn or is heavily contaminated. The next requirement is that the fiber needle must be protected. The needle shields the fiber, allows for introduction of the fiber into an injection port, and provides a diffusion channel for TWA sampling. Fiber protection is necessary throughout the sampling/sample preparation, storage, and transportation period due to the risk of operator injury and fiber damage. The third requirement is that the field sampler should be user-friendly, for acceptance in the industry as an alternative to existing methodologies. For example, a pen-like device would be easy to deploy and transport. The last requirement is that the field sampler should be amenable to automation, which requires that the physical dimensions of the field sampler be small, and the use of the device only involves several simple movements.

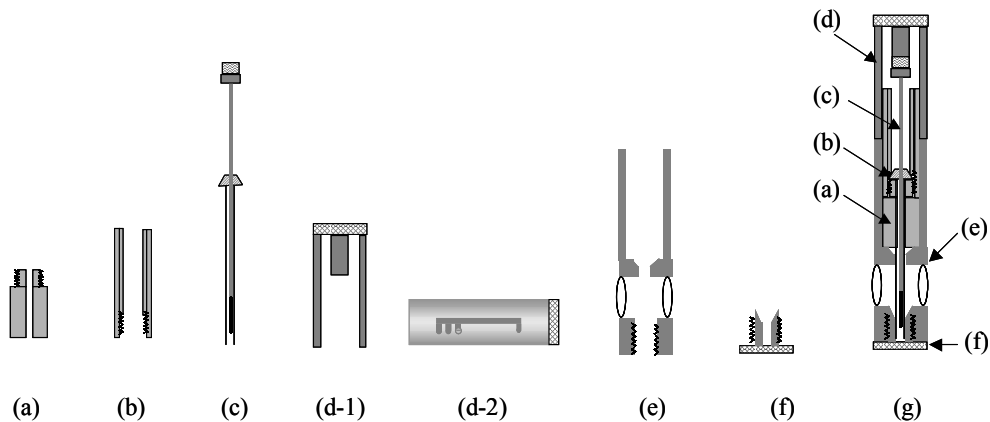


Figure 5-1 Schematic of the new SPME field sampler. Parts (a) and (b) are the fiber holder. Part (c) is a commercialized fiber assembly. Part (d-1) is the cross view of the adjustable cylinder, and Part (d-2) is the side view of the adjustable cylinder. Part (e) is the protecting shield. Part (f) is a replaceable Teflon cap.

Figure 5-1 shows the schematic of the new field sampler. Parts (a) and (b) are two cylinders with matching male and female screws. The needle of the fiber assembly (c) can be put through the central hole of part (a), whose inner diameter is slightly larger than the outside diameter of the needle, until the fiber assembly sits on part (a). Holding part (a) with the fiber assembly on it, the hub of the fiber assembly passes through the central hole of part (b) from the female screw end. Tightly screwing part (a) and (b), the fiber assembly is fixed to the holder. The hub of the fiber assembly can be connected to the inner pistol of part (d-1) by a screw. Part (d) can move along the fiber holder consisting of part (a) and (b). By controlling the position of part (d-2), the fiber can be positioned inside the needle for storage, transportation, or TWA sampling, or outside the needle for fiber injection, or rapid/short-term sampling. Part (e) is a protecting shield. The upper part of the protecting shield can hold and move along the fiber holder. Three side-holes are milled in the middle part of the shield, providing windows for analytes to access the fiber coating. The lower part of the shield is used to support the Teflon sealing cap (f). The Teflon cap can be easily replaced in the case of bad sealing or heavy contamination. (g) is the schematic of the final SPME field sampler, and resembles a large pen. The overall dimensions of the field sampler are 137 mm×13 mm. The prototype field sampler is larger than the final goal for the design, because this field sampler is designed for commercialized fibers. Since the dimensions of the SPME fibers can be decreased significantly, it can be expected that future SPME field samplers will be smaller.

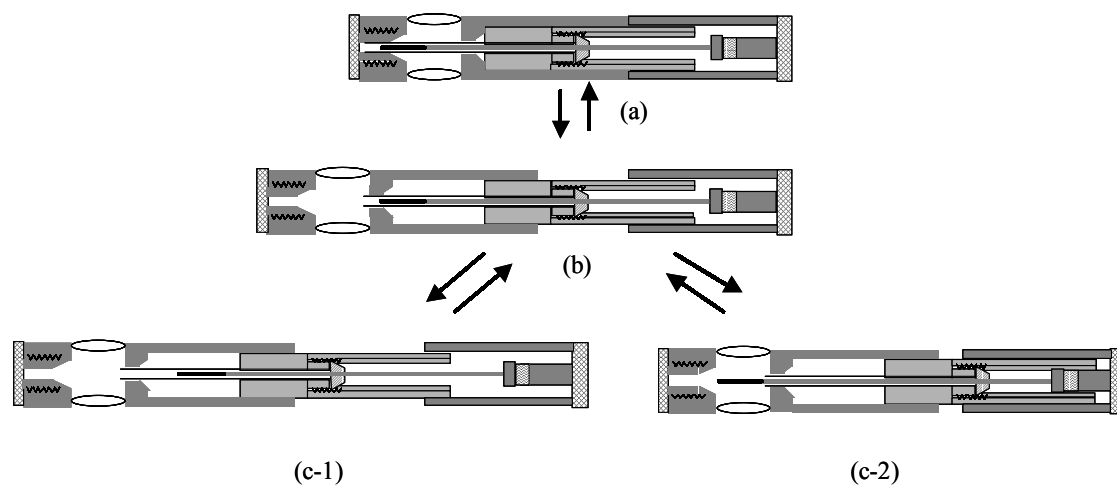


Figure 5-2 Operation of the new SPME field sampler. (a) is the status of standby, storage, or transportation. (b) is the status when the protecting shield is pulled outward and locked at the sampling position. (c-1) is the model for TWA sampling, and (c-2) is the model for grab sampling.

The field sampler is very easy to use and the operation is schematically shown in Figure 5-2. (a) is the field sampler in the status of standby, storage, or transportation. To use the sampler, first, unlock the protecting shield (part (e) in Figure 5-1), pull the shield outward until it stops and is locked at the sampling position (b). Second, unlock the adjustable cylinder (part (d) in Figure 5-1), adjust and lock the adjustable cylinder so that the fiber can be positioned further inside the needle—for TWA sampling (c-1), or exposed completely outside the needle—for rapid/short-term sampling (c-2). After sampling, restore and lock the position of the adjustable cylinder (b), then restore and lock the protecting shield (a). When the sampler is transported to a laboratory, unlock the protection shield, take off it from the sampler (Figure 5-3 (b)). Then the needle can be introduced into the injection port of a GC for desorption (Figure 5-3 (c)).

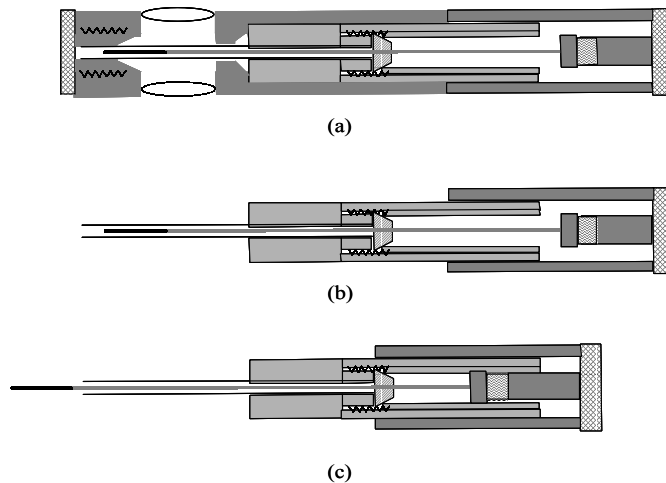


Figure 5-3 Introduction of the fiber into a GC injector. (a): the fiber is protected. (b): the protecting shield is removed. (c): exposure of the fiber.

5.3.2 Preservation of Sample Integrity

As a field sampler, it must preserve the integrity of the collected analytes following sampling until up to the analysis time. There are a number of ways to ensure this, such as the use of a highly efficient sorbent, the development of a holder that will perfectly seal the fiber, and storage of the fiber at sub-ambient temperatures.

A high efficient sorbent has a strong affinity and a large capacity toward VOCs, and thus can retain VOCs for a long time. Decreasing the storage temperature increases the affinity and capacity of a sorbent. Sealing the fiber needle tightly avoids potential losses of analytes and contamination from the ambient environment.

The use of a high efficient sorbent to preserve sample integrity is always the first choice, as demonstrated from the following experiment. When a Carboxen fiber was assembled in the field sampler, 30 min of TWA passive sampling was used to load BTEX

onto the Carboxen fiber. Storage of the sampler for 1 day and 2 weeks at room temperature shows that there is no significant loss of BTEX from the fiber. This is because, Carboxen is very effective at retaining BTEX and the sealing of the needle with the Teflon cap is very tight.

When the sorbent used is not very efficient for retaining VOCs, the choice of the sealing materials is crucial. PDMS is known to exhibit the least storage capacity towards VOCs among available commercialized fibers. PDMS fibers were chosen to study the “worst situation” for the sake of gaining a better understanding of the preservation of sample integrity.

When a PDMS fiber was assembled in the field sampler, exposing the fiber to a BTEX standard gas mixture for 2 min was followed by immediate desorption or storage under different conditions to evaluate the storage capacity of the field sampler. The extraction of BTEX using PDMS is based on equilibrium extraction. When the PDMS fiber is in storage, desorption of the BTEX from the fiber occurs until there is an equilibrium between BTEX in the fiber and those in the ambient air inside the needle. If the sealing of the needle is not tight, analytes in the ambient air inside the needle will be lost, causing further desorption of analytes from the fiber. If the sealing material absorbs analytes, the same results will be observed. In this study, different sealing materials, septum and Teflon were compared, followed by temperature effects on the storage capacity, and finally the reusability of the Teflon cap.

First, when a piece of septum was used to seal the fiber needle for 24 h at room temperature ($\sim 25^{\circ}\text{C}$), the amounts of BTEX left on the PDMS fiber were found to be ~ 4 , 9, 8, and 8%, respectively. Under the same conditions, when a Teflon cap was used, the

amounts of BTEX left on the PDMS fiber were found to be ~12, 40, 60, and 65%, respectively. Obviously, Teflon is better than septum for the preservation of analytes during storage. This is because septum, a soft material that can seal the needle tightly, is made of PDMS, which absorbs BTEX. Teflon is a relatively inert material, minimizing the absorption of BTEX. The loss of BTEX occurred even when the Teflon cap was used probably because the septum used to support the fiber and seal the other end of the needle absorbed the analytes. This might therefore limit the potential storage capacity of the system if PDMS fibers are used.

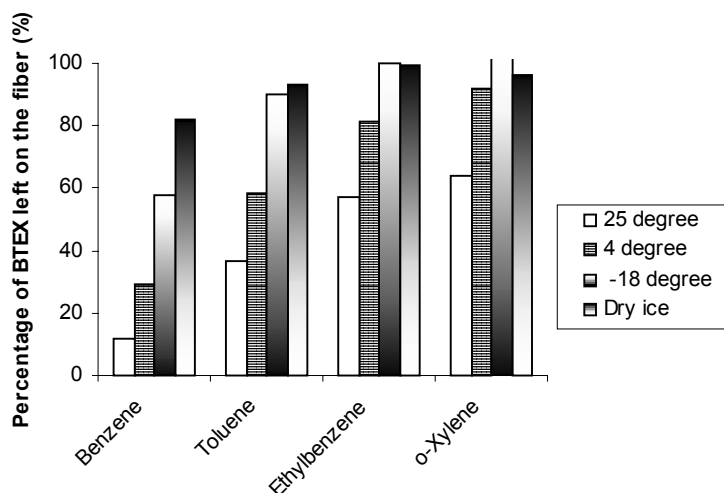


Figure 5-4 Effect of storage temperature. A PDMS fiber was used. The storage time was 24 h.

To enhance the preservation of sample integrity, storage of fibers at sub-ambient temperatures is an efficient solution. Absorption/adsorption is an exothermic process. Decreasing temperature favors the process of the absorption/adsorption of analytes onto fiber coatings, characterized by a larger distribution constant. Thus, more analytes can be retained at lower temperatures under the same conditions. Figure 5-4 presents the results of the temperature effect. In this study, a PDMS fiber was loaded with BTEX, sealed with a Teflon

cap, and then stored for 24 h at different temperatures. For compounds as volatile as benzene, decreasing the storage temperature significantly increases the percentage of analytes remaining on the fiber. However, even when the fiber was stored in dry ice, there was roughly a 20% loss of benzene after 24 h. Further decreasing the storage temperature will help retain more benzene on the fiber. For other components of BTEX, the same results were observed. However, when the storage temperature was as low as -18 degree, almost 100% of the ethylbenzene and the o-xylene were retained on the fiber. Further decreasing the storage temperature is not necessary if the storage time remains within 24 h of sample collection.

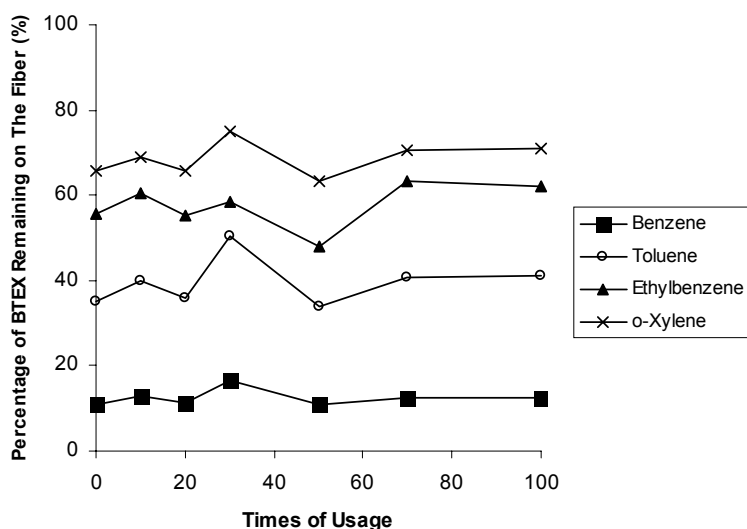


Figure 5-5 The reusability of a Teflon cap with the use of a PDMS fiber. The storage time was 24 h at $\sim 25^{\circ}\text{C}$.

It has thus been demonstrated that Teflon caps are a very good alternative for sealing fiber needles. The next concern is that if the same Teflon cap can be used repeatedly without any deteriorating sealing effects. To investigate the reusability of Teflon caps, a new Teflon cap was used to seal a PDMS fiber needle. The percentage of BTEX remaining on the fiber

was determined. The same Teflon was used repeatedly for 10, 20, 30, 50, 70, and 100 times. The corresponding percentages of BTEX remaining on the fiber were determined and are also presented in Figure 5-5. It was found that the Teflon cap could be used up to 100 times without any deteriorating sealing effects. This is understandable, because Teflon is a relative soft material.

5.3.3 Cross Contamination

In Section 5.3.2, it was demonstrated that the same Teflon cap could be used up to 100 times without any deteriorating sealing effects. This is a very desirable feature for the system, in terms of convenience and cost. However, when the same Teflon cap is used repeatedly, is there a possibility of cross contamination/memory effect?

To test the cross contamination potential, a series of experiments were performed. First, after extracting *n*-nonane, *n*-decane, and *n*-undecane standard gas mixture, a PDMS fiber was sealed with a Teflon cap and stored at room temperature for 24 h. The fiber was introduced in a GC injector to desorb analytes. The carryover of the fiber was checked to ensure there were no analytes left on the fiber and the GC column. The fiber was then sealed with the same Teflon cap for another 20 min at room temperature. Introduction of the fiber into the GC injector was set to detect if there were any analytes extracted by the fiber from the Teflon cap. Experimental results demonstrated that there were no detectable analytes extracted by the fiber from the Teflon cap. The same results were obtained when the target compounds were changed from *n*-nonane, *n*-decane, and *n*-undecane to *n*-tetradecane.

The next study utilized two PDMS fibers and two Teflon caps. Fiber #1 was used to extract *n*-nonane, *n*-decane, and *n*-undecane, and then sealed with Teflon cap #1. Fiber #2

was used to extract *n*-tetradecane, and then sealed with Teflon cap #2. Both fibers were stored at room temperature. After 24 h, the two Teflon caps were exchanged. In other words, fiber #1 was sealed with cap #2, and fiber #2 was sealed with cap #1. The two fibers were stored at room temperature for another 24 h. Analysis of the two fibers indicated that there were about 0.2% of *n*-tetradecane found on the fiber #1 and 1.3 to 3% of *n*-nonane, *n*-decane, and *n*-undecane found on fiber #2.

From the first study involved only one fiber and one Teflon cap (case 1), no memory effect was found. However, cross contamination was found from the second study involved two fibers and two Teflon caps (case 2). Why is there a big difference between the two studies? Careful inspection of the conditions of the two studies indicates that there are two differences. First, in case 2, the two caps were exchanged and used to seal fibers immediately, while in case 1, there was a 30 min interval between when the cap was detached from the fiber to check the amounts of analytes left on the fiber and the carryover of the fiber and reattachment of the cap to the fiber to check for the cross contamination/memory effect. If analytes were trapped in the air in the Teflon cap hole, the 30 minute exposure of the cap to ambient air might have allowed the escape of the analytes. Second, in case 1, when the cap was re-attached to the fiber to check for cross contamination, the second storage time was 20 min, while in case 2, it was 24 h.

To investigate the effects of these differences, more experiments were performed. In the case 3 study, the same conditions used for case 2 were used, except that there was a 30 min interval between when the two caps were detached and exchanged for the sealing of the fibers. During the interval, two new Teflon caps were used to seal the fibers. Experimental results indicated that cross contamination was found with the same magnitude as those found

in case 2. This suggests that the 30 min interval does not account for the difference between case 1 and case 2. In other words, cross contamination does not come from the analytes trapped in the air of the Teflon cap hole.

So, in case 4, the same conditions used for case 1 were investigated, except that the second storage time was set to 24 h. Cross contamination was found with about the same magnitude as those found in case 2, which means the long storage time accounts for the cross contamination effect.

From these studies, it was noted that Teflon caps do absorb analytes, and cross contamination was found during long storage times. When a Teflon cap was used to seal a PDMS fiber, some of the analytes desorbed from the coating are adsorbed onto the Teflon cap. When the Teflon cap was used to seal a clean fiber, analytes desorbed from the Teflon cap and absorbed onto the coating. Since desorption of analytes from the Teflon cap was slow, and the cross sectional area of the needle was small, it took a long time for the fiber coating to collect a detectable amount of the analytes.

If the analysis of these data is correct, it implies that if a highly efficient sorbent is used, desorption of analytes from the sorbent is negligible, and the adsorption of analytes onto the Teflon cap will be negligible. Correspondingly, cross contamination will be negligible.

To verify this assumption, another experiment was performed. In this study, the same conditions used for case 4 were applied, except that a DVB fiber was used. A 10 s extraction of C₉-C₁₁ was followed by a 24 h storage period at room temperature. After analysis of the fiber and check of the carryover, the same Teflon cap was used to seal the clean DVB fiber for another 24 h at room temperature. Analysis of the DVB fiber indicated that there was no

detectable carryover from the Teflon cap. This proves that the above analysis for the cross contamination is correct.

However, in the case of PDMS fibers being used and stored for a long time, or cross contamination from other sources, how can cross contamination be eliminated?

There are several solutions to eliminate cross contamination. The first solution is the use of other sealing materials. However, Teflon is probably the best material in terms of both sealing effect and memory effect. Septum is good at sealing but absorbs analytes; other materials, such as deactivated stainless steel, may minimize adsorption of analytes, but can't seal the needle very tightly. Alternatively, it might be helpful to coat the hole with deactivated materials.

The second solution is to use a new Teflon cap. This solution completely eliminates memory effect, but results in higher experimental costs. To minimize the size of the Teflon caps, the effect of the depth of the Teflon cap hole was investigated (the depth of the hole is 5 mm, unless otherwise specified). In this study, 3 caps with 3 different depths, namely 2.5, 5, and 10 mm, were used to seal 3 PDMS fibers that were preloaded with BTEX. After storage of the fibers at room temperature for 12 or 24 h, the amount of BTEX remaining each fiber was determined. It was found that the depth of the hole does not affect the retention efficiency of the system, which implies that as long as the needle can be sealed tightly, the size of the Teflon cap can be made as small as possible, thereby helping to reduce experimental costs.

The third solution is to clean the Teflon cap, using a solvent or high temperature. The latter strategy was experimentally investigated. A Teflon cap was conditioned at high temperatures to eliminate memory effect. For the first experiment, the Teflon cap was

conditioned at 125°C for 1 h. In this case, 0.4, 0.4, and 0.2% of *n*-nonane, *n*-decane, and *n*-undecane were found, respectively. Compared with the results when the Teflon was not conditioned, the carryover on the cap decreased, suggesting high temperature helps to eliminate the memory effect. When the conditioning temperature is increased to 200°C, while the conditioning time decreased to 30 min, the memory effect was barely observed.

5.3.4 Deactivated Needles

The SPME fiber needle has several important functions. One of them is to help the introduction of the fiber into a GC injector. When the needle is introduced into a GC injector, analytes adsorbed onto the needle during sampling, storage, and transportation are desorbed and carried into the GC column. Since the adsorption of analytes on the stainless steel needle is poorly predictable, it is always desirable to eliminate the adsorption. To date, the most widely used solution is to use a deactivated needle. A Silicosteel coated needle was found to be a good deactivated needle that could eliminate the adsorption of high boiling compounds, such as *n*-undecane.⁶ To examine this issue, a study was performed to test several kinds of deactivated needles provided by Supelco, to investigate if they could effectively eliminate the adsorption of high boiling compounds.

The empirical method previously described was used to determine if there is adsorption of high boiling compounds on the needle (Section 4.4.2).⁶ The deactivated needle fiber was used to passively sample *n*-undecane standard gas for 10 to 120 min period. Sampling rates at different sampling times were determined. It is suggested that if there is no adsorption of *n*-undecane on the needle, the sampling rate will be constant and equal to the theoretical value. Alternatively, if there is adsorption of *n*-undecane on the needle, the

sampling rate will be larger than the theoretical value, and initial sampling rate will be significantly large, and it decreases with sampling time. This is because at the beginning of sampling, the amount of *n*-undecane extracted by the coating is small and the amount of *n*-undecane adsorbed on the needle is the main component of the total amount of *n*-undecane introduced into the GC injector. With the increase of sampling time, the portion of *n*-undecane extracted onto the fiber coating is dominating. The results from this study are shown in Figure 5-6. Previously reported data obtained by the use of a Silicosteel deactivated needle were translated and presented in the same Figure.

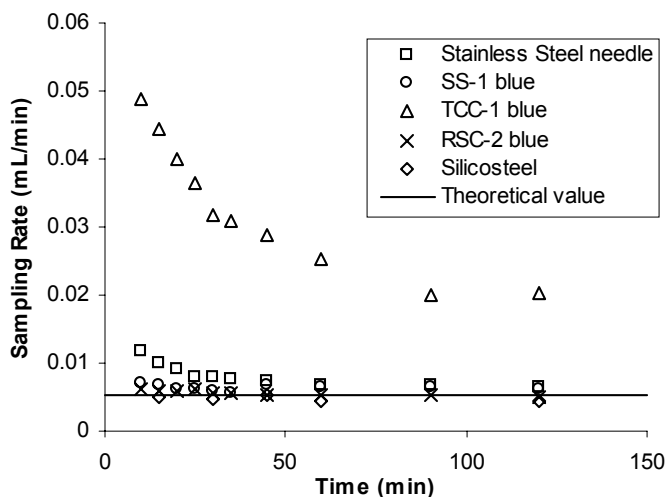


Figure 5-6 Test of adsorption of *n*-undecane onto deactivated needles. The sampling rates of Silicosteel were translated from reference 6.

From Figure 5-6, it can be concluded that the TCC-1 blue (DVB) fiber needle was the worst fiber for eliminating the adsorption of *n*-undecane, and performed more poorly than the ordinary stainless steel needle. In other words, the coating used to coat the TCC-1 blue fiber needle has a stronger affinity towards *n*-undecane than stainless steel. The RSC-2 blue

(DVB) fiber needle was found to be comparable to the Silicosteel deactivated needle. The sampling rates (0.0056 ± 0.00036 mL/min) obtained by the use of the RSC-2 blue (DVB) fiber were close to theoretical value (0.0052 mL/min), with high reproducibility. The SS-1 blue (DVB) fiber needle was also effective at eliminating the adsorption of *n*-undecane. It performed more efficiently than the commercialized stainless steel fiber needle, but not as well as the RSC-2 blue (DVB) fiber needle.

5.4 Field Sampling

The new SPME field sampler was investigated for field applications. The first application involved the extraction of a complex sample—the air near a gas station. Two Carboxen fibers were installed in the field sampler and the commercialized SPME holder, respectively. These two fibers were exposed side-to-side to the air for 5 min. Then both fibers were sealed with Teflon caps and transported to the laboratory. The fiber installed in the commercialized SPME holder was analyzed immediately, while the new SPME field sampler was stored at room temperature for 16 h before being analyzed. The total area counts obtained by the new SPME field sampler are about 94% of those obtained without storage.

The second field application involved the determination of the TWA concentration of toluene in a chemistry laboratory. The SPME field sampler was placed in the TWA sampling model, in which the Carboxen fiber was withdrawn 5 mm inside the needle, and placed on a working bench. NIOSH method 1501 was chosen as the reference method. The TWA concentration of toluene over 3 working days was found to be 3.6 ng/L by SPME and 3.0 ng/L by the NIOSH charcoal tube method, respectively.

5.5 Conclusion

The new SPME field sampler integrated some merits of previously developed SPME field samplers. It was readily deployed, stored, transported, as well as rugged, avoiding fiber failure. The use of a Teflon cap to isolate the fiber coating from the ambient environment provided an effective mechanism for preserving sample integrity and preventing contamination. In addition, the field sampler can be used for both TWA sampling and grab sampling.

The field sampler was demonstrated to be capable of retaining VOCs for up to two weeks without significant loss when a highly efficient sorbent such as Carboxen was used. When a low efficient sorbent such as PDMS was used, storage of the sampler in sub-ambient temperatures is necessary if there are extended storage periods (such as greater than 24 h).

Cross contamination might be an issue only if Teflon caps are used repeatedly, or if PDMS fibers are used at the same time. However, simple solutions such as conditioning the Teflon cap at high temperatures can effectively eliminate the potential for cross contamination.

Upon the use of efficient deactivated needles, the adsorption of high boiling point compounds on the fiber needles during sampling, storage, and transportation will be minimized.

5.6 References

¹ Pawliszyn, J. Solid Phase Microextraction – Theory and Practice; Wiley–VCH; New York, 1997.

² Pawliszyn, J. (ed.); *Applications of Solid Phase Microextraction*; RSC; Cambridge, UK, 1999.

³ Koziel, J.; Jia, M.; Khaled, A.; Noah, J. and Pawliszyn, J. *Anal. Chim. Acta* **1999**, 400, 153.

⁴ Augusto, F.; Koziel, J. and Pawliszyn, J. *Anal. Chem.*, **2001**, 73, 481.

⁵ Koziel, J.; Jia, M. and Pawliszyn, J. *Anal. Chem.* **2000**, 72, 5178.

⁶ Chen, Y. and Pawliszyn, J. *Anal. Chem.* **2003**, 75, 2004.

⁷ Chen, Y.; Koziel, J. and Pawliszyn, J. *Anal. Chem.* **2003**, 75, 6485.

⁸ Górecki, T.; Yu, X. and Pawliszyn, J. *Analyst* **1999**, 124, 643.

⁹ Müller, L.; Górecki, T. and Pawliszyn, J. *Fresenius J. Anal. Chem.*, **1999**, 364, 610.

Chapter 6 Summary

6.1 Calibration for Different Extraction Modes of SPME

Calibration based on physicochemical constants, such as the distribution coefficient and the diffusion coefficient, is simple, rapid, and cost-efficient, especially for on-site analysis. As various theories indicate, these constants, which can be obtained from the literature, determined by simple experiments and/or estimated from various empirical equations, define the extraction process.

SPME is a simple, solvent-free, and reliable microextraction technique. The small dimensions of SPME devices and its solvent-free feature enable on-site sampling/sample preparation. The combination of SPME and calibration based on physicochemical constants thus has great potential to achieve rapid and cost-efficient quantitative on-site sampling/sample preparation. For example, in equilibrium microextraction techniques, the distribution coefficient is used to quantify the concentration of analytes in the sample matrix (equation 1.4). In time-weighted average (TWA) passive sampling techniques, calibration can be based on the diffusion coefficient (equation 1.28). When the conventional calibration step is skipped, sampling/sample preparation is simplified and accelerated, enabling on-site analysis. This reduces errors and the time associated with sample transport and storage, resulting in more accurate, precise, and more time efficient analytical data. Figure 6-1 presents various calibration approaches according to the different arrangements of the extraction phase.

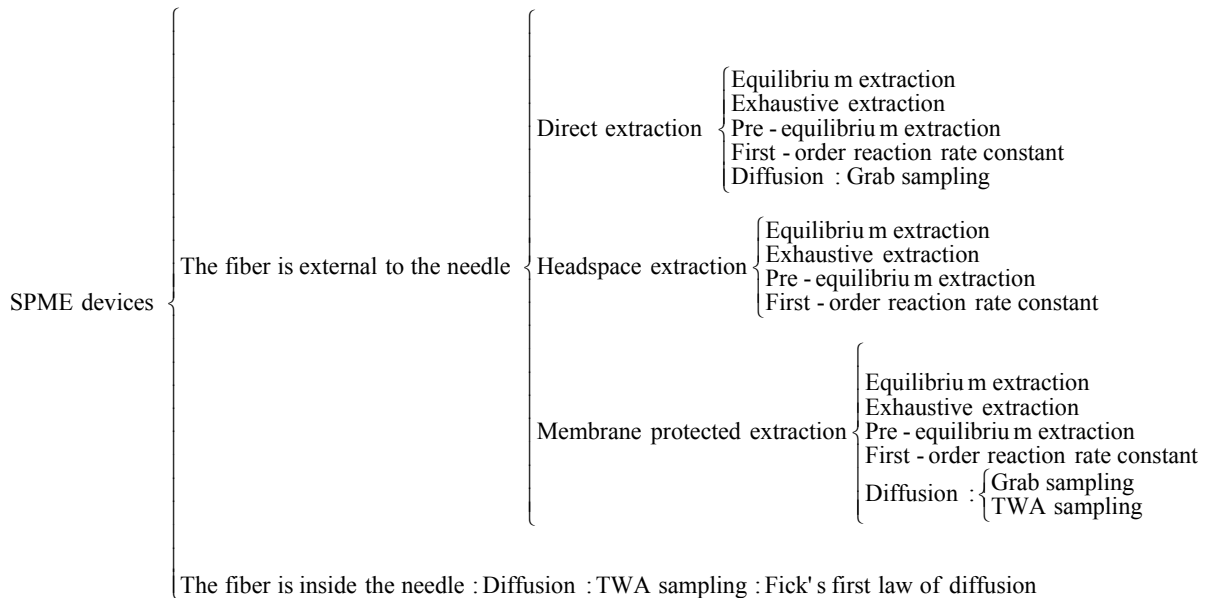


Figure 6-1 Extraction modes of SPME and the corresponding calibration methods

When the fiber is exposed outside its needle, which is usually used for rapid sampling/sample preparation, three basic types of extraction can be performed: direct extraction, headspace extraction, and membrane protected extraction. Figure 6-2 illustrates the differences among these modes. In the direct extraction mode (Figure 6-2 a), the coated fiber is inserted into the sample and the analytes are transported directly from the sample matrix to the extracting phase. To facilitate rapid extraction, some level of agitation is required to transport analytes from the bulk of the solution to the vicinity of the fiber. For gaseous samples, natural convection of air is sufficient to facilitate rapid equilibration. For aqueous matrices, more efficient agitation techniques, such as fast sample flow, rapid fiber or vial movement, stirring, or sonication are required. These conditions are necessary to reduce the effect caused by the "depletion zone", produced close to the fiber as a result of fluid

shielding and slow diffusion coefficients of analytes in liquid matrices. Direct extraction can be calibrated based on equilibrium extraction, exhaustive extraction, pre-equilibrium extraction, first-order reaction rate constant, or diffusion.

In the headspace mode, the analytes need to be transported through the air barrier before they can reach the coating. This modification serves primarily to protect the fiber coating from damage by high molecular mass and other non-volatile interferences present in the sample matrix, such as humic materials or proteins. This headspace mode also allows modification of the matrix, such as a change of the pH, without damaging the fiber. Calibration methods for direct extraction can be readily adapted for headspace extraction by considering the existence of the gas phase. The only difference is that the diffusion-based calibration has not been developed for headspace extraction to date.

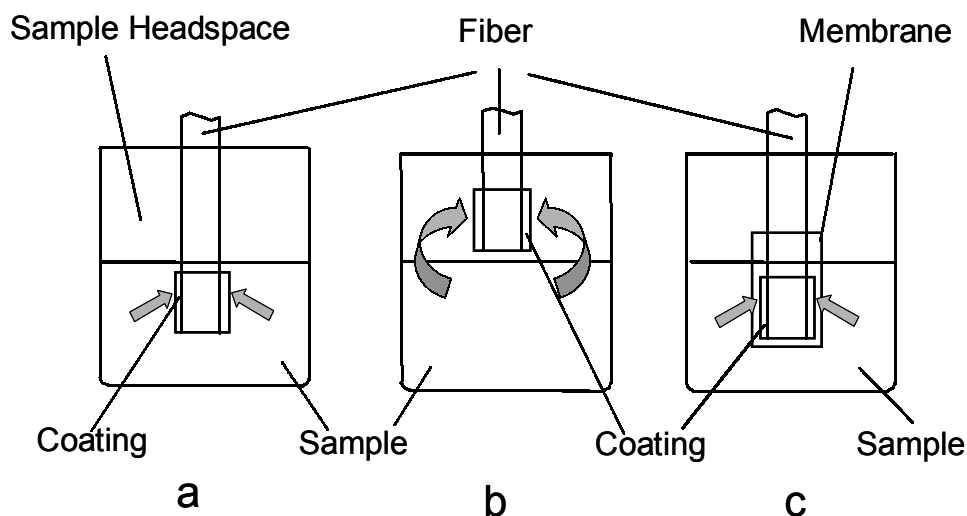


Figure 6-2 Extraction modes of SPME when the fiber is extended outside its needle: (a) direct extraction, (b) headspace extraction, (c) membrane-protected extraction.

Figure 6-2 c illustrates the principle of indirect SPME extraction through a membrane. The initial purpose of the membrane barrier was to protect the fiber against damage, similar to the use of headspace SPME when very dirty samples are analyzed. Membrane protection is advantageous for the determination of analytes that possess volatilities too low for the headspace approach. In addition, a membrane made from an appropriate material can add a certain degree of selectivity to the extraction process. The kinetics of membrane extraction is substantially slower than for direct extraction, however, because the analytes must diffuse through the membrane before they can reach the coating. The use of thin membranes and increased extraction temperatures will result in faster extraction times. The thicker membranes can be used to slow down the mass transfer through the membrane, resulting in the TWA measurement for aqueous and gaseous samples.

When the fiber is withdrawn inside its needle (Figure 1-12), analytes can only access the fiber coating by diffusion through the diffusion gap, between the fiber and the needle opening. This mode is exclusively used for TWA sampling. The uptake of analytes is calibrated with the diffusion law.

6.2 Contributions of this Thesis

The fundamental knowledge related to rapid sampling/sample preparation with SPME has been extended. The first mass transfer model (Chapter 1) was accurate for rapid air sampling, while the new mass transfer model (Chapter 2) was validated for both air and water samples.

In addition, the introduction of ‘standard on a fiber’ further integrates sampling, sample preparation, and sample introduction. The significance of the approach will be most evident for studies in which conventional standardization procedures are difficult, if not impossible, to implement, which is often the case for on-site or *in-vivo* sampling/sample preparation. It is especially critical for on-site or *in-vivo* investigations, where the composition of the sample matrix is very complicated, and/or agitation of the sample matrix is variable or unknown.

TWA sampling with SPME was achieved. The advantages of this approach were recognized by the fundamental understanding of the mass transfer process. With the development of the new SPME field sampler, commercialized SPME products for TWA sampling will soon be available for analytical chemists and industrial hygienists to perform routine measurements of TWA concentrations.

6.3 Perspective

Diffusion-based SPME has achieved breakthroughs for both grab and TWA sampling. The future research in this area could consist of a number of applications.

First, the extension of the TWA sampling technique for water samples is needed across many disciplines. This is a very important yet very difficult project, requiring long-term and collaborative investigation, due to the slow diffusion in water, the difficulty related to implementing the specific SPME devices, adsorption of persistent organic compounds on the needle, and various errors related to long experimental times.

Second, the extension of the standards on a fiber technique for porous coatings is needed. Since the extraction with porous coatings is completely controlled by the diffusion

through the boundary layer, this technique could be used for both air and water sampling, even at highly agitated conditions. The challenge is the validation of quick equilibrium at the interface and the determination of the distribution coefficient or the product of the distribution coefficient and the volume of the coating.

Glossary

a	Time constant
A	Surface area of a SPME fiber
BTEX	Benzene, toluene, ethylbenzene, and xylene
CAR	Carboxen
C_0	Initial analyte concentration
C_f	Analyte concentration in the fiber coating at the interface of the fiber coating and the boundary layer
C'_f	Analyte concentration in the fiber coating at the interface of the fiber coating and the fused silica
C_s	Analyte concentration in the bulk of the sample matrix
C'_s	Analyte concentration in the boundary layer at the interface of the fiber coating and the boundary layer
d	Diameter of the fiber
D_f	Diffusion coefficient in the fiber coating
D_s	Diffusion coefficient in the sample matrix
DVB	Divinylbenzene
FID	Flame ionization detection
GC	Gas chromatograph
h_f	Mass transfer coefficient in the fiber coating
h_s	Mass transfer coefficient in the boundary layer
J	Mass flux
K	Distribution coefficient
K^*	First-order reaction rate constant
MS	Mass spectrometer
n	The amount of analyte absorbed onto the fiber
n_0	The amount of analyte absorbed onto the fiber at equilibrium
NIOSH	National Institute for Occupational Safety and Health

NIST	National Institute of Standards and Technology
\overline{Nu}	Nusselt number
OSHA	Occupational Health and Safety Administration
PAH	Polycyclic aromatic hydrocarbon
PDMS	Poly(dimethylsiloxane)
ppm	Parts per million
q	The amount of standard desorbed from the fiber
q_0	The initial amount of standard extracted onto the fiber
Q	The amount of standard remaining on the fiber
Re	Reynolds number
Sc	Schmidt number
SPME	Solid phase microextraction
u	Linear velocity
ν	Kinematic viscosity
V_f	The volume of the fiber coating
V_s	The volume of the sample matrix
VOC	Volatile organic compound
t	Sampling time
TWA	Time-weighted average
δ_f	The thickness of the fiber coating
δ_s	The thickness of the boundary layer
Z	Diffusion path length